The effect of traumatic brain injury in experimental models of Alzheimer's disease

by

Jessica Marie Collins, BMedRes(Hons)

Submitted in fulfilment of the
requirement for the Degree of
Doctor of Philosophy

Wicking Dementia Research and Education Centre,
School of Medicine, Faculty of Health,
University of Tasmania
(October, 2015)

COPYRIGHT STATEMENT

This thesis contains no material which has been accepted for a degree or diploma by the University or any other institution, except by way of background information and duly acknowledged in the thesis, and to the best of the my knowledge and belief no material previously published or written by another person except where due acknowledgement is made in the text of the thesis, nor does the thesis contain any material that infringes copyright.

Jessica Marie Collins

STATEMENT OF AUTHORITY OF ACCESS

This thesis may be made available for loan and limited copying and communication in accordance with the Copyright Act 1968.

Part of the work submitted in this thesis has been published or submitted for publication as follows:

Collins, J. M., King, A. E., Woodhouse, A., Kirkcaldie, M. T. & Vickers, J. C. 2015. The effect of focal brain injury on beta-amyloid plaque deposition, inflammation and synapses in the APP/PS1 mouse model of Alzheimer's disease. *Experimental Neurology,* 267, 219-29.

ABSTRACT

Traumatic brain injury (TBI) can cause persistent cognitive changes and ongoing neurodegeneration in the brain. Accumulating epidemiological and pathological evidence implicates TBI in the development of Alzheimer's disease (AD). Furthermore, repetitive TBI is shown to cause the neurodegenerative condition chronic traumatic encephalopathy, which has many clinical and pathological similarities to AD.

AD is characterized by three main pathological hallmarks: extracellular plaques composed of beta-amyloid (Aβ), dystrophic neurites and intracellular neurofibrillary tangles composed of tau. The amyloid cascade hypothesis posits that the accumulation of Aβ in the brain is a principal factor in AD pathogenesis, and genetic mutations causing enhanced Aβ formation result in early-onset AD.

Aβ plaques have been demonstrated in approximately 30% of severe TBI cases, however the effects of mild/moderate non-fatal TBI on Aβ plaque deposition remains unclear. Furthermore, the underlying mechanisms and risk factors for Aβ plaque deposition after TBI are unknown. Thus, this thesis investigated the effects of a single TBI on the onset and progression of Aβ plaque deposition in the APPswe/PS1dE9 (APP/PS1) transgenic mouse model of AD.

Two models of TBI were utilized in this thesis. The first model was a focal cortical brain injury, which involved the insertion of a needle into the somatosensory cortex of the brain, inducing localized structural brain damage with minimal secondary pathology. The results demonstrated that focal cortical brain injury before the onset of plaque deposition and mid-way into deposition did not alter Aβ plaque load post-injury. Furthermore, these studies indicated that APP/PS1 mice with established amyloidosis have the same microglial, astrocytic and synaptic responses to focal cortical brain injury as wild type mice, despite the presence of AD-related neuropathology.

The second model of TBI utilized in this thesis was the lateral fluid percussion injury (LFPI) which produces widespread diffuse brain damage with evolving secondary pathology such as diffuse axonal injury (DAI). These studies demonstrated that LFPI prior to the onset of Aβ plaque deposition caused an increase in plaque load after injury,

whereas LFPI during Aβ plaque deposition caused a decrease in plaque load post-injury. Thus, the results indicated that the stage of amyloidosis at the time of LFPI affected whether Aβ plaque deposition was enhanced or reduced in APP/PS1 mice after injury. Furthermore, as LFPI but not focal cortical brain injury altered Aβ plaque deposition after injury, the results indicate that diffuse TBI may be required for the modulation of Aβ plaque deposition after injury.

DAI can result in impaired axonal transport and the intra-axonal accumulation of amyloid precursor protein (APP). Impaired axonal transport is caused by TBI-induced cytoskeletal damage and may be a potential mechanism for post-injury Aβ plaque formation. Neurofilaments are an integral part of the axonal cytoskeleton and undergo various pathological changes following TBI however, the role of NF in DAI and impaired axonal transport is unclear. Thus, the final study in this thesis investigated the effect of altering the NF cytoskeleton on the axonal response to injury. The results demonstrated that genetically altered mice lacking NF light gene showed an increased number of axonal APP accumulations, indicating higher levels of impaired axonal transport and thus DAI following LFPI.

The research in this thesis provides insight into the effects of different types of TBI on Aβ plaque dynamics. The results indicated that diffuse but not focal TBI can alter Aβ plaque deposition after injury and that this modulation is dependent on the stage of amyloidosis at the time of injury. Lastly, this thesis demonstrated that the axonal cytoskeleton is important in the axonal response to TBI and may be a potential therapeutic target.

ACKNOWLEDGMENTS

First and foremost I would like to thank my supervisors James Vickers, Anna King, Adele Woodhouse and Matthew Kirkcaldie for all their support, guidance, help and patience throughout my PhD journey.

I would also like to thank our technical staff Graeme McCormack and Justin Dittmann for spending the time to teach and assist me with the animal work and protocols that are included in this thesis.

Thank you to the animal facility staff, past and present for all your help in the breeding and care of the laboratory animals. The research in this thesis would not have been possible without your hard work.

To my fellow students, both past and present, thank you so much for making my PhD fun and for all your friendship. In particular, I would like to thank the members of the Wicking laboratory group for all their help and encouragement.

I would like to show my appreciation to all of my friends and family for their support and understanding. I would especially like to thank and acknowledge my partner Lachlan Davey who has shared my PhD journey with me. Also, to my cat Maverick, thanks for sitting on my lap and listening to me ramble on about my PhD without complaint.

Finally, thank you to the JO and JR Wicking Trust (Equity Trustees) and the National Health and Medical Research Council for providing funding for this work.

Table of Contents

ABBREVIATIONS

Beta-amyloid (Aβ)

Amyloid intracellular domain (AICD)

Alzheimer's disease (AD)

Apolipoprotein E (APOE)

Amyloid precursor protein (APP)

Aquaporin 4 (AQP4)

B-secretase (BACE)

Bone marrow derived macrophage (BMDM)

Controlled cortical impact (CCI)

Cerebrospinal fluid (CSF)

Chronic traumatic encephalopathy (CTE)

Carbon 11-labelled Pittsburgh compound B ([^{11}C]PiB)

Diffuse axonal injury (DAI)

Interstitial fluid (ISF)

Lateral fluid percussion injury (LFPI)

Loss of consciousness (LOC)

Mild cognitive impairment (MCI)

Neurofilament (NF)

Neurofilament heavy (NFH)

Neurofilament light (NFL)

Neurofilament medium (NFM)

Positron emission tomography (PET)

Presenilin 1 (PS1)

Presenilin 2 (PS2)

Standard error of the mean (SEM)

Traumatic brain injury (TBI)

Wild-type (WT)

1 Introduction

1.1 Traumatic brain injury

A traumatic brain injury (TBI) is commonly induced by an impact to the head or by acceleration/deceleration and/or rotational forces. The major causes of TBI in high-income countries are motor vehicle accidents and falls (Baguley et al., 2012, Feigin et al., 2013, Myburgh et al., 2008). It is typically a prime of life disability, affecting predominantly younger individuals during their most productive years of life (Maas et al., 2008, Feigin et al., 2013). However, in recent decades, the median age of TBI patients has increased in high-income countries (Maas et al., 2008, Roozenbeek et al., 2013). This may be attributed to increased life expectancy and thus an increase in the 'aging' of the population as well as better traffic safety (Maas et al., 2008, Roozenbeek et al., 2013). The main cause of TBI in the elderly is falls, with people aged over 75 years having the highest rates of hospitalisations and deaths (McIntyre et al., 2013).

Severe TBI may lead to profound disability or even death, whereas moderate and mild forms of TBI can result in significant morbidity and disability (Khan et al., 2003). TBI can cause both short-term and long-term cognitive deficits. Characteristically, these deficits occur in attention, higher order executive functions, short-term memory and learning, speech and language functions and speed of information processing, reflecting the regions of the brain most vulnerable to TBI-induced damage (McAllister, 2011). Moderate to severe TBI causes enduring cognitive deficits, whereas deficits from mild TBI may resolve within months. However, persistent cognitive disturbances and neurobehavioural symptoms occur in up to 15-30% of mild TBI cases (reviewed in Shenton et al., 2012). Additionally, evidence suggests that (single or repetitive) TBI can lead to ongoing neurological decline including the development of conditions such as chronic traumatic encephalopathy (CTE) (Corsellis et al., 1973, Martland, 1928, McKee et al., 2009) and Alzheimer's disease (AD) (Mortimer et al., 1991, Fleminger et al., 2003).

1.2 The epidemiological link between traumatic brain injury and Alzheimer's disease

Several epidemiological studies have concluded that a history of TBI increases the risk of AD (Heyman et al., 1984, French et al., 1985, Sullivan et al., 1987, Graves et al., 1990, Mortimer et al., 1991, Mayeux et al., 1993, Kondo et al., 1994, Rasmusson et al., 1995, O'Meara et al., 1997, Schofield et al., 1997, Guo et al., 2000, Fleminger et al., 2003, Wang et al., 2012, Plassman et al., 2000), although others have shown no such relationship (Amaducci et al., 1986, Shalat et al., 1987, Chandra et al., 1989, Broe et al., 1990, Li et al., 1992, Fratiglioni et al., 1993, Tsolaki et al., 1997, Mehta et al., 1999, Launer et al., 1999). Many of these studies may be limited by small sample sizes and thus a lack of statistical power to detect an association (Button et al., 2013). In support of this notion, meta-analyses by Mortimer et al. (1991) and Fleminger et al. (2003) have both shown statistically significant associations between TBI and AD, but only for males. This increased risk of AD after TBI in males but not females is also reported in other independent studies (O'Meara et al., 1997, Salib and Hillier, 1997). Conversely, a study by Mayeux et al. (1993) has demonstrated an association between head injury and AD in females only, although it may have included insufficient males to detect an association. It is important to note, however, that TBI is three times more common in men than in women (Khan et al., 2003, Nemetz et al., 1999), which may be a confounding factor.

Another variable that may determine whether TBI increases an individual's risk of AD is injury severity. For example, epidemiological studies have variously defined TBI as head injury with loss of consciousness (LOC) (Fratiglioni et al., 1993, Mayeux et al., 1995), head injury with LOC >15 minutes (Broe et al., 1990), head injury requiring medical care and/or LOC (O'Meara et al., 1997) and head injury causing memory loss, confusion or coma (Amaducci et al., 1986). Plassman and colleagues demonstrated in a cohort of Navy and Marine veterans that moderate (LOC or post-traumatic amnesia > 30 minutes but < 24hrs) and severe (> 24 hours), but not mild (< 30 minutes), TBI increased the risk of AD (Plassman et al., 2000). Additionally, Schofield et al. (1997) found that TBI increased the odds of developing AD only if LOC is more than 5 minutes;

similarly, Guo et al. (2000) found that only TBI with LOC significantly increased AD risk. Thus, a particular level of injury severity may be required to initiate and/or accelerate the development of AD pathology.

Due to the identification of several risk factor genes in the development of AD, the interaction between genetics, TBI and AD has also been the focus of several studies. The strongest identified genetic risk factor for AD is the gene encoding apolipoprotein E (*APOE*), with inheritance of the *ε4* allele increasing the risk of developing the disease relative to the *ε3* allele (Pericak-Vance et al., 1991, Strittmatter et al., 1993). Studies have demonstrated that TBI is only significantly associated with AD in the presence of the *APOE ε4* allele (Mayeux et al., 1995, Katzman et al., 1996) and that there is a 10-fold increase in the risk of AD following TBI in association with the *ε4* allele (Mayeux et al., 1995). Additionally, it has been reported that the frequency of the ε*4* allele is higher in TBI cases with AD or mild cognitive impairment (MCI) compared to TBI cases without AD and TBI-/AD-free controls (Mauri et al., 2006). This suggests that TBI and *APOE ε4* may act synergistically in the development of AD. However, other studies have shown no additive or synergistic effects between *APOE* ε*4* and TBI in increasing the relative risk of AD (O'Meara et al., 1997, Mehta et al., 1999) and there is evidence that those lacking the *APOE* ε*4* allele are at a higher risk of developing AD following TBI compared to those carrying the allele (Guo et al., 2000, Jellinger et al., 2001a, Jellinger et al., 2001b).

Several studies have also shown that a family history of AD, which may indicate a genetic predisposition, does not augment the relative risk of developing the disease after TBI (Mayeux et al., 1995, Mortimer et al., 1991, Guo et al., 2000, van Duijn et al., 1992, Mayeux et al., 1993). Thus, TBI may instead be a risk factor for the more common sporadic form of AD. In contrast, a study by Nemetz et al. (1999) demonstrated there was no increase in the incidence of AD in a TBI cohort (as compared to a population-based incidence rate) however, the observed time to AD onset was significantly less than the expected time (as determined using a life table based on a TBI-free AD cohort) (Nemetz et al., 1999). This suggests that TBI may not necessarily increase the risk of developing AD, but might accelerate the disease process in predisposed individuals. However, studies

by Mortimer et al. (1991), Rasmusson et al. (1995) and Guo et al. (2000) showed no effect of TBI on the age of AD onset.

Overall, the epidemiological data indicates that TBI may increase the risk of developing AD (Fleminger et al., 2003, Mortimer et al., 1991) and may accelerate its onset in some cases (Nemetz et al., 1999). To elucidate the underlying mechanisms we must understand the pathology of TBI and AD, and how they may be related.

1.3 The pathology of Alzheimer's disease

AD is a neurodegenerative disorder causing progressive cognitive decline. The AD brain is characterised by three main pathological hallmarks: extracellular amyloid beta (Aβ) plaques, intracellular neurofibrillary tangles composed of hyperphosphorylated tau (Braak and Braak, 1991) and dystrophic neurites (Woodhouse et al., 2009, Dickson and Vickers, 2001). The Aβ peptide is derived from the proteolytic cleavage of a larger protein called the amyloid precursor protein (APP). Two proteolytic pathways exist by which APP can be processed: a non-amyloidogenic pathway where cleavage by α-secretase then γ-secretase produces the peptides sAPPα, p3 and the amyloid intracellular domain (AICD); and an amyloidogenic pathway in which cleavage by β-secretase then γ-secretase produces Aβ, sAPPβ and AICD. Several sites within APP can be cleaved by γ-secretase, producing Aβ peptides ranging from 38 to 43 amino acids in length, with Aβ40 and Aβ42 being the most common (reviewed by O'Brien and Wong, 2011).

Increased Aβ production via the amyloidogenic pathway is hypothesised to underlie, at least in part, the series of neurodegenerative changes associated with AD (Hardy & Allsop, 1991). Several mutations resulting in familial AD have been identified in the *APP* gene (Goate et al., 1991, reviewed in Bagyinszky et al., 2014). Many of these mutations are near the γ-secretase and β-secretase cleavage sites and cause aberrant processing of APP, leading to increased formation of Aβ (reviewed in Bagyinszky et al., 2014). Additionally, mutations in the genes presenilin 1 and 2 (PS1 and PS2), which are components of the γ-

secretase complex, also result in familial AD (reviewed in Bertram and Tanzi, 2008, Sherrington et al., 1995). These mutations cause increased production of the more amyloidogenic Aβ42 peptide relative to the Aβ40 peptide, leading to Aβ aggregation and plaque formation (Duff et al., 1996, Jankowsky et al., 2004).

The APP and thus Aβ protein sequence is highly conserved throughout species (Podlisny et al., 1991), however, the rodent Aβ sequence has 3 amino acid differences at residues 5, 10 and 13 (Yamada et al., 1987). Normally, a proportion of aged humans and mammals including primates, dogs, pigs and polar bears develop Aβ plaques (Selkoe et al., 1987, Johnstone et al., 1991) whereas aged rodents do not (Selkoe, 1989). Experimental evidence has demonstrated that rodent Aβ does not aggregate as readily as human Aβ (Kirschner et al., 1987, Kirkitadze et al., 2001, Otvos et al., 1993) and this may be why rodents do not form plaques with aging. Thus, to study the mechanisms of Aβ plaque formation and associated pathology, transgenic mouse models of Alzheimer's amyloidosis have been created. These mice typically overexpress human APP with familial AD mutations and develop plaques composed of human Aβ (Hall and Roberson, 2012).

1.4 The pathology of traumatic brain injury

Head trauma can result in two main forms of brain damage, focal and diffuse, however, both can occur simultaneously. Moderate and severe cases of TBI, involving severe direct impact to the brain, causes focal damage such as intracranial bleeds, lacerations and cortical and subcortical contusions (Andriessen et al., 2010, Adams et al., 1991). Diffuse injury, however, does not necessarily involve a direct hit to the head and thus can occur in mild, moderate and severe TBI's (Andriessen et al., 2010). Diffuse injury is multifocal and caused by the straining, shearing and compression of brain tissue (Adams et al., 1989, Adams et al., 1991, Strich, 1956, Holbourn, 1943, Holbourn, 1945, Strich and Oxon, 1961). This results in pathology such as diffuse axonal and vascular injury, brain swelling and hypoxic-ischemic injury (Andriessen et al., 2010). Diffuse axonal injury (DAI) is the most common pathology seen and occurs due to acceleration/deceleration forces on the brain causing shear stress to axons

(Adams et al., 1982, Gennarelli et al., 1982, Strich, 1956, Strich and Oxon, 1961).

Two common types of DAI that occur in brain injury are 'bulbs' and 'varicosities'. Axonal bulbs appear as a single large swelling, still in continuation with either the proximal (proximal axonal bulb) or the distal axonal segment (distal axonal bulb) (Hanell et al., 2014). Axonal varicosities are swellings that occur periodically along intact neurites (Hanell et al., 2014, Tang-Schomer et al., 2012). Both types of axonal pathology have been suggested to reflect the force distribution along the axon at the time of injury (Smith and Meaney, 2000). Varicosities are thought to occur in axons that have experienced a uniform strain along their length, whereas bulbs occur in axons that have undergone a highly localized area of strain, causing axonal disconnection (Smith and Meaney, 2000).

These swellings are caused by interrupted axonal transport, resulting in the accumulation of incompletely transported proteins and organelles (Tang-Schomer et al., 2010, Tang-Schomer et al., 2012). Such transport deficits may be due to the stretching of axons, which results in the breakage, disorganization and disassembly of microtubules, a component of the axonal cytoskeleton (Tang-Schomer et al., 2012, Tang-Schomer et al., 2010). The accumulation of proteins and organelles following progressive damage to the neuronal cytoskeleton may eventually lead to disconnection of the axon via secondary axotomy, subsequently forming an axonal bulb (Tang-Schomer et al., 2010, Smith and Meaney, 2000). It is believed that the disconnected distal axon will then undergo Wallerian degeneration (Smith and Meaney, 2000). However, in some axons there are periodic breaks of individual microtubules causing only partial interruption of axonal transport and the formation of varicosities (Tang-Schomer et al., 2012). It is possible that intact axons with varicosities may undergo repair if cytoskeletal integrity can be restored.

Although transport deficits and swellings do not occur in all axons, other important pathological changes induced by TBI can cause axonal dysfunction and/or degeneration. Diffuse brain injury can lead to the compaction of neurofilaments (NFs), another component of the axonal cytoskeleton (Povlishock

et al., 1997, Pettus et al., 1994). It has been proposed previously that NF compaction and microtubule disassembly were both parts of the same progressive pathology ultimately leading to impaired axonal transport (Povlishock and Pettus, 1996, Pettus et al., 1994). However, current evidence now suggests that, in the majority of injured axons, NF compaction is not associated with impaired axonal transport and swelling, and thus is a different injury phenotype (Stone et al., 2001, Marmarou et al., 2005).

TBI can also perturb the axonal ionic balance, including elevated intra-axonal sodium and calcium levels (Wolf et al., 2001, Kilinc et al., 2009). Elevated intra-axonal calcium levels can activate certain proteases, such as calpain (Kilinc et al., 2009, Iwata et al., 2004), which can damage the axonal cytoskeleton and ion channels (Iwata et al., 2004, Kilinc et al., 2009, McGinn et al., 2009). Additionally, TBI-induced oxidative stress and lipid peroxidation can cause cytoskeletal degradation and mitochondrial dysfunction in the axon (reviewed in Johnson et al., 2013b).

Enduring axonal pathology has been seen years after TBI (Chen et al., 2009). Axonal injury is a significant pathology in both TBI and AD and thus may be an important mechanistic link between these conditions.

1.5 Pathological links between traumatic brain injury and Alzheimer's disease

The axonal responses to TBI and AD are pathologically similar. Dystrophic neurites surrounding Aβ plaques have been shown to have accumulations of NF protein aggregates, organelles and tau (Stokin et al., 2005, Woodhouse et al., 2009, Dickson and Vickers, 2001). Furthermore, Stokin et al. (2005) found impaired axonal transport resulting in axonal swellings in both AD transgenic mouse models and early AD. These swellings occurred in areas of the brain devoid of amyloid and morphologically resembled those seen in axonal injury and senile plaque-associated dystrophic neurites (Stokin et al., 2005).

As mentioned previously, Aβ is cleaved from its precursor protein APP by the proteolytic enzymes γ-secretase (incorporating PS1) and β-secretase (BACE) (reviewed in O'Brien and Wong, 2011). Fast anterograde axonal transport, mediated by kinesin-I, traffics APP along with PS1 and BACE, during which APP may be cleaved to form Aβ (Kamal et al., 2001). Reducing kinesin-I in an AD mouse model has been shown to increase axonal swellings and overall levels and deposition of Aβ in the brain (Stokin et al., 2005). This indicates that impaired axonal transport could be an early initiating event in Aβ plaque development and the pathogenesis of AD. As TBI causes widespread axonal injury, including axonal transport deficits, this could be a mechanism by which TBI triggers Aβ plaque deposition and the development of AD.

1.5.1 Traumatic brain injury and intra-neuronal accumulation of APP

The accumulation of APP in axons following TBI is now well recognized as a pathological hallmark of axonal injury (Gentleman et al., 1993, Otsuka et al., 1991, Sherriff et al., 1994). Otsuka et al. (1991) first showed the accumulation of APP following a cortical stab wound injury in rats. APP immunoreactivity was demonstrated in dystrophic axonal swellings as early as 30 minutes post-injury and in glial cells resembling astrocytes at 3 hours post-injury (Otsuka et al., 1991). Shortly after, Gentleman et al. (1993) confirmed this result in human post-mortem brain tissue from cases of severe head injury. APP immunoreactivity was demonstrated in neuronal cell bodies and dystrophic neurites of the cortical grey matter and in damaged axons of the white matter (Gentleman et al., 1993).

The presence of APP within damaged axons has now been extensively described, in both human TBI cases (Gentleman et al., 1993, Sherriff et al., 1994, McKenzie et al., 1996) and multiple rodent TBI models, including mild compression contusion trauma (Lewen et al., 1995), fluid percussion injury (FPI) (Bramlett et al., 1997, Pierce et al., 1996, Iwata et al., 2002) and controlled cortical impact (CCI) injury (Ciallella et al., 2002). Extensive axonal APP accumulations are found in white matter following injury, matching the pattern of DAI detected by silver staining (Gentleman et al., 1993, Sherriff et al., 1994, McKenzie et al., 1996). Furthermore, these APP-immunoreactive axons demonstrate the features

of DAI, including undulating morphologies, varicose swellings and axonal end bulbs (Tang-Schomer et al., 2012).

In severe human TBI, axonal APP immunoreactivity is present as early as 35 minutes post-injury (Al-Sarraj et al., 2004), with the amount of immunoreactivity increasing with post-injury survival time (McKenzie et al., 1996). APP is present within axonal bulbs, which progressively increase in number and size post-injury (Sherriff et al., 1994, McKenzie et al., 1996). Additionally, axonal APP accumulations have been shown to persist for years after a single TBI, indicating ongoing axonal pathology and neurodegeneration (Roberts et al., 1994, Chen et al., 2009, Johnson et al., 2012). TBI does not need to be severe for this pathology to arise, with milder forms of non-fatal head injury in humans still showing APP accumulation within injured axons (Blumbergs et al., 1994). However, animal models have shown that as injury severity increases, so too does the number of APP-immunoreactive axonal swellings (Bramlett et al., 1997, Tran et al., 2011a).

Upregulation of APP mRNA and protein following TBI has been demonstrated in multiple experimental models, and is part of the acute response of the brain to trauma (Murakami et al., 1998, Van den Heuvel et al., 1999, Masumura et al., 2000, Ciallella et al., 2002). The function of APP is largely unknown, although APP's cleavage product sAPPα has been shown to be neuroprotective after TBI (Thornton et al., 2006). Additionally, the APP cleavage product, AICD, is proposed to be a transcriptional regulator (Rajendran and Annaert, 2012). Thus, following TBI, APP may be upregulated to exert a neuroprotective effect and/or regulate genes involved in the acute post-trauma reaction. Conversely, increased levels of APP in conjunction with its localized accumulation in axonal swellings, may lead to enhanced Aβ generation and accumulation.

1.5.2 Traumatic brain injury and intra-neuronal accumulation of beta-amyloid

In addition to APP, Aβ has also been shown to accumulate in neurons post-TBI. Axonal Aβ accumulations have been described in post-mortem brain samples from both short- and long-term TBI-survivors (Chen et al., 2009, Uryu et al.,

2007, Smith et al., 2003) as well as in animal models of TBI (Smith et al., 1999, Iwata et al., 2002, Chen et al., 2004, Abrahamson et al., 2006, Tran et al., 2011a, Tran et al., 2011b).

In animal models of TBI including parasagittal FPI (Iwata et al., 2002), rotational acceleration injury (Chen et al., 2004, Smith et al., 1999) and CCI (Abrahamson et al., 2006, Tran et al., 2011a, Tran et al., 2011b), Aβ accumulation has been demonstrated in axonal swellings and end bulbs in the injured cortex, pericontusional white matter, hippocampus and dentate gyrus. Additionally, Aβ has also been shown to accumulate within neuronal cell bodies of the cortex and the hippocampus (Iwata et al., 2002). Several studies have noted Aβ accumulation in axons and neurons after TBI in $APP^{NLh/NLh}$ (APPK670N/M671L knocked in to endogenous APP gene), 3xTg-AD (APPK670M/N671L, PSEN1M146L, TauP301L) and APP/PS1 (APPK595N/M596L, PSEN1dE9) transgenic mouse models of AD, but not in wild-type controls (Abrahamson et al., 2006, Tran et al., 2011a, Tran et al., 2011b). Notably, other groups have also shown this pathology in brain injured wild-type mice and rats (Iwata et al., 2002, Murai et al., 1998).

Accumulated intra-neuronal Aβ has been detected as early as one hour and as late as one year post-injury in animal models of TBI (Iwata et al., 2002, Tran et al., 2011b). The size and number of Aβ accumulations increases across the first 24 hours post-injury (Tran et al., 2011b) and the total number of Aβ-positive axonal swellings increases with injury severity (Tran et al., 2011a).

Following TBI, Aβ co-accumulates with APP, BACE and PS1 in axonal bulbs (Chen et al., 2009, Uryu et al., 2007), and amyloidogenic processing of APP is enhanced. For example, in a rodent CCI model, increased mRNA and protein expression of BACE-1 was seen in the ipsilateral cortex and hippocampus, along with elevated levels of its cleavage product sAPPβ (Blasko et al., 2004). An increase in Aβ production via BACE-1 APP cleavage has also been shown in 3xTg-AD mice following CCI injury. Thus, TBI appears to augment amyloidogenic processing of APP, leading to Aβ accumulation within injured

neuronal cell bodies and axons. Studies in both human AD cases and AD transgenic mouse models have demonstrated the accumulation of Aβ intraneuronally before the appearance of plaques (Takahashi et al., 2002, Billings et al., 2005, Gouras et al., 2000). Thus, the TBI-induced accumulation of Aβ may seed plaque formation if it is focally released into the brain parenchyma from axonal swellings or lysing cells. Relatedly, in a swine model of TBI, Aβ plaques were shown to be in close proximity to Aβ-positive axonal bulbs (Chen et al., 2009).

1.5.3 Beta-amyloid plaque deposition following traumatic brain injury

Numerous studies have shown the presence of Aβ plaques in the brain from hours up to years following TBI (Roberts et al., 1991, 1994, Nicoll et al., 1995, Smith et al., 2003, Ikonomovic et al., 2004, Uryu et al., 2007, DeKosky et al., 2007, Chen et al., 2009, Johnson et al., 2012). However, only about 30% of individuals dying after a severe TBI demonstrated Aβ plaques (Roberts et al., 1991, 1994), suggesting that other factors such as the location or type of TBI, as well as genetic background, may influence the development of plaques post-injury. The frequency of the *APOE ε4* allele has been shown to be significantly higher in a Aβ plaque-positive TBI group at post-mortem as compared to a plaque-negative TBI group (Nicoll et al., 1995). Furthermore, there was a gene-dose effect, with the proportion of TBI cases with Aβ deposits increasing with the number of *ε4* alleles (Nicoll et al., 1995).

Aβ plaques have been observed in cases of non-fatal TBI up to 47 years post-injury (Johnson et al., 2012). However, due to the advanced age of many of these cases, it is unclear whether the plaques were due to the TBI sustained or a product of pathological aging and/or prodromal AD. Johnson and colleagues (2012) described plaques in both TBI cases and age-matched controls (without a history of TBI, neurodegenerative or neurological disease), with no significant difference in the incidence of plaque pathology between the two groups (Johnson et al., 2012). Nevertheless, the density of plaques was higher in the TBI cases, and were often fibrillar, unlike control cases in which they were mostly diffuse

(Johnson et al., 2012) thus, TBI may have accelerated the progression of Aβ pathology.

Despite reports of TBI-induced Aβ deposition in individuals as young as 10 years old (Roberts et al., 1994), the ageing brain appears to be more vulnerable to Aβ plaque pathology post-injury. One study found that the incidence of plaques increased with advancing age in both TBI and control cohorts, however the TBI cohort had more plaques and a higher plaque-positivity rate than the control cohort (Roberts et al., 1994). This indicates that TBI and pathological aging may synergistically increase abnormal Aβ burden in the brain.

Recent advances in neuroimaging using carbon 11-labelled Pittsburgh compound B ([^{11}C]PiB) positron emission tomography (PET) allows researchers to detect Aβ deposits within the brains of living subjects following TBI. A significant increase in the [^{11}C]PiB distribution volume ratio was reported in the cortical grey matter of TBI patients within 1 year of their injury compared to controls, indicating the presence of Aβ deposits in these patients (Hong et al., 2014). [^{11}C]PiB imaging has also demonstrated that MCI and a history of head injury are associated with higher global brain amyloid levels compared to MCI with no history of head injury, although this association was not found in cognitively normal people with a history of head injury (Mielke et al., 2014), supporting the hypothesis that TBI may accelerate AD progression in predisposed individuals. These and future studies using this technique will provide evidence for a cause and effect mechanistic link between TBI and AD.

1.5.4 Beta-amyloid plaque deposition in animal models of traumatic brain injury

Despite studies demonstrating Aβ plaques in human cases of TBI, no non-transgenic rodent TBI models have recapitulated these findings (Pierce et al., 1996, Iwata et al., 2002, Bramlett et al., 1997, Ciallella et al., 2002, Masumura et al., 2000). Thus, to assess the relationship between TBI and AD, transgenic mouse models of Alzheimer's amyloidosis have served as a useful tool. The results of these studies, however, have been conflicting with increased (Uryu et

al., 2002), decreased (Nakagawa et al., 1999, Nakagawa et al., 2000) and no change in plaque pathology (Smith et al., 1998) reported following experimental TBI. Several factors have complicated the comparison of these studies, including the transgenic mouse model used, the age and stage of plaque deposition at the time of injury, the timepoints analysed post-injury and the severity and method of injury used. The most commonly used experimental TBI model for examining the effect of brain injury on Aβ plaque pathology is the CCI, however other models, including rotational acceleration injury and FPI have also been used. This injury involves the intact dura being hit at a certain depth and speed by a pneumatically or electromagnetically controlled piston (reviewed in Xiong et al., 2013). This model causes a primarily focal injury with elements of DAI to underlying white matter tracts (reviewed in Morales et al., 2005).

Many studies have focused on chronic changes in plaque burden or distribution after the usual onset of plaque deposition in injured AD-transgenic mice, and therefore reveal the effects of TBI on the progression of amyloidosis. Studies on PDAPP (APP V717F) mice subjected to CCI injury prior to the onset of amyloidosis have shown no change in the number or distribution of Aβ plaques at 2 months post-injury (Smith et al., 1998) but a decreased abundance of plaques when examined at 8 months post-injury (Nakagawa et al., 1999). Similarly, PDAPP mice with overt amyloidosis at the time of CCI injury had an ongoing reduction in plaques when examined from 1-16 weeks after injury (Nakagawa et al., 2000). In contrast to these studies, Uryu et al. (2002) demonstrated that both single and repetitive modified CCI prior to the onset of amyloidosis increases plaque burden at 16 weeks post-TBI in Tg2576 (APP K670M/N671L) mice, however repetitive injury was shown to increase plaque burden to a greater extent than single injury.

The effect of TBI on the onset of plaque pathology has also been examined in a number of different transgenic AD mouse models. For example, Tran and colleagues have demonstrated no Aβ plaque deposition at 1 to 24 hours or at 7 days after CCI injury in pre-plaque 3xTg-AD mice, or 24 hours after injury in pre-plaque APP/PS1 mice, despite extensive intra-axonal Aβ accumulation (Tran

et al., 2011a, Tran et al., 2011b). This indicates that although TBI can cause intra-axonal Aβ accumulation in mouse models of TBI, it does not cause Aβ plaque formation acutely after injury. A more recent study reported cloudy Aβ42-positive accumulations within the injured cortex of a pre-plaque 3xTg-AD mouse, 24 hours post-injury, although only in 1 of 7 mice examined (Washington et al., 2014).

Studies have also been performed using transgenic mouse models which do not spontaneously form Aβ plaques, including the YAC mouse which expresses wild-type human APP at levels 2-fold higher than endogenous mouse APP (Murai et al., 1998) and the $APP^{NLh/NLh}$ mouse which expresses mutant human APP at normal levels under the endogenous mouse APP promoter (Reaume et al., 1996). CCI injury was not sufficient to induce plaque formation in either $APP^{NLh/NLh}$ mice at 24 hours post-injury (Abrahamson et al., 2006) or YAC mice 1 week after injury (Murai et al., 1998).

Mouse models have also been used to determine the effect of APOE alleles on plaque deposition post-TBI. Hartman et al. (2002) performed CCI injury on PDAPP mice expressing human *APOE* ε4, human *APOE* ε3 or no *APOE* at 9-10 months of age. Three months after injury (12-13-months of age), all groups had Aβ-immunoreactive deposits, but only APOE ε4 expressing mice had thioflavine-S-positive deposits. Additionally, PDAPP APOE ε4 mice had significantly more Aβ-immunoreactive plaques in the molecular layer of the dentate gyrus compared to PDAPP APOE ε3 mice (Hartman et al., 2002). These results support the notion that APOE genotype may affect Aβ plaque dynamics and thus AD progression post-TBI.

Despite the lack of plaques observed in the brains of injured wild-type rodents, and the variable results demonstrated in injured transgenic AD mouse models, studies in swine have shown Aβ deposition similar to that seen in human TBI cases within days, and up to months, post-injury. Aβ plaque-like deposits were found in the grey and white matter of pigs following non-impact head rotational acceleration brain injury, although only in 30% of injured animals (Smith et al., 1999, Chen et al., 2004). This is in general accordance with human studies, in

which only 30% of TBI sufferers are shown to have Aβ deposits post TBI (Roberts et al., 1991, Roberts et al., 1994). Interestingly, the TBI-induced plaques were located in the white matter of pigs with the most extensive axonal pathology (Smith et al., 1999) suggesting a relationship between axonal injury and Aβ deposition. Additionally, some of these plaques were shown to be fibrillar in nature, staining with both thioflavin-S and Congo red (Chen et al., 2004). The amino acid sequence of the Aβ peptide in pigs is homologous to the human sequence, and thus these studies demonstrate that diffuse TBI can cause Aβ plaque-like aggregates in mammals with human Aβ (Johnstone et al., 1991).

From these studies it is apparent that TBI can affect Aβ plaque dynamics in animal models. Whether TBI results in increased or decreased plaque formation post-injury, and which factors may influence this effect, remain to be elucidated. The mechanism of Aβ deposition, source of Aβ and possible degradation of Aβ plaques by injury-activated glia and enzymes, all require further investigation and clarification. Animal models of experimental TBI will provide a useful platform for the continued investigation of post-injury plaque deposition.

1.6 Beta-amyloid clearance after traumatic brain injury

Following TBI, multiple mechanisms may contribute to clearance of accumulated Aβ. However, if clearance mechanisms are defective or become overwhelmed by the amount of Aβ produced, then initiation of the amyloid cascade and the development of AD may ensue. Mechanisms for Aβ removal after TBI may include enzymatic degradation by neprilysin (Iwata et al., 2000), phagocytosis by activated glia (Funato et al., 1998, Simard et al., 2006, Wyss-Coray et al., 2003a) and the more recently described glymphatic system (Iliff et al., 2012).

1.6.1 Neprilysin

Many enzymes within the brain can degrade Aβ, such as neprilysin, insulin-degrading enzyme, endothelin-converting enzymes, matrix metalloproteinases and plasmin (reviewed in Miners et al., 2008). Of these, neprilysin has been the

most extensively studied in TBI. Neprilysin is a cell-surface metalloendopeptidase (Turner et al., 2001) and is a major extracellular Aβ-degrading enzyme in the brain (Iwata et al., 2000). Polymorphisms in the neprilysin gene may increase the risk for AD (Helisalmi et al., 2004, Sakai et al., 2004, Shi et al., 2005) and reduced neprilysin mRNA and protein levels were observed in the AD brain (Yasojima et al., 2001), particularly in areas susceptible to Aβ plaques (Yasojima et al., 2001, Akiyama et al., 2001, Caccamo et al., 2005).

Studies in neprilysin-knockout mice have shown a gene-dose dependent increase in brain Aβ levels (Iwata et al., 2001). Furthermore, intracerebral injection of a lentiviral vector expressing human neprilysin decreases Aβ plaques by half in the treated hemisphere compared to the untreated hemisphere in AD transgenic mouse models (APPV717F and APP V717I/K670M/N671L) (Marr et al., 2003). These studies provide evidence that changes in the activity and levels of neprilysin in the brain may alter Aβ clearance, and thus could be an important determinant of Aβ plaque formation post-TBI. In support of this notion, a study by Chen and colleagues has demonstrated extensive neprilysin immunoreactivity in neurons and a virtual absence of Aβ plaques in long-term survival cases of TBI (1 month to 3 years) despite the presence of plaques in short-term survival cases of TBI (< 1 week survival) (Chen et al., 2009). This suggests that neprilysin up-regulation may be an Aβ removal mechanism in the brain following TBI.

As noted above, only 30% of TBI cases exhibit Aβ plaques (Johnson et al., 2012, Roberts et al., 1991, Roberts et al., 1994), suggesting that other factors such as genetics may influence post-TBI plaque deposition. The neprilysin gene has a 19-22 GT-repeat polymorphism in its promoter region (Sodeyama et al., 2001). Numerous studies (Wood et al., 2007, Lilius et al., 2003, Sodeyama et al., 2001) have examined whether this polymorphism alters the risk of developing AD, with the study by Sakai et al. (2004) showing a positive association. Accordingly, a study by Johnson et al. (2009) has demonstrated that the length of the neprilysin GT-repeat polymorphism affects acute post-TBI Aβ plaque deposition. Specifically, cases with more than 41 total repeats in two alleles, or

22 in at least one allele, had an increased risk for Aβ plaques after injury, whereas having 20 repeats in one allele was independently associated with reduced plaque deposition (Johnson et al., 2009).

These studies indicate that neprilysin may be important in post-injury Aβ degradation. Polymorphisms in the neprilysin gene (Sodeyama et al., 2001) and other factors affecting its expression and activity may increase susceptibility to AD following TBI.

1.6.2 Glia

Another possible mechanism of plaque removal post-TBI is via activated glia. TBI results in neuroinflammation characterized by the activation of microglia and astrocytes (reviewed in Kumar and Loane, 2012). Following activation, microglia proliferate and are recruited to the site of injury. Activated microglia can assume a phagocytic phenotype, and release cytokines and other soluble factors, which may be pro- or anti-inflammatory (reviewed in Loane and Byrnes, 2010).

In addition to microglial activation, peripheral macrophages migrate into the brain after injury (reviewed in Kumar and Loane, 2012). These macrophages are morphologically indistinguishable from microglia, and currently no markers exist to differentiate between them (Loane and Byrnes, 2010). Thus, studies of TBI may be examining either cell type and therefore, from herein, this chapter will refer to both cell types as microglia.

In response to the cytokines and molecules induced by TBI and produced by activated microglia, astrocytes become activated (astrogliosis) (reviewed in Zhang et al., 2010). Astrogliosis is characterized by the proliferation, migration and hypertrophy of astrocytes (reviewed in Sofroniew, 2009). Both microglia (Liu et al., 2010, Paresce et al., 1996) and astrocytes (Funato et al., 1998, Wyss-Coray et al., 2003a) have been shown to internalize Aβ. Thus, following TBI, activated microglia and astrocytes may phagocytose newly formed and accumulated Aβ. In support of this notion, Aβ-immunoreactive glial cells of

unidentified lineage have been shown in human TBI (Ikonomovic et al., 2004). Additionally, in animal models of TBI, microglia have been shown to be immunoreactive for Aβ (Chen et al., 2004) and the aforementioned Aβ-degrading enzyme, neprilysin (Chen et al., 2009).

Despite the ability of glia to remove Aβ from the brain (Funato et al., 1998, Liu et al., 2010, Paresce et al., 1996, Wyss-Coray et al., 2003a), they have also been demonstrated to have detrimental effects following TBI (Kumar and Loane, 2012, Parachikova et al., 2010). Neuroinflammation has been shown to persist chronically after TBI (Johnson et al., 2013a, Gentleman et al., 2004) and may cause neurodegeneration and the development of AD.

1.6.3 The glymphatic system

The glymphatic system is a brain-wide pathway used for the transport of fluid and the removal of interstitial solutes from the brain (Iliff et al., 2012). Subarachnoid cerebrospinal fluid (CSF) enters the brain interstitium via influx from the para-arterial space surrounding arteries, and interstitial fluid (ISF) is cleared into spaces around large-diameter draining veins (Iliff et al., 2012). The convective flow of CSF from the para-arterial space into the interstitium is facilitated by the water channel aquaporin 4 (AQP4), expressed on the astrocytic endfeet wrapping the space (Iliff et al., 2012). Waste products are forced away from arteries and towards the veins as the CSF and ISF exchange (Iliff et al., 2012). The ISF containing the waste products then enters the paravenous space and exits the brain (Iliff et al., 2012). This pathway is responsible for the removal of 40-80% of large proteins and solutes from the brain (Nedergaard, 2013). In addition to the glymphatic system, a lymphatic system has recently been identified in the brain (Louveau et al., 2015). Lymphatic vessels line the dural sinuses and transport immune cells and fluid from the CSF to the deep cervical lymph nodes (Louveau et al., 2015). It is suggested that these lymphatic vessels transport CSF to the periphery following drainage of ISF from the brain parenchyma to the CSF by the glymphatic system (Louveau et al., 2015).

AQP4 expression is highly polarized to the endfeet of astrocytes and AQP4 knock-out mice have a 70% reduction in the rate of interstitial solute clearance from the brain compared to wild-type mice (Iliff et al., 2012). Additionally, AQP4 deletion results in a 55% reduction in Aβ clearance from the brain (Iliff et al., 2012). AQP4-mediated glymphatic clearance is clearly important for the removal of soluble Aβ, and dysregulation of this pathway could potentiate post-TBI Aβ clearance following TBI, hence, leading to its accumulation.

TBI causes astrocytes to activate, changing their morphology and molecular make-up (reviewed in Sofroniew, 2009). Severe TBI can lead to the formation of a glial scar (reviewed in Sofroniew, 2009) whereas more moderate forms can cause widespread and long-lasting reactive astrogliosis, which has been observed up to 1 month post-injury (Ren et al., 2013). As AQP4 is expressed by astrocytes, alterations in its expression are common in TBI-induced reactive astrogliosis (Higashida et al., 2011, Marmarou et al., 2014). An investigation by Ren et al. (2013) of mild and moderate TBI found that up to 1 month following mild TBI, AQP4 expression in astrocytes localizes to the soma rather than the endfeet (Ren et al., 2013). This loss of AQP4 polarity could greatly impair the clearance of interstitial solutes, leading to the build-up of waste products and Aβ in the brain.

The ageing mouse brain has a reduced capacity to clear intraparenchymally injected Aβ, due in part to widespread astrogliosis and the loss of AQP4 perivascular polarization along penetrating arterioles (Kress et al., 2014). This reduced glymphatic capacity may potentiate age-related Aβ deposition in the brain. Reductions in glymphatic Aβ clearance due to ageing may also act synergistically with TBI to increase the Aβ burden in the brain. In support of this notion, a post-mortem study has shown that the number of plaque-positive TBI cases increase with advancing age (Roberts et al., 1994).

These studies demonstrate that the glymphatic system potentially plays an important role in the removal of Aβ from the interstitium of the brain. Following TBI, astrogliosis and the dysregulation of this system may result in reduced clearance of Aβ. Additionally, increased production of Aβ due to TBI-induced

changes in APP processing may overwhelm the capacity of the glymphatic system to remove Aβ.

1.7 Chronic traumatic encephalopathy

This review has concentrated on the effects of a single TBI on Aβ dynamics and the development of AD. However, repetitive brain trauma can cause the development of the neurodegenerative condition CTE, which shares many clinical and pathological features with AD (Corsellis et al., 1973, McKee et al., 2009). Clinical presentations of CTE include cognitive changes such as dementia, behavioural and psychiatric changes and Parkinson-like symptoms (McKee et al., 2009). Pathologically, CTE is characterized by brain atrophy, astrocytic tau tangles, TDP-43 accumulation as well as the pathological hallmarks of AD, tau-neurofibrillary tangles, and in some cases Aβ plaques (McKee et al., 2009, Stein et al., 2015, McKee et al., 2013). CTE is defined pathologically as a tauopathy, with the abnormal tau accumulations occurring primarily perivascularly and at the depths of the cortical sulci (McKee et al., 2009, McKee et al., 2013). This pattern of abnormal tau accumulation is distinct from other tauopathies, however, the neurofibrillary tangles and Aβ plaques are immunohistochemically identical to those seen in AD (McKee et al., 2009). Additionally, CTE frequently occurs in conjunction with other neurodegenerative disorders including AD (McKee et al., 2013). A recent study has characterized Aβ plaque deposition in CTE and has found that it occurs in approximately 50% of cases (Stein et al., 2015). Furthermore, its findings suggested that CTE with Aβ plaques is a more aggressive and distinct subtype of the disease, with a greater amount of tauopathy and worse clinical outcome (Stein et al., 2015). The overlap between CTE and AD suggests a common underlying pathogenesis between these neurodegenerative conditions.

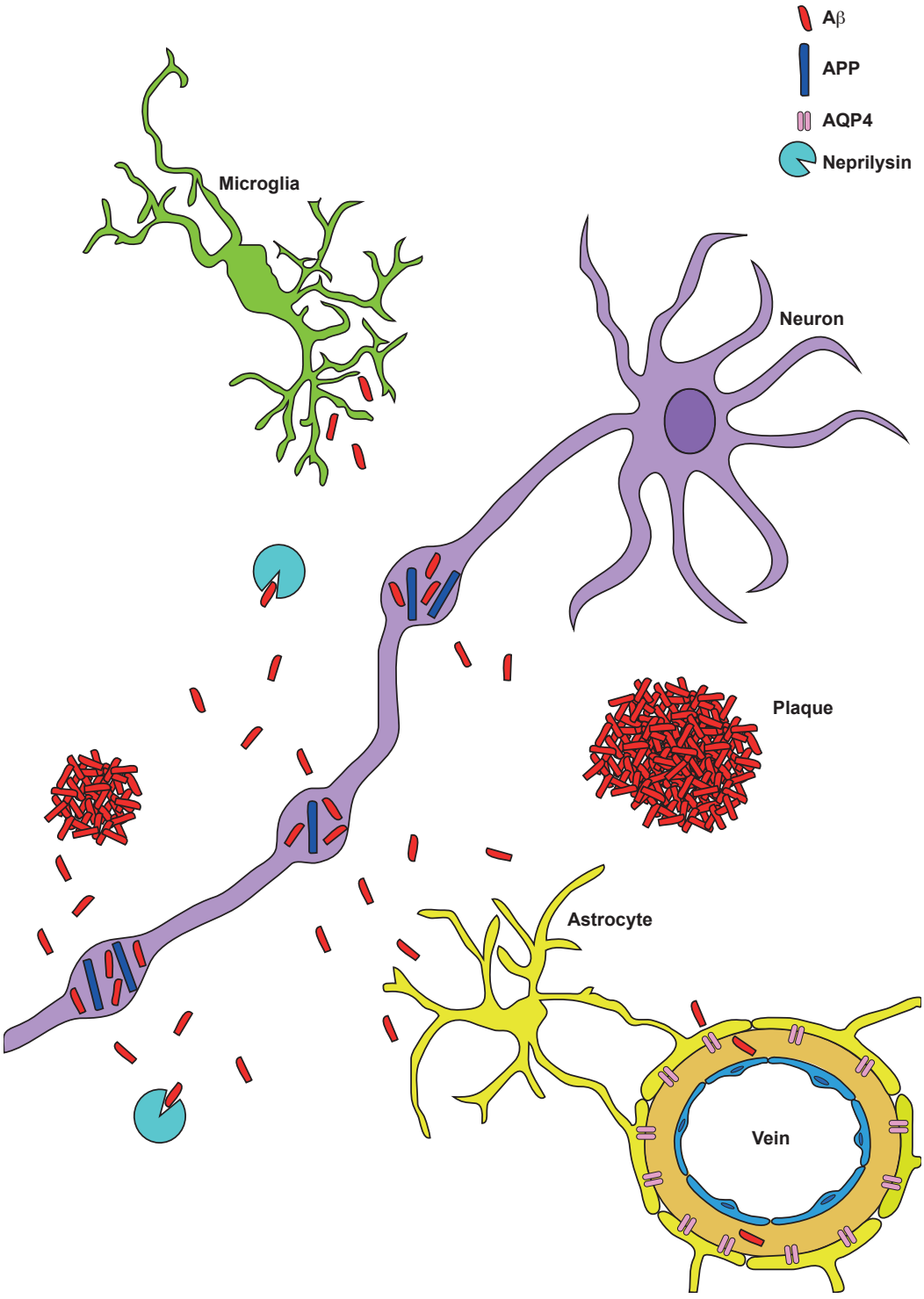

Figure 1.1 A β dynamics following TBI. TBI results in the accumulation of APP and A β within axonal swellings. Accumulated A β may then be released from the axon, into the brain parenchyma, if it undergoes degeneration and lyses. This A β may then aggregate forming plaques or be cleared via several mechanisms including: enzymatic degradation by neprilysin, phagocytosis by microglia and/or astrocytes and AQP4-mediated glymphatic clearance.

1.10 Project Aims

The balance of epidemiological and pathological studies supports the hypothesis that TBI is a risk factor for the development of AD, however, the cellular basis for this remains to be elucidated. Additionally, the effect of TBI on the onset and progression of AD pathology and the response of the brain to trauma in the setting of AD-associated neurodegeneration are unknown. Examining the underlying mechanisms by which TBI causes the development of AD will result in a greater understanding of the disease etiology, and may lead to the identification of therapeutic targets to intervene in the process. Thus, this thesis investigated how TBI affects Aβ plaque pathology dependent on the stage of amyloidosis at the time of injury, as well as how the brain responds to TBI in the setting of amyloidosis. The effect of alterations in the NF cytoskeleton on the axonal response to TBI was also evaluated.

For Aims 1 and 2 of this thesis the APP_{SWE}/PSENdE9 (APP/PS1) mouse model of AD was used, which replicates some, but not all, aspects of human AD. The APP/PS1 mouse model is an early Aβ plaque model (reviewed in Zahs and Ashe, 2010) and begins depositing a limited number of plaques at 4 months of age, and by 6 months of age, plaques are easily detectable (Garcia-Alloza et al., 2006, reviewed in Lee and Han, 2013). APP/PS1 mice develop behavioural deficits beginning around 6-8 months of age, but do not develop neurofibrillary tangles or overt neuronal loss and thus is a model of the pre-dementia phase of AD (reviewed in Lee and Han, 2013).

Aim 1: To determine the effect of focal brain injury on beta-amyloid plaque deposition, inflammation and synapses.

The effect of TBI on the onset and progression of Aβ plaque pathology is unclear. Additionally, the inflammatory and synaptic responses to TBI in the setting of amyloidosis are not well characterized. This aim assesses the effect of a focal brain injury model, which causes discrete structural brain damage without substantial secondary pathology, on Aβ plaque pathology in APP/PS1 transgenic AD mice. Three-month-old pre-plaque APP/PS1 mice, 9-month-old APP/PS1

mice with extensive Aβ plaque pathology and wild-type controls of the same ages were subjected to focal brain injury, immunohistochemical techniques were then used to examine Aβ plaque pathology, inflammation and synaptic changes.

Aim 2: To determine the effect of diffuse brain injury on beta-amyloid dynamics.

Aim 2 employed the lateral fluid percussion injury (LFPI) model to examine the effects of a clinically relevant model of diffuse TBI, with more widespread secondary pathology than the focal model of Aim 1, on Aβ plaque deposition. Three- and 6-month old APP/PS1 mice and 6-month-old wild-type mice were subjected to LFPI and immunohistochemical methods were used to assess plaque load, APP and Aß relative to axonal pathology and inflammatory changes.

Aim 3: To determine the effect of alterations to the neurofilament cytoskeleton on the axonal response to diffuse traumatic brain injury.

A significant pathology in TBI and a possible mechanism for TBI-induced Aβ plaque pathology is DAI. NFs have been proposed to be important in the mechanical strength of axons, which is vital in determining how an axon will respond to the forces imparted by TBI. Thus, aim 3 examines the effect of alterations in the NF cytoskeleton on the axonal response to diffuse TBI. Transgenic mice lacking the NF light chain gene (NFLKO) and wild-type mice were exposed to LFPI and the axonal response to injury was quantified by examining axonal APP accumulations. Furthermore, Western blotting was utilized to examine the expression of APP in NFLKO versus wild-type mice after TBI.

2 Materials and Methods

2.1 Mice

Animals were housed in standard conditions (20°C, 12/12hrs light/dark cycle), with access to food and water *ad libitum* and were monitored daily for signs of illness and stress. All experimental procedures were performed in accordance with the Australian Code of Practice for the Care and Use of Animals for Scientific Purposes and approved by the Animal Ethics Committee of the University of Tasmania (A12780, A13170).

2.2 Genotyping

Tail clippings removed from mice at weaning were incubated in 45ul of extraction solution (QUANTA Biosciences, cat no. 95091-025) for 30 minutes at 95°C to extract genomic DNA. Genotypes were then determined by standard PCR using the MyTaq^{TM} Red Mix (Bioline, cat no. BIO-25044) and primers (GeneWorks) to the different transgenes and to an internal control gene as per the manufacturer's protocol (refer to Chapter 3 section 3.2.2 and Chapter 5 section 5.2.2 for specific genotyping information). PCR products and a 100bp ladder (Hyperladder V, Bioline, BIO-33031) were then electrophoresed in a 2% agarose gel (Bioline, cat no. BIO-41025) with 0.0001% SYBR safe DNA gel stain (Invitrogen, cat.no S33102) at 120V for 35 minutes. Gels were then visualized using a Carestream 4000MM Pro image station.

2.3 *In vivo* model of focal brain injury

In vivo focal brain injury was performed as previously described (King et al., 2001). Following gas anesthesia (isoflurane 1-3%, 0.7 L/min), mice were given a subcutaneous injection of analgesic (Meloxicam, 5mg/kg) and immobilised in a Stoelting stereotaxic frame. A burr hole was then progressively drilled into the skull over the somatosensory cortex (3 mm lateral, 1 mm posterior to bregma) with frequent irrigation using 4°C 0.01M PBS (phosphate buffered saline) to cool the site. A 26 gauge needle was then lowered to a depth of 1 mm from the

top of the dura into the cortex and left *in situ* for 10 minutes before being removed and the wound sutured closed. Mice were left to recover on a heat pad set at 37°C until mobile and feeding.

2.4 *In vivo* model of diffuse traumatic brain injury

Mice were subjected to lateral fluid percussion brain injury (LFPI) or sham treatment, as described previously (Alder et al., 2011). Briefly, following anaesthesia with isoflurane, mice were given a subcutaneous injection of buprenorphine (Temgesic, 0.1mg/kg), and the scalp hair removed. Mice were then immobilised in a stereotaxic frame (Stoelting, USA). A midline scalp incision was made and bupivacaine (0.025%) was applied topically to the skull. The periosteum was removed with a scalpel blade and the area in the middle of the parietal plate was marked. A 1mm disk of whipper snipper line was attached to the skull over the mark with cyanoacrylate glue and surgical glue (Vetbond, 3M, USA) was applied to the skull to stabilize the sutures and hold the surrounding skin away from the craniotomy site. Using the whipper snipper line as a guide, a craniotomy was performed using a 3mm (outside diameter) trephine attached to a handheld drill. The drilling was done slowly with frequent irrigation with 4°C artificial CSF, to cool the skull, remove bone dust and to help release the skull bone from the underlying dura. The bone flap was then gently pulled from the underlying dura, leaving it intact. An injury hub (a sterile Luer-Loc syringe hub cut from a 23 gauge needle) was affixed to the skull using Loctite glue and dental cement and then filled with sterile saline. Mice were then allowed to recover for 2 hours prior to induction of injury. Injury was induced using a fluid percussion device connected to a pressure measurement instrument (American Scientific Model FP 302). The animal was re-anaesthetised, the hub filled with sterile saline and connected to the fluid filled tube of the injury device. Anaesthesia was then removed and the mouse allowed to recover until a breathing pattern indicative of light anaesthesia (but not full consciousness) was gained. The pendulum of the device was then released transmitting a fluid pressure pulse to the intact dural surface. The injury induced was of a mild to moderate severity (1.25-1.35 atm). The mice were then removed from the injury device, re-anaesthetised with isoflurane and placed back into the stereotaxic

frame. The injury hub was removed, the injury site examined and then the skin sutured closed. Sham surgeries were performed in the same manner, omitting release of the pendulum.

2.5 Tissue preparation

Mice were terminally anesthetized with sodium pentobarbitone (110mg/kg delivered intraperitoneally) and transcardially perfused with 4% paraformaldehyde in 0.01M PBS for immunohistochemical studies and in 0.01M PBS for biochemical studies. Tissue was then dissected immediately and post-fixed for 24 hours in 4% paraformaldehyde in 0.01M PBS for immunohistochemical studies or snap frozen in liquid nitrogen and stored at -80°C for biochemical analyses.

2.6 Immunohistochemistry and histological staining

2.6.1 Indirect fluorescent immunohistochemistry

Free-floating brain sections were incubated 3 × 10 minutes in 0.01M PBS with 0.25% Triton-X-100 followed by Dako serum-free protein block (Dako, cat no. X0909) for 15 minutes at room temperature. Sections were then immunolabelled with combinations of mouse monoclonal and rabbit polyclonal primary antibodies diluted in 0.01M PBS with 0.3% Triton-X-100, for 1 hour at room temperature then overnight at 4°C. Following incubation in primary antibodies, sections were washed in 0.01M PBS with 0.25% Triton-X-100 6 × 10 minutes. Primary antibody labelling was visualized by incubation in Alexa-fluorophore conjugated secondary antibodies (Molecular Probes) diluted in 0.01M PBS with 0.3% Triton-X-100 at 1:1000 for 2 hours at room temperature. Following incubation in secondary antibodies, sections without thioflavin-S staining were incubated in a solution of 4',6-diamidino-2-phenylindole (DAPI, 5µg/ml, Invitrogen, cat no. D3571) for 10 minutes at room temperature prior to washing. Sections were then washed 3 × 10 minutes in 0.01M PBS with 0.25% Triton-X-100, once in 0.01M PBS, and mounted used Dako fluorescent mounting medium (Dako, cat no. 53023).

2.6.2 Formic acid antigen retrieval

For MOAB-2 Aβ plaque labelling, formic acid antigen retrieval was performed. Sections were incubated in 88% formic acid (Sigma-Aldrich, cat no. 399388-500ML, lot. 06098KJ) for 8 minutes at room temperature and then washed in 0.01M PBS 6 x 5 minutes. Immunohistochemistry was then performed as described.

2.6.3 Thioflavin-S staining

Thioflavin-S (Sigma-Aldrich, cat no. T-1892, lot. 123H0598) staining was also used to determine Aβ plaque load. This stain labels a subset of fibrillar and dense-core plaques that are composed of Aβ with a β-pleated sheet conformation (Dickson and Vickers, 2001, Lindgren and Hammarstrom, 2010). Brain sections were incubated in thioflavine-S solution (0.125% thioflavine-S diluted in 60% absolute ethanol, 40% 0.01M PBS) for 3 minutes at room temperature. Sections were then washed 2 × 1 minute in a 50% absolute ethanol in 50% 0.01M PBS solution followed by 3 × 5 minute washes in 0.01M PBS. Immunohistochemistry was then performed as outlined above.

2.7 Western Blotting

2.7.1 Protein extraction

Frozen brain tissue was transferred immediately into 250ul of RIPA buffer (Sigma-Aldrich, R0278-50mL) with protease (Complete Mini Protease Inhibitor Cocktail tablets Roche, cat no. 11 836 153 001) and phosphatase inhibitors (Phosphatase Inhibitor Cocktail, A.G. Scientific, Inc., P-1549) and homogenized using an UltraTurrax. Homogenates were then incubated with shaking for 30 minutes at 4°C followed by centrifugation at 13000rpm for 15 minutes at 4°C. The supernatant was then transferred to a clean tube and the pellet discarded. Protein concentration was then determined by performing a Bradford assay as per manufacturer's protocol (BioRad Protein Assay, BioRad, 500-006)

2.7.2 Gel electrophoresis and Western Blot

Gel electrophoresis was performed as per the manufacturer's protocols (Life Technologies). Bolt® 4×Lithium dodecyl sulphate (LDS) sample buffer (Life Technologies, cat no. B0007) and 10× Bolt® Sample reducing buffer (Life Technologies, cat no. B0009) were added to the protein samples and the samples heated at 80°C for 10 minutes. The samples were then loaded onto 4-12% Bolt® Bis-TRIS Plus gels (Life Technologies, cat no. NW04125BOX) and electrophoresed at 200V for 20 minutes in Bolt® MES running buffer (Life Technologies, cat no. B0002). The gels were then transferred at 20V for 1 hour at 4°C in Bolt® Transfer buffer (Life Technologies, BT0006) to 0.2µm PVDF membranes (BioRad, cat no. 162-0177) and blocked in 5% skim milk powder in Tris-buffered saline with 0.1% Tween-20 (TBST). The membranes were then incubated in the primary antibodies in 5% skim milk powder in TBST for 2 hours at room temperature, washed 3 × 10 minutes in TBST and then incubated in a HRP-conjugated antibody (goat anti-mouse HRP, Dako, cat no. P0447; goat anti-rabbit HRP Dako, cat no.P0448) at 1/7000 diluted in 5% skim milk powder in TBST for 2 hours at room temperature. The Immobilon™ chemiluminescent HRP Substrate (Millipore cat no. WBKL50500) was then used to detect immunoreactivity and images were captured using a Carestream 4000MM Pro image station. A pre-stained molecular ladder (Thermo Scientific, cat no. 26619, lot. 00188551) was used to determine the molecular weights of immunoreactive bands.

Table 2.1 Primary antibody information

Name	Species	Immunogen/ Immunoreactivity	Application	Concentration	Company	Catalogue Number
6E10	M IgG1	Amino acids 1-16 of Aβ. Labels Aβ40 and Aβ42 and APP.	Immuno WB	1/1000 1/5000	Covance	SIG-39320
APP C-Terminal	R	C-terminal of human APP amino acid 676-695.	Immuno	1/1000	Sigma	A8717
APP	R	C-terminal human and mouse APP.	WB	1/1000	Invitrogen	36-6900
AT8	M IgG1	Human paired helical filament-tau (phosphoSer202/ phosphoThr205).	Immuno	1/1000	Thermo Fisher Scientific	MN1020
GAPDH	M IgG1	Glyceraldehyde-3-phosphate dehydrogenase.	WB	1/5000	Millipore	MAB374
GFAP	R	Human brain glial fibrillary acidic protein. Labels astrocytes.	Immuno	1/2000	Dako	20334
Iba-1	R	Ionized calcium binding adaptor molecule 1. Labels microglia and macrophages.	Immuno	1/1000	Wako	019-19741
MOAB-2	M IgG2b	N-terminus of Aβ (amino acids 1-4). Labels Aβ40 and Aβ42 (not APP).	Immuno WB	1/2000 1/5000	Novus Biologicals	NBP2-13075
SMI-32	M IgG1	A non-phosphorylated epitope in NFH. Visualises neuronal cell bodies, dendrites and some thick axons.	Immuno	1/2000	Covance	SMI-32P
SMI-312	M IgG1 cocktail	Phosphorylated neurofilaments. Visualises axons.	Immuno	1/2000	Covance	SMI-312R
Synaptophysin	R	Synaptophysin.	Immuno	1/200	Millipore	AB9272

M, mouse; R, rabbit; Immuno, Immunohistochemistry; WB, Western blotting.

Table 2.2 Secondary antibody information

Emission (nm)	Reactivity	Species	Dilution	Supplier, Catalogue Number
488	M IgG1	G	1/1000	Molecular Probes, A-21121
546	M IgG2b	G	1/1000	Molecular Probes, A-21143
488	M IgG	G	1/1000	Molecular Probes, A-11034
546	R IgG	G	1/1000	Molecular Probes, A-11035
594	R IgG	G	1/1000	Molecular Probes, A-11037

M, mouse; R, rabbit; G, goat.

3 The effect of focal brain injury on Aβ plaque deposition, inflammation and synapses

3.1 Introduction

As discussed in Chapter 1, previous studies in AD mouse models have demonstrated that the effect of TBI on the onset and progression of Aβ plaque deposition is complex and not completely understood. The influence of TBI on Aβ plaque dynamics may differ depending on the stage of amyloidosis in the model at the time of injury as well as the type of injury model used. Thus, the present study aimed to investigate the effects of a focal cortical brain injury on Aβ plaque deposition in a transgenic mouse model of AD at stages before the onset of plaque deposition and mid-way into deposition. It also investigated, in the setting of increased APP production and amyloidosis, whether the microglial, astrocytic and synaptic responses to brain injury were altered by comparing transgenic APP/PS1 mice to WT mice of the same genetic background.

The focal model of brain injury used in this study involved the acute insertion of a fine gauge needle through a small craniotomy to induce a discrete lesion to the somatosensory cortex. This injury model was selected to provide a localized model of structural brain damage, with a less substantial distribution of secondary pathology (eg oedema, inflammatory changes, diffuse axonal injury) relative to fluid percussion or impact models. The focal brain injury model has been well described and involves a relatively well-defined sequence of cellular changes, including the localized proliferation and infiltration of glial cells, tissue remodeling, glial scar formation and neovascularization with minimal tissue destruction and loss (King et al., 2001, Blizzard et al., 2011, Carbonell et al., 2005). This model therefore permitted the examination of local changes in Aβ plaque deposition, inflammation and synapses surrounding the injury site by immunohistochemical techniques.

3.2 Materials and Methods

3.2.1 Mice

All experimental procedures utilized male APP_{SWE}/PSENdE9 (APP/PS1) (Jankowsky et al., 2001) and C57BL/6 wild-type (WT) littermate control mice at either 3- or 9-months of age.

3.2.2 Genotyping

Genotyping was performed as outlined in the Material and Methods section 2.2. To detect the presence of the APP and PS1 transgenes, primers to the PS1 gene were utilized and primers to the IL-2 were used as an internal control. The primers sequences and expected product sizes are outlined in Table 3.1.

Table 3.1 Primers sequences and expected product sizes.

Gene	Primer sequence	Product Size (bp)
PS1	forward 5'-AATAGAGAACGGCAGGAGCA-3' reverse 5'-GCCATGAGGGCACTAATCAT-3'	608
IL-2	Forward 5'-CTAGGCCACAGAATTGAAAGATCT-3' reverse 5'-GTAGGTGGAAATTCTAGCATCATCC-3'	324

3.2.3 In vivo model of focal brain injury

Three- and 9-month-old APP/PS1 and WT controls (n=3-4 mice per group, per time-point, 52 total) were subjected to focal brain injury or sham treatment (surgery omitting the injury) as outlined in the Materials and Methods section 2.3.

3.2.4 Tissue preparation

Mice were terminally anaesthetized, transcardially perfused and tissue was prepared for either immunohistochemistry or Western blotting as outlined in the Materials and Methods section 2.5.

3.2.5 Protein extraction Western Blotting

Protein extraction and Western blotting with the MOAB-2 and 6E10 antibodies was performed as outlined in the Materials and Methods section 2.7 (refer to Table 2.1 in the Materials and Methods section for antibody concentrations. For each sample 30μg of protein was loaded onto the gel.

3.2.6 Immunohistochemistry

For immunohistochemical studies, mice were terminally anesthetized and transcardially perfused at either 24 hours or 7 days post-injury as outlined in the Materials and Methods section 2.5. Serial 50μm tangential sections were then cut on a vibratome (Leica VT1000). In each animal 10 tangential sections were obtained from the injury site, numbered from the dura inwards, which were labelled for MOAB-2 (3,6,8,10), thioflavine-S (4,9), Iba-1 (6,10), GFAP (7) and synaptophysin (3) as outlined in the Materials and Methods section 2.6. For MOAB-2 Aβ plaque labelling, formic acid antigen retrieval was performed as outlined in the Materials and Methods section 2.6.2. For immunolabelling of fibrillar Aβ deposits, thioflavin-S was used and for all Aβ, and the recently characterized antibody MOAB-2, was used to label mouse and human unaggregated, oligomeric and fibrillar forms of Aβ42 and unaggregated forms of Aβ40, but not APP from either species (Youmans et al., 2012a, Youmans et al., 2012b, Perez et al., 2013, Katsouri et al., 2014, Zhao et al., 2014a, Zhao et al., 2014b), was used. This antibody has previously been demonstrated to have strong intra-neuronal and extra-cellular immunoreactivity for Aβ in the 3×Tg (APP_{SWE}, $MAPT_{P301L}$, $PSEN1_{M146V}$) mouse model of AD (Youmans et al., 2012a). We therefore used brain tissue from 3×Tg mice as a positive control for intra-neuronal Aβ labelling. The antibody SMI-32 which labels non-phosphorylated epitopes in neurofilament M and H was used to label a subset of neurons (Goldstein et al., 1983). For assessment of the microglial response and synaptic changes, the antibodies anti-Iba-1 and anti-synaptophysin were used, respectively. The astrocytic response was examined using the GFAP antibody and the AT8 antibody against hyperphosphorylated tau was used to assess the presence of abnormal tau processing after injury.

3.2.7 Confocal microscopy and quantification

Imaging was performed on a Perkin-Elmer Ultraview VOX confocal imaging system using Volocity 6.3 software for image capture and processing. For each analysis, all images were acquired with the same laser power and exposure settings. Plaque loads (percentage area thioflavin-S or MOAB-2 positive) were calculated for a 2000x2000μm field of view (20× objective) encompassing the injury site, or corresponding area in the sham, from 2 × thioflavin-S stained and 4 × MOAB-2 immunolabelled sections per mouse. The Multithresholder plug-in on ImageJ (NIH, v1.46) was used to automatically segment the image (RenyiEntropy method for thioflavine-S and GFAP, Li method for MOAB-2 and Iba-1). The percentage area of Iba-1 labelling was calculated for a 500×500μm area (20× objective) of the injury site or the corresponding site in the sham on 2 sections per mouse. Similarly the percentage area for GFAP labelling was calculated for a 1000×1000μm (20× objective) of the injury site or the corresponding site in the sham on 1 section per mouse. For quantification of synaptophysin labelling, 2 images were taken "near" (60μm) and "distant" (120μm) to the injury site per section (60× objective). Using ImageJ, blinded to case type, images were Gaussian blurred (σ =1) and thresholded at the same level, before puncta were identified using a watershed plugin (http://bigwww.epfl.ch/sage/soft/watershed) as previously described (Mitew et al., 2013a). Synaptophysin positive puncta between 0.15-1.5μm^2 were assessed and the number of boutons counted per field (synaptophysin density) and the percentage area covered was recorded.

3.2.8 Statistical analysis

All data was analyzed using IBM SPSS Statistics (Version 19). For thioflavin-S and MOAB-2 plaque load data, a two-way analysis of variance (ANOVA) model with the factor variables treatment (injury, sham) and post-treatment time (24 hours, 7 days) was used. The microglial data was examined using ANOVA for the main effects of the four factor variables: treatment (injury and sham), post-treatment time (24 hours and 7 days), age (3 months and 9 months) and genotype (APP/PS1 and WT). A full factorial ANOVA was then used to test for

interactions between the variables. The synaptophysin data was also analyzed using ANOVA methods for the main effects of the four factor variables: treatment (injury and sham), post-treatment time (24 hours and 7 days), distance from injury site (near and distant) and genotype (APP/PS1 and WT), followed by a full factorial ANOVA. All data is reported as means ± standard error of the mean (SEM), with significance set at $p<0.05$ and estimates of effect size (partial η^2) reported for significant effects.

3.3 Results

3.3.1 Verification of the MOAB-2 antibody

To confirm the specificity and labelling pattern of the MOAB-2 antibody, we performed co-labelling with the commonly used anti-Aβ antibody 6E10 in APP/PS1 mouse brain tissue (see Figure 3.1A). Western blotting was also performed on 9-month-old APP/PS1 and WT cortical tissue to ensure the MOAB-2 antibody was specific for Aβ and did not cross-react with full length APP (Figure 3.1B).

3.3.2 Aβ plaque load in 3-month-old APP/PS1 mice

Three-month-old APP/PS1 mice were used to examine the effects of focal brain injury on plaque deposition prior to the onset of frank amyloidosis. A very small number of MOAB-2 positive Aβ plaques were present in sections from injured and sham APP/PS1 mice at both 24 hours and 7 days post-injury. No change in plaque deposition was detected in injured mice compared to sham mice following focal brain injury at either 24 hours or 7 days post-injury (Figure 3.2). Although plaques were present in the brains of these mice, they were rare in the area used for quantification, and so plaque load was not quantified. Furthermore, no intra-neuronal or intra-axonal accumulations of MOAB-2 labelled Aβ were detected at any time-point (Figure 3.2). As the MOAB-2 antibody has been shown previously to label intra-neuronal Aβ in 3×Tg mice (Youmans et al., 2012a), we used brain tissue from these mice as a positive control. MOAB-2 labelled intra-neuronal Aβ in the brain tissue of 3×Tg mice as expected (Figure 3.2).

3.3.3 Aβ plaque load in 9-month-old APP/PS1 mice

Nine-month-old APP/PS1 mice had established amyloidosis, with plaques that labelled with both thioflavin-S and the Aβ antibody, MOAB-2. Following focal brain injury the thioflavin-S plaque load surrounding the injury site was not significantly different ($p>0.05$) to the corresponding area in sham mice at either

Figure 3.1 Verification of the MOAB-2 antibody. (A) Co-immunolabelling with MOAB-2 and 6E10 in 9-month-old APP/PS1 cortex. MOAB-2 (red) and 6E10 (green) plaque labelling co-localised. Scale bar = 200μm. (B) MOAB-2 and 6E10 immunoblots of cortical brain samples from 9-month-old APP/PS1 and WT mice. MOAB-2 and 6E10 both labelled Aβ and only 6E10 labelled APP.

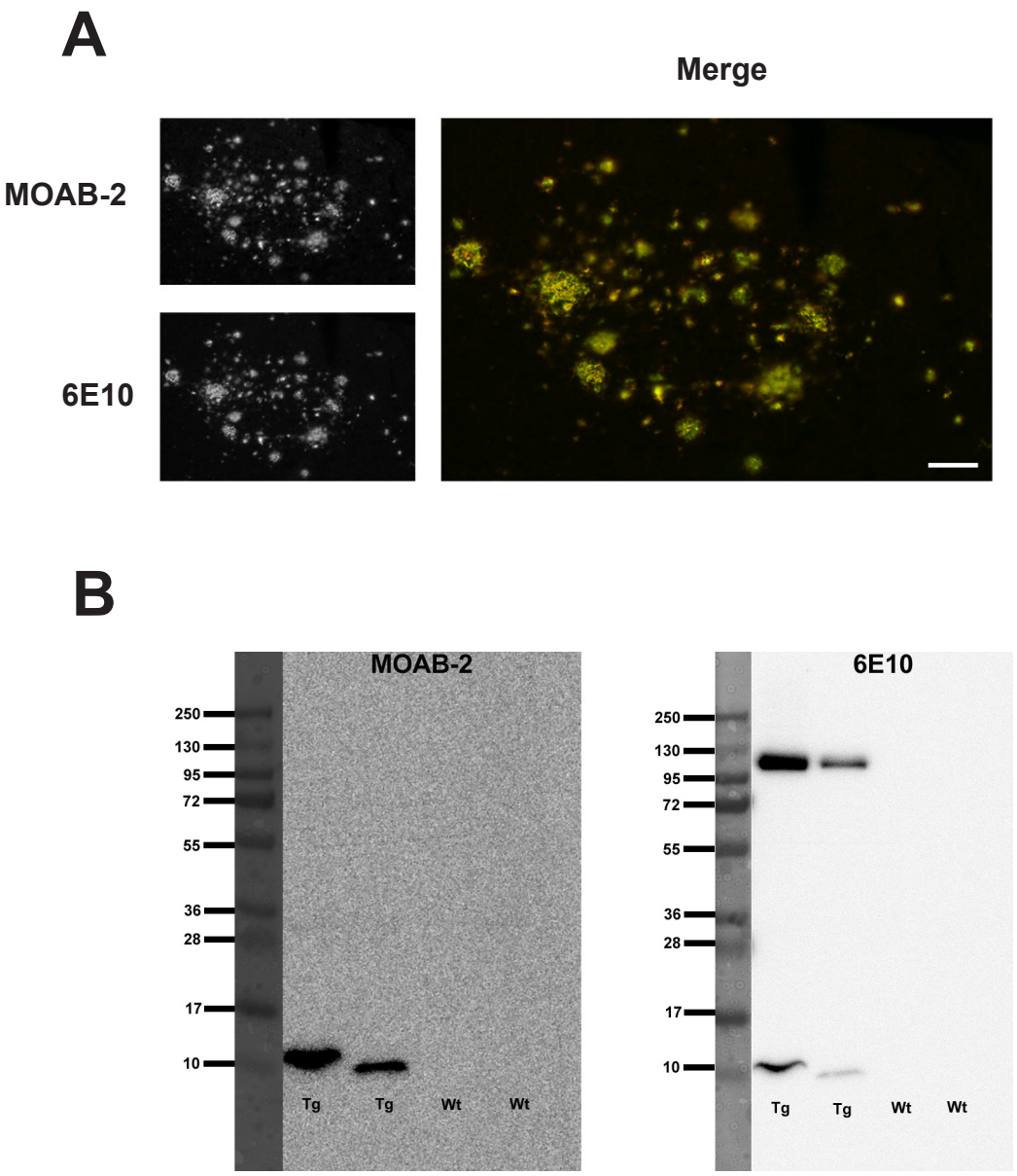
A
Merge
MOAB-2
6E10
B
MOAB-2
6E10
250
130
95
72
55
36
28
17
10
Tg
Tg
Wt
Wt

Figure 3.2 Focal brain injury does not induce intra-neuronal Aβ accumulations in 3- or 9-month-old APP/PS1 mice, or Aβ plaques in 3-month-old mice at 24 hours or 7 days post-injury. 3xTg tissue was used as a positive control for intra-neuronal Aβ. Representative sections labelled with the Aβ antibody MOAB-2 (red), the neuronal antibody SMI-32 (green) and the nuclei marker DAPI (blue). Aβ plaques can be seen in 9-month-old injured mice, but no intra-neuronal or intra-axonal Aβ accumulation can be seen. * Marks the injury site. Scale Bar = 50μm.

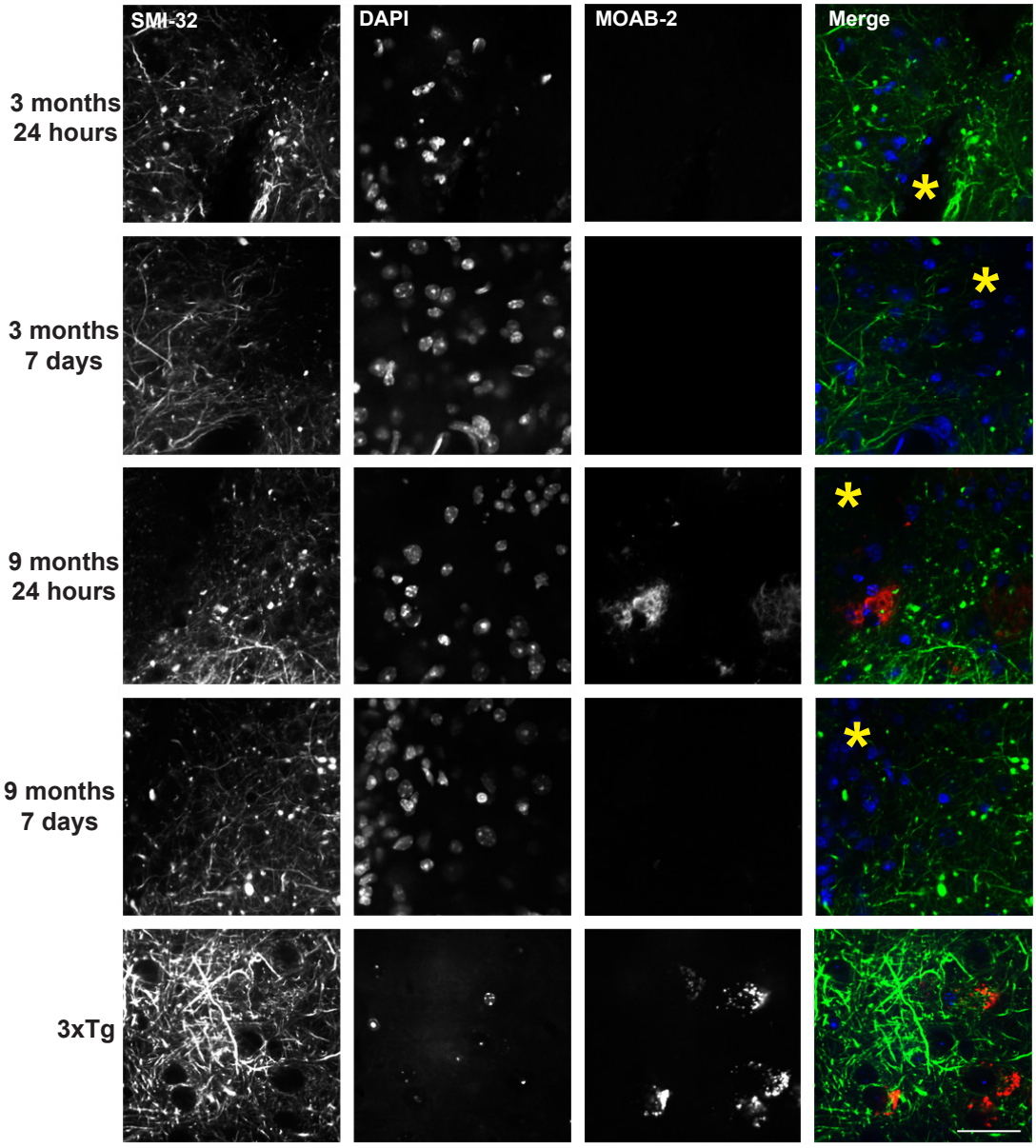
SMI-32
DAPI
MOAB-2
Merge
3 months
24 hours
3 months
7 days
9 months
24 hours
9 months
7 days
3xTg

24 hours (0.09 ± 0.02% vs 0.10 ± 0.04%) or 7 days (0.14 ± 0.07% vs 0.08 ± 0.02%) post-injury (Figures 3.3A and B). The MOAB-2 plaque load surrounding the injury site in APP/PS1 mice was also not significantly different ($p>0.05$) to the corresponding area in sham mice at either 24 hours (3.72 ± 0.99% vs 3.03 ± 0.55%) or 7 days post-injury (2.71 ± 0.40% vs 2.70 ± 0.23%) (Figures 3.3A and B). Additionally, no intra-neuronal or intra-axonal accumulations of Aβ were observed in injured or sham brains at either time-point stained with thioflavin-S or MOAB-2 (Figure 3.2).

3.3.4 Aβ plaque dynamics in wild-type mice

Focal injuries in WT mice were also examined with MOAB-2 and thioflavin-S staining. As expected, no plaques were present at either 24 hours or 7 days post-injury in sections from WT mice injured at either 3- or 9-months of age (Figure 3.4). Furthermore, no intra-neuronal or intra-axonal accumulations of Aβ were detected at either time-point (Figure 3.4).

3.3.5 Hyperphosphorylated tau

As previously described in other transgenic mouse models of AD (Woodhouse et al., 2009), AT8-immunoreactivity was detected in a subset of dystrophic neurites surrounding Aβ plaques in APP/PS1 mice (Figure 3.5). However, no AT8-immunoreactivity was detected around the injury site in either APP/PS1 or WT mice (Figure 3.5).

3.3.6 Microglial/macrophage response

The microglial/macrophage response following focal cortical brain injury was examined at 24 hours and 7 days post-injury in 3- and 9-month-old WT and APP/PS1 mice. The sham treatment did not cause visible microglial proliferation and/or activation at either 24 hours or 7 days post-injury (Figure 3.6A). The percentage areas occupied by Iba-1-positive microglia/macrophages are presented in Table 3.2. There was a significant main effect of treatment [$F(1,47) = 72.2$, $p<0.001$, partial $\eta^2 = 0.61$] with injury increasing the percentage area

Figure 3.3 Focal brain injury does not effect Aβ plaque deposition in 9-month-old APP/PS1 mice. (A) Representative sections stained with thioflavin-S or labelled with the Aβ antibody MOAB-2. Dotted yellow line indicates injury site. Scale bar = 200μm. (B) There was no significant difference ($p>0.05$) in thioflavin-S plaque load between injured and sham APP/PS1 mice at either 24 hours or 7 days post-injury. (C) There was no significant difference ($p>0.05$) in MOAB-2 plaque load between injured and sham APP/PS1 mice at either 24 hours or 7 days post-injury. Bars represent mean ± standard error.

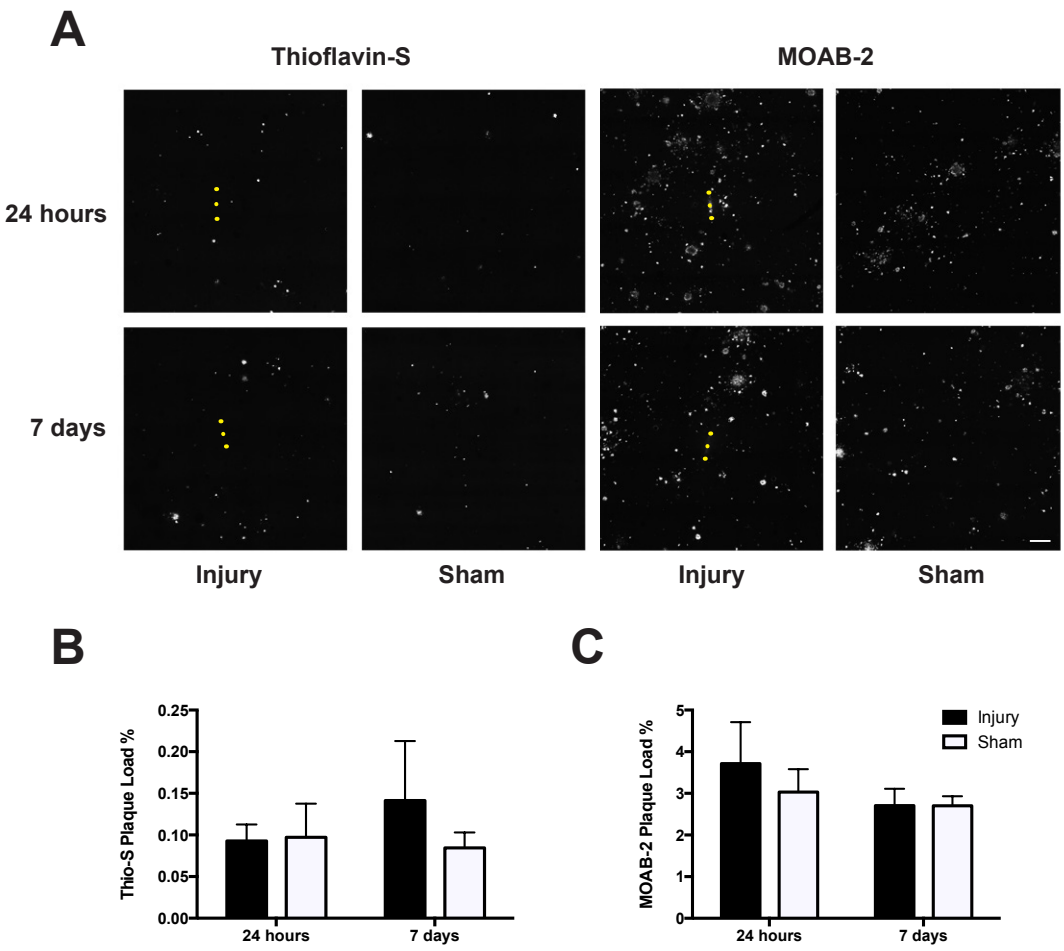
A
Thioflavin-S
MOAB-2
24 hours
7 days
Injury
Sham
Injury
Sham
B
Thio-S Plaque Load %
0.25
0.20
0.15
0.10
0.05
0.00
24 hours
7 days
C
MOAB-2 Plaque Load %
5
4
3
2
1
0
24 hours
7 days
Injury
Sham

Figure 3.4 Focal brain injury does not induce Aβ plaques or intra-neuronal accumulations of Aβ in WT mice at 24 hours or 7 days post-injury. Representative sections labelled with the Aβ antibody MOAB-2 (red), the neuronal antibody SMI-32 (green) and the nuclei marker DAPI (blue). * Marks the injury site. Scale bar = 50μm.

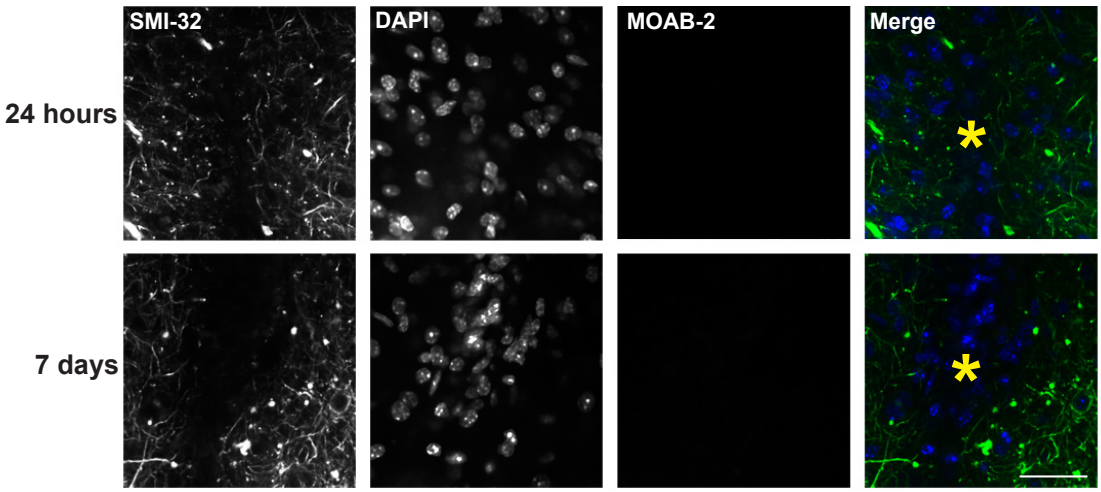
SMI-32
DAPI
MOAB-2
Merge
24 hours
7 days

Figure 3.5 Focal brain injury does not induce hyperphosphorylated tau in APP/PS1 or WT mice. Representative sections labelled with the hyperphosphorylated tau antibody AT8 (green) and the Aβ antibody MOAB-2 (red). AT8-positive dytrophic neurites (yellow arrows) can be observed surrounding Aβ plaques. Scale bars = 50μm.

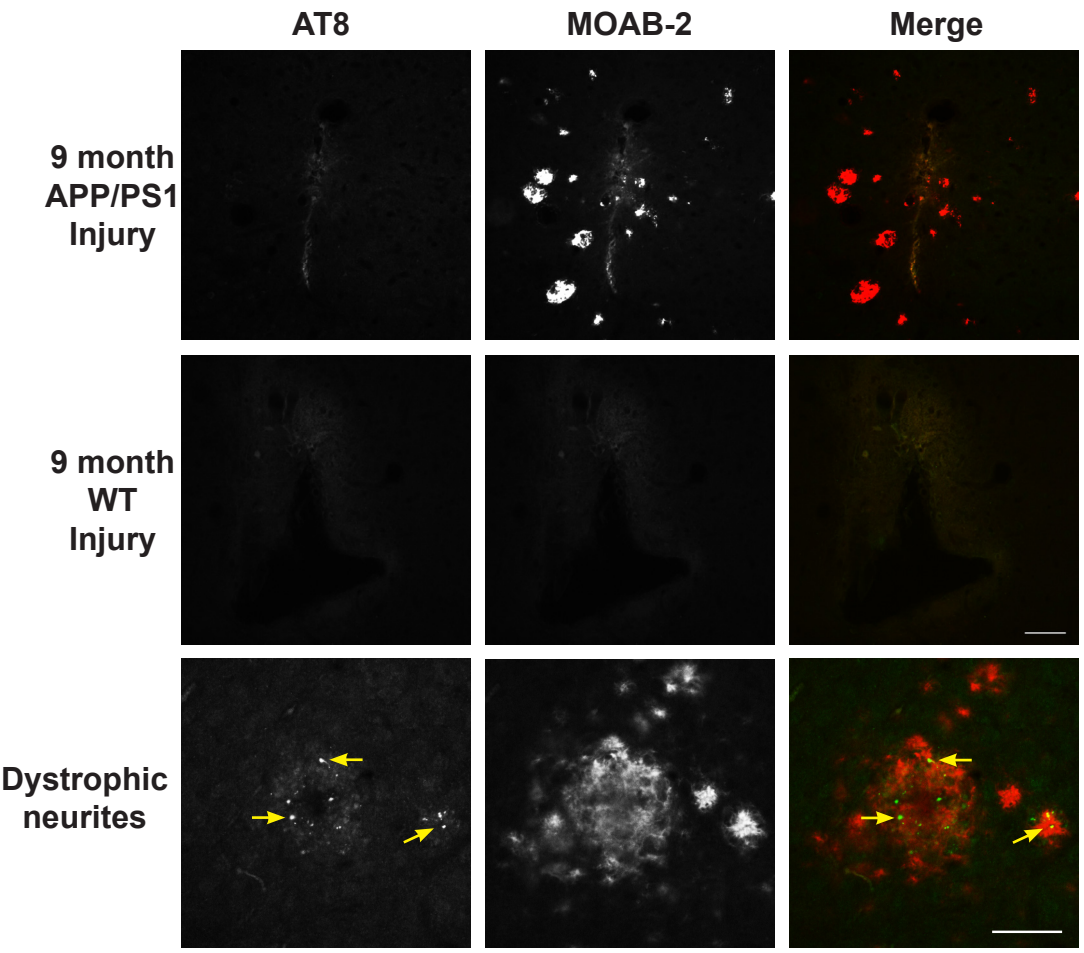
AT8
MOAB-2
Merge
9 month APP/PS1 Injury
9 month WT Injury
Dystrophic neurites

occupied by Iba-1-positive microglia/macrophages compared to sham (Figures 3.6A, B and C). There was also a significant main effect of post-treatment time [$F(1,47) = 25.7$, $p<0.001$, partial $\eta^2 = 0.35$] with the percentage area occupied by Iba-1-positive microglia/macrophages higher at 7 days post-injury compared to 24 hours post-injury (Figures 3.6A, B and C). A significant treatment×time interaction was observed [$F(15,1) = 25.7$, $p<0.001$, partial $\eta^2 = 0.42$] with the percentage area occupied by Iba-1-positive microglia/macrophages higher at 7 days post-injury compared to 24 hours post-injury, in injured but not sham mice (Figures 3.6A, B and C). There were no significant main effects or interactions for genotype or age ($p>0.05$) (Figures 3.6A, B and C).

Table 3.2 Percentage of area covered by Iba-1-positive microglia/macrophages (means ± SEM)

Genotype	Treatment	Age	Time-point	Area (%)
APP/PS1	Injury	3 months	24 hours	15.0 ± 1.1
			7 days	24.7 ± 2.1
		9 months	24 hours	13.0 ± 1.7
			7 days	27.1 ± 4.6
	Sham	3 months	24 hours	8.90 ± 0.48
			7 days	10.3 ± 0.76
		9 months	24 hours	8.52 ± 0.67
			7 days	9.96 ± 0.89
WT	Injury	3 months	24 hours	14.2 ± 1.6
			7 days	21.5 ± 2.1
		9 months	24 hours	12.2 ± 3.5
			7 days	24.8 ± 2.7
	Sham	3 months	24 hours	10.2 ± 0.69
			7 days	10.2 ± 0.52
		9 months	24 hours	8.80 ± 0.40
			7 days	9.70 ± 0.58

Figure 3.6 APP/PS1 mice have the same microglial/macrophage response to focal brain injury as WT mice. (A) Representative sections labelled with Iba-1 for microglia. At 24 hours post-injury microglia/macrophages have an activated phenotype and local migration has occurred resulting in the accumulation of microglia/macrophages at the edge of the injury site in both APP/PS1 and WT mice of both ages. By 7 days post-injury a large accumulation of activated microglia/macrophages can be seen at the injury site. Scale bar = 200μm. (B) There was a significant increase ($p<0.001$) in the percentage area Iba-1-positive in 3-month-old injured mice compared to sham mice at both 24 hours and 7 days post-injury. There was also a significant increase ($p<0.001$) in injured mice at 7 days compared to 24 hours post-injury. There was no effect of genotype ($p>0.05$). (C) There was a significant increase ($p<0.001$) in the percentage area Iba-1-positive in 9-month-old injured mice compared to sham mice at both 24 hours and 7 days post-injury. There was also a significant increase ($p<0.001$) in injured mice at 7 days compared to 24 hours post-injury. There was no effect of genotype ($p>0.05$). Values represent mean ± standard error. * = significance $p<0.001$ for injured vs sham. + = significance $p<0.001$ for injured mice at 24 hours vs 7 days post-injury.

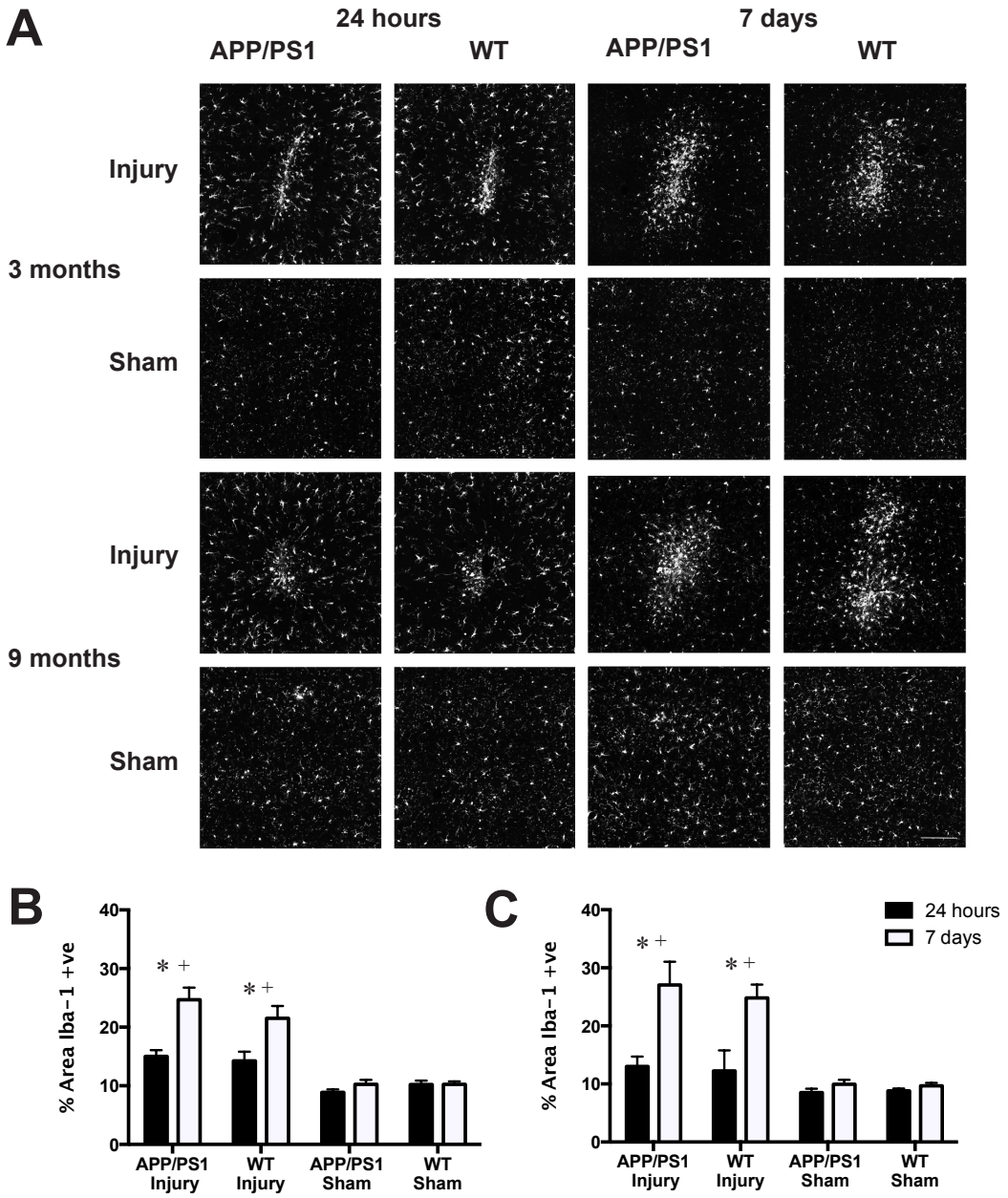
A
24 hours
7 days
APP/PS1
WT
APP/PS1
WT
Injury
3 months
Sham
Injury
9 months
Sham
B
% Area Iba−1 +ve
40
30
20
10
0
* +
* +
APP/PS1 Injury
WT Injury
APP/PS1 Sham
WT Sham
C
% Area Iba−1 +ve
24 hours
7 days
* +
* +
APP/PS1 Injury
WT Injury
APP/PS1 Sham
WT Sham

3.3.7 Astrocytic response

The response of astrocytes to focal cortical brain injury was assessed using the GFAP antibody in both 3- and 9-month-old mice. The sham treatment did not induce any observable astrocytic response at either 24 hours or 7 days post-injury (Figure 3.7A). As expected, activated astrocytes were present near MOAB-2 positive plaques in both sham and injured 9-month old APP/PS1 mice (Figure 3.7A). The percentage areas occupied by GFAP-positive astrocytes are presented in Table 3.3. There was a significant main effect of treatment [$F(1,46) = 55.29$, $p<0.001$, partial $\eta^2 = 0.55$] with an increase in the percentage area occupied by GFAP-positive astrocytes in injured compared to sham mice (Figures 3.7A, B and C). There was also a significant main effect of post-treatment time [$F(1,46) = 35.18$, $p<0.001$, partial $\eta^2 = 0.43$] with an increase in the percentage area occupied by GFAP-positive astrocytes at 7 days post-injury compared to 24 hours post-injury Figures 3.7A, B and C). A significant treatment×time interaction was also detected [$F(1,35) = 130.33$, $p<0.001$, partial $\eta^2 = 0.79$] with the percentage area occupied by GFAP-positive astrocytes higher at 7 days post-injury compared to 24 hours post-injury, in injured but not sham mice (Figures 3.7A, B and C). There were no significant main effects or interactions for genotype or age ($p>0.05$) (Figures 3.7A, B and C).

Figure 3.7 APP/PS1 mice have the same astrocytic response to focal brain injury as WT mice. (A) Representative sections labelled with GFAP for astrocytes. At 24 hours post-injury astrocytes surrounding the injury site have an activated phenotype. Activated astrocytes can also be seen surrounding plaques in 9-month old APP/PS1 mice. By 7 days post-injury a large accumulation of activated astrocytes can be seen at the injury site. Scale bar = 200μm. (B) There was a significant increase ($p<0.001$) in the percentage area GFAP-positive in 3-month-old injured mice compared to sham mice at both 24 hours and 7 days post-injury. There was also a significant increase ($p<0.001$) in injured mice at 7 days compared to 24 hours post-injury. There was no effect of genotype ($p>0.05$). (C) There was a significant increase ($p<0.001$) in the percentage area GFAP-positive in 9-month-old injured mice compared to sham mice at both 24 hours and 7 days post-injury. There was also a significant increase ($p<0.001$) in injured mice at 7 days compared to 24 hours post-injury. There was no effect of genotype ($p>0.05$). Values represent mean ± standard error. * = significance $p<0.001$ for injured vs sham. + = significance $p<0.001$ for injured mice at 24 hours vs 7 days post-injury.

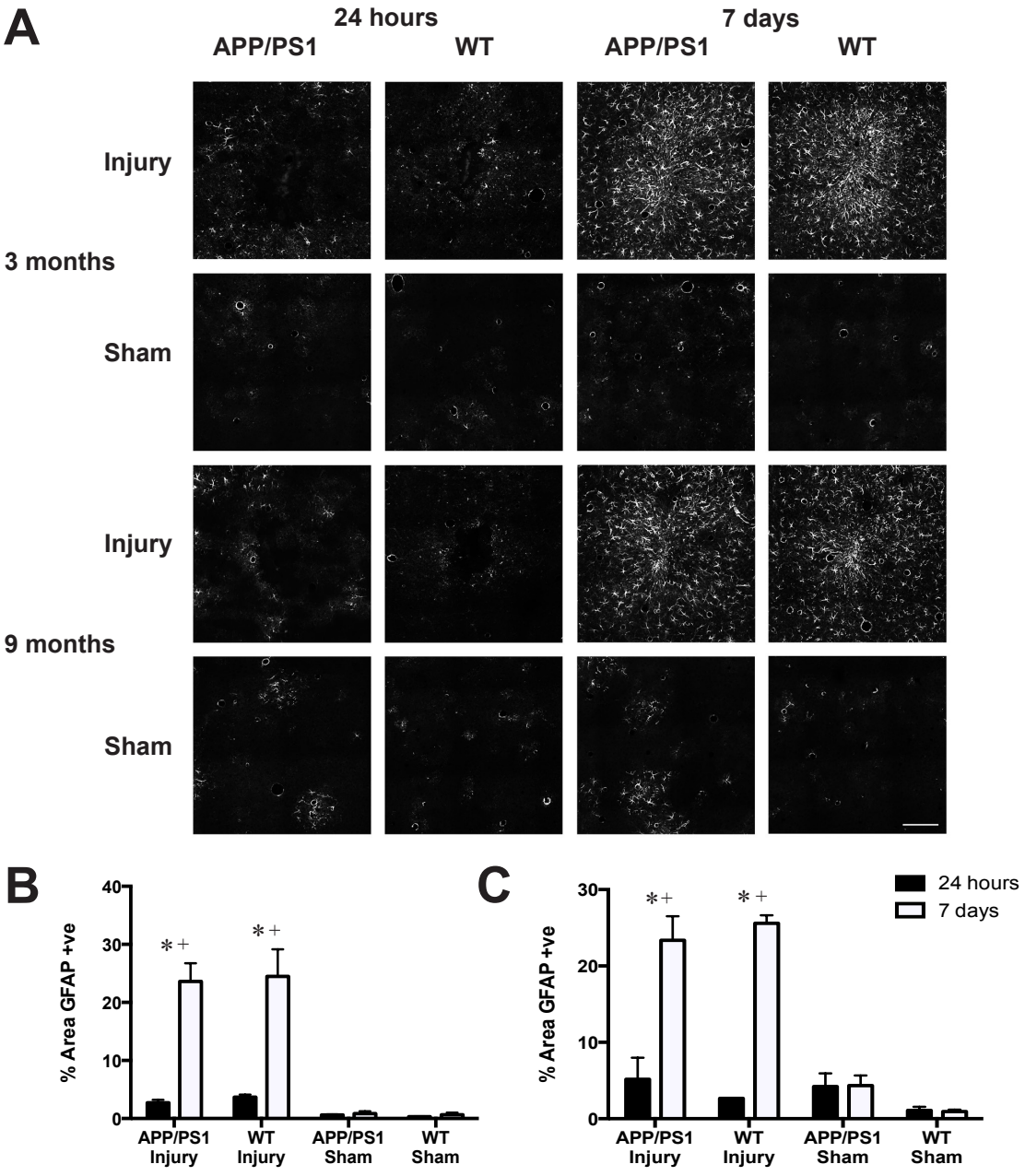
A
24 hours
7 days
APP/PS1
WT
APP/PS1
WT
Injury
3 months
Sham
Injury
9 months
Sham
B
% Area GFAP +ve
40
30
20
10
0
*+
*+
APP/PS1 Injury
WT Injury
APP/PS1 Sham
WT Sham
C
% Area GFAP +ve
30
20
10
0
*+
*+
24 hours
7 days
APP/PS1 Injury
WT Injury
APP/PS1 Sham
WT Sham

Table 3.3 Percentage of area covered by GFAP-positive astrocytes (means ± SEM)

Genotype	Treatment	Age	Time	Area (%)
APP/PS1	Injury	3 months	24 hours	2.71 ± 0.49
			7 days	23.61 ± 3.14
		9 months	24 hours	5.16 ± 2.81
			7 days	23.37 ± 3.15
	Sham	3 months	24 hours	0.62 ± 0.09
			7 days	0.86 ± 0.39
		9 months	24 hours	4.20 ± 1.73
			7 days	4.34 ± 1.34
WT	Injury	3 months	24 hours	3.68 ± 0.44
			7 days	24.47 ± 4.69
		9 months	24 hours	2.66 ± 0.06
			7 days	25.59 ± 1.05
	Sham	3 months	24 hours	0.31 ± 0.06
			7 days	0.61 ± 0.35
		9 months	24 hours	1.08 ± 0.48
			7 days	0.50 ± 0.25

3.3.8 Synaptic Response

The synaptic response to focal brain injury was investigated using an antibody to synaptophysin, which labels the majority of pre-synaptic terminals (Calhoun et al., 1996). This analysis was only undertaken in 9-month-old mice. The number of synaptic puncta per μm^2 (synaptophysin density), the percentage area covered and the average size of puncta was calculated. Table 3.4 shows synaptophysin densities and percentage areas occupied by synaptophysin puncta.

There was a significant main effect of treatment [$F(1,51) = 7.69$, $p<0.01$, partial $\eta^2 = 0.13$] with decreased synaptophysin density in injured compared to sham treated mice (Figures 3.8A and B). There was also a significant main effect of time on synaptophysin density [$F(1,51) = 6.90$, $p<0.05$, partial $\eta^2 = 0.12$] with lower densities at 24 hours post-injury compared to 7 days post-injury (Figures

3.7A and B). A significant treatment×time×distance interaction was observed [$F(1,40) = 5.08$, $p<0.05$, partial $\eta^2 = 0.11$]. This interaction was due to a significant reduction in synaptophysin density at 24 hours post-injury near the site in injured but not sham mice (Figures 3.8A and B). There was no main effect of either genotype or distance on synaptophysin density ($p>0.05$) (Figures 3.8A and B).

Similarly, when looking at the percentage area covered by synaptophysin-positive puncta, there was a significant main effect of treatment [$F(1,51) = 5.23$, $p<0.05$, partial $\eta^2 = 0.09$] with a reduction in injured compared to sham treated mice (Figures 3.8A and C). There was also a significant main effect of time [$F(1,51) = 6.72$, $p<0.05$, partial $\eta^2 = 0.12$] with an increase in the percentage area covered by synaptophysin-positive puncta at 7 days post-injury compared to 24 hours post-injury (Figures 3.8A and C). A significant [$F(1,51) = 5.41$, $p<0.05$, partial $\eta^2 = 0.10$] distance-related reduction in percentage area was also observed for sites near versus sites distant (Figures 3.8A and C). A significant treatment×time×distance interaction was also detected [$F(1,40) = 4.63$, $p<0.05$, partial $\eta^2 = 0.10$] due to a significant reduction in the percentage area covered by synaptophysin-positive puncta at 24 hours post-injury near the site in injured but not sham mice. There was no significant main effect of genotype on this response ($p>0.05$) (Figures 3.8A and C).

The average size of synaptophysin puncta was also measured. There was no significant main effects of treatment, post-treatment time or distance from the injury site ($p>0.05$). However, there was a significant main effect of genotype [$F(1,51) = 8.96$, $p<0.01$, partial $\eta^2 = 0.15$] with APP/PS1 mice having smaller puncta than WT mice (0.39 ± 0.004 vs 0.41 ± 0.003, data not shown). A full factorial analysis showed no significant interactions with treatment ($p>0.05$), post-treatment time ($p>0.05$) or distance from the injury site ($p>0.05$).

Figure 3.8 Focal brain injury reduces synaptophysin-postive synapses near the injury site at 24 hours post-injury. (A) Representative sections labelled with the presynaptic marker synaptophysin (green) and DAPI (blue) to label nuclei. The injury site was 60 μm from the edge of the image marked by the yellow *. Scale Bar = 20μm. (B) There was a significant reduction ($p<0.05$) in synaptophysin density near (60 μm from the injury site) at 24 hours post-injury compared to distant (120 μm from the injury site) and sham sites. (C) There was a significant reduction ($p<0.05$) in the percentage area occupied by synaptophysin puncta near (60 μm from the injury site) at 24 hours post-injury compared to distant (120 μm from the injury site) and sham sites. Bars represent mean ± standard error. * = significance $p<0.05$ for 24 hours near vs distant and sham.

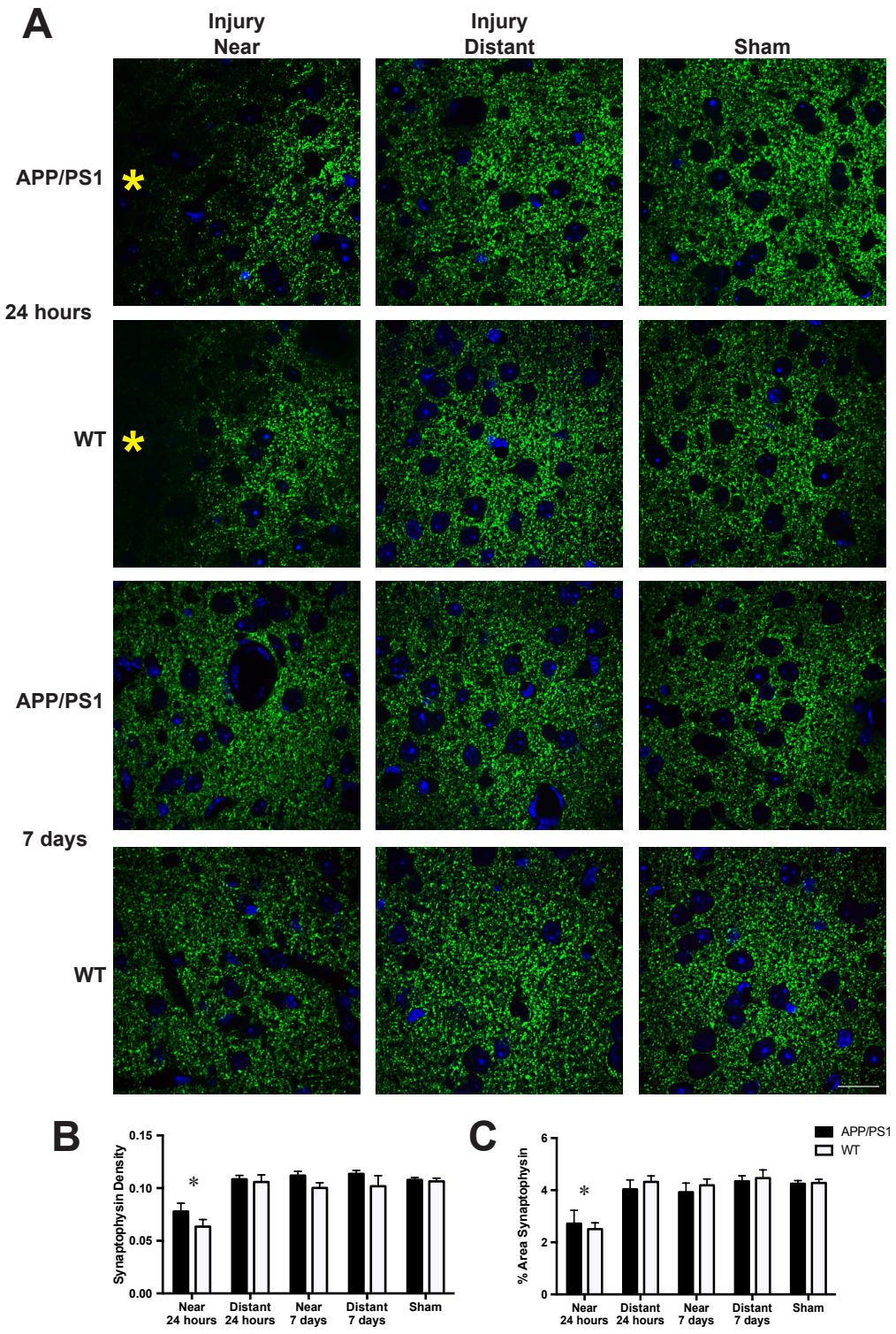
A
Injury
Near
Injury
Distant
Sham
APP/PS1
24 hours
WT
APP/PS1
7 days
WT
B
Synaptophysin Density
0.15
0.10
0.05
0.00
Near
24 hours
Distant
24 hours
Near
7 days
Distant
7 days
Sham
C
% Area Synaptophysin
6
4
2
0
APP/PS1
WT
Near
24 hours
Distant
24 hours
Near
7 days
Distant
7 days
Sham

Table 3.4 Synaptophysin density and percentage of area covered by synaptophysin-positive puncta (means ± SEM)

Genotype	Treatment	Distance	Time	Density	% Area
APP/PS1	Injury	Near	24 hours	0.073 ± 0.011	2.72 ± 0.27
			7 days	0.100 ± 0.006	3.92 ± 0.41
		Distant	24 hours	0.102 ± 0.009	4.03 ± 0.20
			7 days	0.114 ± 0.003	4.34 ± 0.32
	Sham	Near	24 hours	0.111 ± 0.006	4.35 ± 0.24
			7 days	0.107 ± 0.005	4.16 ± 0.23
		Distant	24 hours	0.111 ± 0.004	4.47 ± 0.28
			7 days	0.104 ± 0.004	4.14 ± 0.37
WT	Injury	Near	24 hours	0.064 ± 0.007	2.51 ± 0.39
			7 days	0.100 ± 0.005	4.19 ± 0.17
		Distant	24 hours	0.106 ± 0.007	4.32 ± 0.23
			7 days	0.102 ±0.010	4.46 ± 0. 27
	Sham	Near	24 hours	0.105 ± 0.005	4.21 ± 0.51
			7 days	0.114 ± 0.003	4.51 ± 0.36
		Distant	24 hours	0.095 ± 0.009	3.89 ± 0.40
			7 days	0.108 ±0.005	4.39 ± 0.24

3.4 Discussion

TBI has been proposed to be a risk factor for the development of AD (Mortimer et al., 1991, Nemetz et al., 1999, Guo et al., 2000, Plassman et al., 2000, Fleminger et al., 2003), but the mechanisms underlying this relationship remain to be elucidated. The current study sought to examine the effects of focal brain injury on Aβ deposition, as well as the microglial and astrocytic responses and synaptic changes in the APP/PS1 mouse model of AD relative to WT mice.

Several studies have investigated Aβ after experimental brain injury in transgenic AD mice, reporting both increased and decreased plaque loads (Nakagawa et al., 1999, Nakagawa et al., 2000, Uryu et al., 2002). However, this and other studies (Smith et al., 1998, Tran et al., 2011a, Tran et al., 2011b) show no evidence of injury-induced changes in Aβ plaque dynamics. These data demonstrate that focal brain injury does not acutely induce Aβ plaque deposition in the somatosensory cortex of pre-plaque APP/PS1 mice, or acutely promote deposition after the onset of amyloidosis in older animals. The wide range of reported effects of TBI on Aβ might be attributable to the type and severity of the experimental brain injury used; the injury used in this study was focal and affected only the neocortex. This allowed the examination of local plaque dynamics without the introduction of confounding variables such as large cortical tissue loss, widespread inflammation or DAI to the white matter tracts. The choice of time points may also have influenced the outcomes: past studies demonstrated more chronic changes in plaque deposition between 2- and 8-months post-injury (Nakagawa et al., 1999, Nakagawa et al., 2000, Uryu et al., 2002). Although Aβ plaques accumulate within hours following human TBI (Ikonomovic et al., 2004), it is possible that, in mouse models of AD, amyloid deposition is a slower process following brain injury. However, *in vivo* multiphoton microscopy in APP/PS1 mice has demonstrated that Aβ plaques can form in as quickly as 24 hours (Meyer-Luehmann et al., 2008).

In the wake of TBI, activated microglia might plausibly reduce Aβ plaque load by phagocytosing plaques (Simard et al., 2006), although microglia have also

been implicated in plaque formation (Wegiel et al., 2000, reviewed in Nagele et al., 2004). Additionally, microglia have been shown to be detrimental following TBI (Reviewed in Kumar and Loane, 2012) and in AD (Reviewed in Streit, 2004b) due to the release of pro-inflammatory cytokines. The findings of the current study suggest that the microglial/macrophage response stimulated by localized brain injury neither acutely induces nor reduces Aβ plaques: no change in plaque load was observed despite an evident microglial/macrophage response. This study also demonstrated that the microglial/macrophage response to brain injury in 9-month-old APP/PS1 mice is comparable to WT mice and 3-month-old pre-plaque APP/PS1 mice. Thus, despite the presence of Aβ plaque-related microglia activation and neurodegeneration, the microglial/macrophage response to focal brain injury is not augmented on this background of neuroinflammation.

Similar to microglia, astrocytes are implicated in both the degradation of Aβ plaques (Funato et al., 1998, Wyss-Coray et al., 2003b) as well as in contributing to the pathogenesis of AD (Pike et al., 1995, Reviewed in Verkhratsky et al., 2010). However, the findings of the current study demonstrate the astrocytic response elicited by focal brain injury did not cause any acute changes to Aβ plaque deposition. Additionally, the astrocytic response to brain injury, like the microglial/macrophage response, was the same in all groups, indicating that AD-associated astrocytic changes do not impair the response to focal brain injury.

APP accumulation is a well characterized marker of axonal injury in TBI (Gentleman et al., 1993, Otsuka et al., 1991), but there is some uncertainty about whether Aβ accumulates intra-neuronally and intra-axonally. Unlike many other commonly used antibodies for Aβ such as 6E10 (Youmans et al., 2012a), the antibody used for the current study, MOAB-2, does not cross-react with APP (Youmans et al., 2012a). The current study found no intra-neuronal or intra-axonal Aβ in either APP/PS1 or WT mice after injury, in contrast to previous studies demonstrating acute accumulation of Aβ in white matter axons following CCI in the 3×Tg-AD (APP_{SWE}, $MAPT_{P301L}$, $PSEN1_{M146V}$) and APP/PS1 mouse models of AD (Tran et al., 2011a, Tran et al., 2011b). It is possible that white matter axons accumulate Aβ only after either a more substantial injury and/or in relation to shear-forces present in CCI models.

This model of focal brain injury causes a highly reproducible, discrete lesion to the cortex with minimal tissue loss (King et al., 2001, Blizzard et al., 2011). Furthermore, substantial tissue remodeling occurs within 7 days post-injury (this study and Blizzard et al., 2013). The current results demonstrate that despite a significant acute loss of synaptophysin immunoreactivity near the injury site, by 7 days post-injury, synaptophysin-positive puncta density was restored to baseline levels in both APP/PS1 and WT mice. This indicates that the mouse brain possessed a significant capability to recover lost synaptophysin immunoreactivity following injury, although the functional significance of this recovery is unknown. Further experiments using combinations of antibodies against synaptic proteins are required to determine the significance of this result.

If the change in synaptophysin immunoreactivity is due to a loss and recovery of synapses, this data suggests an equal capacity for the recovery of synapses following injury despite the presence of AD-related neuropathology that causes local and remote loss of synapses in the APP/PS1 model at 12-months of age (Mitew et al., 2013a). With respect to the latter study, this also suggests that the synapse loss in APP/PS1 mice occurs via highly specific mechanisms.

Two limitations must be taken into account when interpreting the results of this chapter. First, this model of focal cortical brain injury is not a clinical representation of most human brain injuries. However, it is a well characterized model (King et al., 2001, Chung et al., 2003, Chung et al., 2004, Chung et al., 2007, Chung et al., 2008, Blizzard et al., 2011, Blizzard et al., 2013) that produces a well delineated injury in which the effect of the injury on nearby plaques could be easily quantified. Second, this study utilized the APP/PS1 transgenic mouse model of AD amyloidosis, which harbors two mutations implicated in familial AD. Whilst most human TBI cases are not genetically predisposed to AD, such mutations are necessary in mice to produce Aβ plaques as WT rodents do not form plaques with aging (Selkoe, 1989) or after TBI (Pierce et al., 1996, Bramlett et al., 1997, Murai et al., 1998).

In conclusion, this study demonstrates that focal cortical brain injury does not accelerate the onset or progression of Aβ plaque deposition acutely in APP/PS1 mice. Furthermore, it shows that APP/PS1 mice with established amyloidosis have normal microglial, astrocytic and synaptic responses to focal brain injury despite existing AD-like neuropathology. It remains to be seen however, whether a clinically relevant model of diffuse brain injury with a more widespread distribution of secondary pathology might alter Aβ plaque deposition after injury.

4 The effect of diffuse brain injury on Aβ dynamics in APP/PS1 mice

4.1 Introduction

The previous chapter demonstrated that focal cortical damage does not alter Aβ plaque dynamics in APP/PS1 mice. However, the focal model of brain injury used causes structural brain damage to a very localized region of the cortex and does not damage underlying subcortical structures or cause extensive secondary pathology (Blizzard et al., 2011, King et al., 2001). Previous studies using the CCI model of experimental brain injury, which induces widespread brain damage and DAI to underlying white matter tracts (Xiong et al., 2013), have shown changes in Aβ plaque deposition post-injury (Nakagawa et al., 1999, Nakagawa et al., 2000, Uryu et al., 2002). Hence, widespread or diffuse injury may be required for TBI-induced alteration in Aβ plaque deposition.

TBI-induced DAI causes impaired axonal transport and the formation of axonal swellings (Hanell et al., 2014, Tang-Schomer et al., 2012, Tang-Schomer et al., 2010). Impaired axonal transport may be a primary event in the formation of Aβ plaques (Stokin et al., 2005), suggesting that DAI may be an important factor in the development of AD following TBI.

The LFPI model is a clinically relevant, and highly reproducible, model of TBI that causes both focal and diffuse injury (Xiong et al., 2013, Alder et al., 2011). Unlike the CCI model, which causes widespread cortical damage and cortical loss (Lighthall, 1988, Smith et al., 1995), at a mild severity, LFPI does not cause cortical loss (Hylin et al., 2013), and hence allows the quantification of Aβ plaque load in the underlying injured cortical tissue.

Thus far, the LFPI model has not been used to assess Aβ plaque dynamics after injury in transgenic AD mice. Therefore, the current study sought to investigate the acute and chronic effects of LFPI on Aβ dynamics in the APP/PS1 mouse model of AD. Previous CCI studies on the effect of TBI on Aβ plaque dynamics

in transgenic AD mouse models are heterogeneous in their experimental design. This makes comparing earlier studies difficult, and consequently the effect of TBI on Aβ plaque dynamics remains unclear. One experimental factor that has differed between various studies is the stage of amyloidosis present in transgenic mouse model at the time of injury. Thus, this chapter aimed to investigate the effect of diffuse TBI on Aβ plaque load in the APP/PS1 mouse at two different stages of amyloidosis, 30 days after injury. Furthermore, as astrocytes and microglial cells have been implicated in both the formation (Nagele et al., 2004, Pike et al., 1995, Verkhratsky et al., 2010, Wegiel et al., 2000) and clearance (Funato et al., 1998, Liu et al., 2010, Paresce et al., 1996, Simard et al., 2006, Wyss-Coray et al., 2003a) of Aβ plaques, this chapter also assesses the glial response to LFPI in APP/PS1 mice. To this end, 3-month-old pre-plaque mice and 6-month-old plaque accumulating mice were subjected to mild LFPI. Immunohistochemical methods were used to assess changes in Aβ plaque deposition as well as astrocytes and microglia post-injury.

4.2 Materials and Methods

4.2.1 Mice

All experimental procedures utilized male APP_{SWE}/PSENdE9 (APP/PS1) (Jankowsky et al., 2001) and C57BL/6 wild-type (WT) littermate control mice at either 3- or 6-months of age.

4.2.2 Genotyping

Genotyping was performed as outlined in the Material and Methods section 2.2 using the primers specified in Chapter 3 section 3.2.2. Primers and expected PCR product sizes are as specified in Chapter 3 Table 3.1.

4.2.3 *In vivo* model of diffuse traumatic brain injury

In vivo diffuse traumatic brain injury was performed as outlined in the Materials and Methods section 2.4. For the 24 hours time-point, 3-month-old APP/PS1 and C57/Bl6 WT mice were used (n=3-4 mice per group, total n=14). For the 30 day time point, 3- and 6-month old APP/PS1 mice (n=5 mice per age and treatment, total=20) were used. A cohort of 6-month-old C57/Bl6 mice (n=5 per treatment, total=10) were also used to determine if LFPI caused plaque deposition in WT animals and if their response to injury differed to mice with established plaque pathology. Three- and 6-month-old mice were perfused at 30 days post-injury making them 4- and 7-months-old at analysis, respectively.

4.2.4 Tissue preparation

At either 24 hours or 30 days post-injury, mice were terminally anesthetised and transcardially perfused as per the Materials and Methods section 2.5. Serial 50um coronal sections were cut on a vibratome (Leica VT1000). For total Aβ labelling the MOAB-2 antibody was used following formic acid antigen retrieval as described in Materials and Methods section 2.6.2. Immunohistochemistry was then performed.

4.2.5 Immunohistochemistry

Immunohistochemistry was performed as described in the Materials and Methods section 2.6. Thioflavin-S staining for fibrillar Aβ deposits and immunolabelling with the following antibodies was performed: MOAB-2 for Aβ deposits, APP, Iba-1 for microglia, GFAP for astrocytes, AT8 for hyperphosphorylated tau and SMI-312 for axons and SMI-32 for neuronal cell bodies, dendrites and thick axons (refer to Table 2.1 in the Materials and Methods section for antibody information).

4.2.6 Confocal microscopy and quantitation

Confocal microscopy was performed on a Perkin-Elmer Ultraview VOX confocal imaging system using Volocity 6.3 software for image capture and stitching (10% overlap, no corrections). MOAB-2 and thioflavin-S were imaged using a 10x objective and GFAP and Iba-1 with a 20x objective. MOAB-2 and thioflavin-S plaque loads (percentage area positive) were calculated independently for each hemisphere, from the midline to the rhinal fissure. Four sections per mouse, for both MOAB-2 and thioflavin-S were used spanning the cortex from bregma +0.5mm to −2.5mm. This region was chosen for analysis after visual survey of APP- and Aβ-labelled axonal and neuronal pathology across the whole brain at 24 hours after LFPI. Iba-1 and GFAP analyses were performed on 2 sections per mouse, per marker in the same regions used for plaque analyses. Glial markers were quantified across a wedge shaped area spanning 1.5mm across the ipsilateral cortex, beginning at the cingulum. And centered beneath the injury site. The markers were quantified as a percentage of area covered by labelled cells. Images were processed to 8-bit greyscale and segmented using ImageJ 1.48r (NIH; Schneider et al., 2012). Segmentation was performed using custom plug-ins written in Java, including an automated random forest classifier (Samaroo et al., 2012, Sommer et al., 2011). The custom random forest classifier was developed using data generated for this thesis by O'Mara and Kirkcaldie (Manuscript in preparation). Briefly, this required an independent image classifier for each antibody or marker (ie. MOAB-2, thioflavin-S, GFAP and Iba-1). These classifiers were trained using manual annotation of 'labelling' and 'background' in a representative set of example images, from which the

random forest classifier optimised its automated image segmentation rules. The separate classifiers were then used for their respective labels to segment the pixels of the original images into label and background classes. An image mask of the region of interest was then applied to the segmented images, after which ImageJ Particle Analysis tool was used to quantify the percentage area of labelling. Analysis was performed on the stitched images acquired on the Perkin-Elmer Ultraview VOX confocal imaging system using Volocity 6.3 software for image capture and stitching (10% overlap, no corrections). The stitched images had a grid-like pattern due uneven illumination across the field of view. The orientation of the mounted sections was the same for all samples and thus the orientation of the grid pattern was also the same for all samples. This grid-like pattern did not influence the results due to the use of the random forest classifier for segmentation. The random forest segmenter was created by supervised machine learning, using images with the same grid pattern. The classifier calculates a range of image derivatives as inputs to the segmentation process thus using local image context (eg texture, edges) to evaluate each pixel. Therefore, intensity shifts (as seen in the grid-like pattern) do not impact the segmentation (Sommer et al., 2011). See Appendix B for an example of an original image and its segmentation using the random forest segmenter.

4.2.7 Statistical analysis

IBM SPSS statistics (Version 19) was used for all statistical analyses and graphs were made using GraphPad Prism (Version 6.0c). The MOAB-2 and thioflavin-S data were analysed using a two-way analysis of variance (ANOVA) model for the main effects of the factor variables: treatment (LFPI and sham) and hemisphere (ipsilateral and contralateral to the LFPI/sham site), and then a full factorial ANOVA was used to test for interactions between the variables. For the GFAP and Iba-1 data ANOVA methods were also used. The 3-month-old and 6-month-old cohorts were analysed separately. For the 3-month-old cohort, Student's t-test was used for the factor variable treatment (LFPI or sham). The 6-month-old cohort had both APP/PS1 mice and WT mice and thus a two-way ANOVA was performed for the main effects of the factor variables treatment (LFPI or sham) and genotype (APP/PS1 and WT) and the interaction effect

between these two variables. All data are expressed as means ± standard error of the mean (SEM) with significance set at $p < 0.05$ and estimates of effect size (eta squared) reported for significant effects.

4.3 Results

4.3.1 Characterisation of the LFPI model

A fluid pressure pulse of 1.25-1.35atm (Figure 4.1A) was delivered to the intact dura and, thus, this LFPI was considered of mild severity (Alder et al., 2011). The average pressure for each of the injury groups was 1.28±0.02 for 3 month APP/PS1 mice, 1.27±0.05 for 6 month APP/PS1 mice and 1.25±0.01 for 6 month WT animals and was not significantly different between the groups ($p>0.05$) (Figure 4.1B). This injury did not induce prolonged unconsciousness, with the animals able to right themselves immediately following the injury.

Following LFPI, the dura remained intact. There was no overt cavitation or hemorrhage at either 24 hours or 30 days post-injury. At the macroscopic level, the brains of injured and sham mice were indistinguishable.

4.3.2 Diffuse axonal injury and amyloid beta accumulation at 24 hours post-LFPI

Three-month-old APP/PS1 mice were used to examine the pattern of DAI produced by LFPI acutely after injury and to confirm previous finding of intra-neuronal and intra-axonal Aβ accumulation in APP/PS1 mice. APP immunohistochemistry was used to assess axonal pathology following LFPI, as it is a well-described pathological hallmark of DAI (Gentleman et al., 1993, Otsuka et al., 1991, Sherriff et al., 1994). Intra-neuronal and intra-axonal Aβ accumulation was assessed using the MOAB-2 antibody. The presence of intra-neuronal labelling was determined by cellular morphology.

At 24 hours post-injury, APP labelling accumulated in neuronal processes within the cortex, white matter tracts and hippocampus in APP/PS1 and WT mice (Figure 4.2). In the cortex, APP was present in cell bodies, injured neuronal processes extending from cell bodies, axonal varicosities resembling ‘beads on a string’ and axonal bulbs. In the white matter tracts and hippocampus, APP labelling was present in axonal varicosities resembling a ‘beads on a string’

Figure 4.1 Average injury severity as determined by the fluid pressure pulse delivered did not vary between groups. (A) Representative pressure trace recorded during a LFPI. The trigger point refers to the point at which the pendulum of the device moves past the sensor point on the device. (B) The was no signficant difference ($p>0.05$) in the average pressure pulse delivered between any of the injured groups. Bars represent means ± standard error.

A

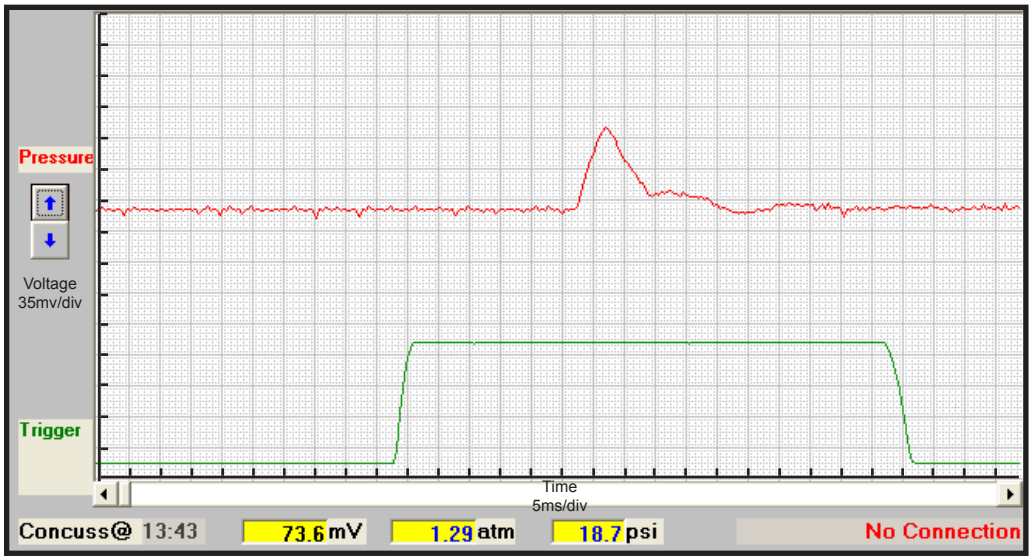
Pressure
Voltage
35mv/div
Trigger
Time
5ms/div
Concuss@ 13:43
73.6 mV
1.29 atm
18.7 psi
No Connection

B

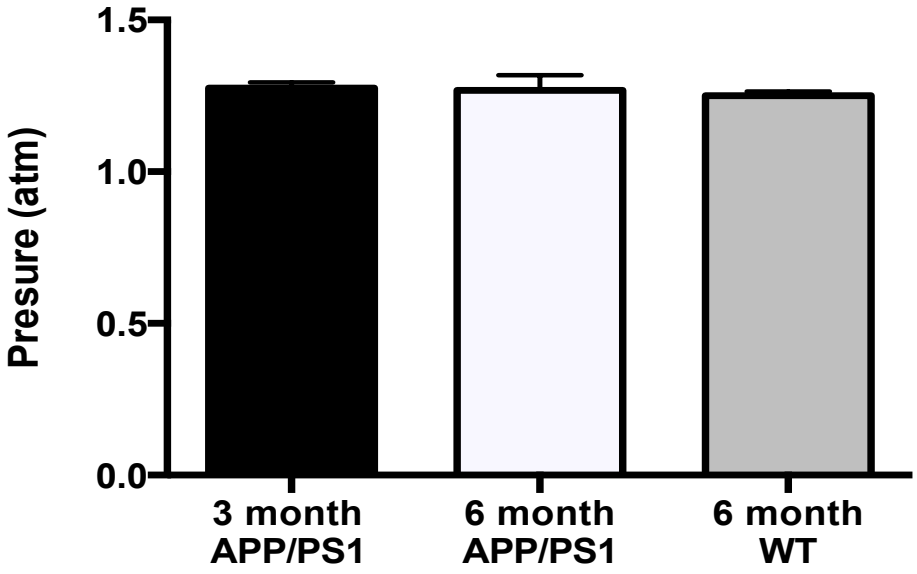
Presure (atm)
1.5
1.0
0.5
0.0
3 month
APP/PS1
6 month
APP/PS1
6 month
WT

morphology. The amount of APP-labeled axonal pathology did not appear to differ between APP/PS1 or WT mice. This pathology was not seen in sham treated APP/PS1 or WT mice.

In injured APP/PS1 mice, MOAB-2 labeled Aβ was specifically localised within neurons in the cortex, white matter tracts and the hippocampus (Figure 4.2). This labelling was typically co-localised with APP labelling, however, it appeared less abundant. In the cortex, Aβ labelling was present in the cell bodies, injured neuronal processes, axonal varicosities and axonal end bulbs. It was also observed in axonal varicosities in the white matter tracts and the hippocampus. Aβ labelling was observed to be less abundant than APP labelling and appeared primarily in larger axonal varicosities and in axonal bulbs. No intraneuronal or intra-axonal Aβ accumulations were present in either injured or sham WT mice or sham injured APP/PS1 mice (Figure 4.2).

4.3.3 Plaque load in 3-month-old APP/PS1 mice 30 days post-LFPI (4-months-old at pathological analysis)

This study sought to investigate the chronic effects of LFPI on the onset of plaque deposition in 3-month-old pre-plaque APP/PS1 mice. APP/PS1 mice were subjected to LFPI or sham treatment and perfused at 30 days post-injury (4-months-old). The MOAB-2 antibody was used to label all Aβ and the stain thioflavin-S was used to label fibrillar plaques. No intra-neuronal Aβ labeling was detected in LFPI or sham treated 3-month-old APP/PS1 mice at 30 days post-injury. Very few Aβ plaques were detected in sham treated APP/PS1 mice at 30 days post-injury (Figures 4.3A, 4.4A) as has been previously reported for this age (Garcia-Alloza et al., 2006). However, at 30 days post-LFPI, thioflavin-S-labeled and numerous MOAB-2-labeled Aβ plaques were present in APP/PS1 mice (Figures 4.3A, 4.4A).

At 30 days post-injury, ANOVA demonstrated there was a significant main effect of treatment, with LFPI increasing the MOAB-2-labelled Aβ plaque load compared to sham treatment (0.29 ± 0.02% vs 0.12 ± 0.01% in both hemispheres, [$F(1,17) = 50.1$, $p<0.001$, partial η^2 0.75], Figure 4.3B). Likewise,

Figure 4.2 LFPI causes diffuse axonal injury and the intra-neuronal accumulation of Aβ in APP/PS1 mice at 24 hours post-injury. APP and Aβ immunohistochemistry in 3-month-old APP/PS1 and WT mice. Scale bar = 50μm. APP accumulations can be seen within axonal swellings and bulbs as well as in neuronal cell bodies in both APP/PS1 and WT mice. Aβ labelling is seen within neuronal cell bodies and axonal swellings and bulbs in APP/PS1 mice only, but not WT mice. APP and Aβ labelling co-localise (yellow arrows), however Aβ labelling appears less abundant than APP labelling.

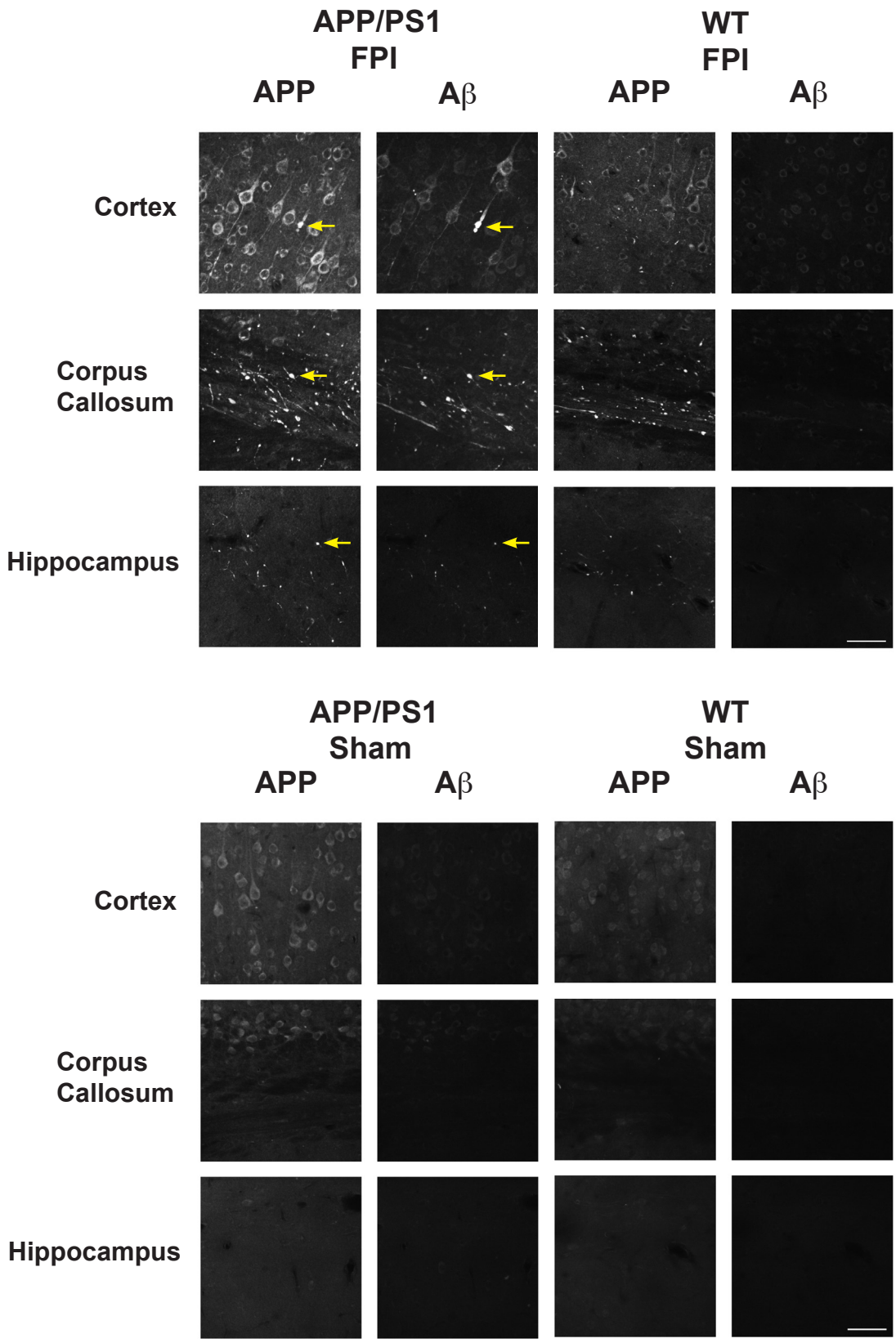
APP/PS1
FPI
WT
FPI
APP
Aβ
APP
Aβ
Cortex
Corpus
Callosum
Hippocampus
APP/PS1
Sham
WT
Sham
APP
Aβ
APP
Aβ
Cortex
Corpus
Callosum
Hippocampus

there was also a significant main effect of treatment on thioflavin-S plaque load in injured compared to sham mice (0.055% ± 0.006 vs 0.022 ± 0.003% in both hemispheres, [$F(1,17) = 27.8$, $p<0.001$, partial η^2 0.62], Figure 4.4B). For both MOAB-2 labelling and thioflavin-S staining, there was no significant main effect of hemisphere ($p > 0.05$) and there was no treatment x hemisphere interaction ($p > 0.05$). Therefore, LFPI caused a significant increase in the MOAB-2-labelled Aβ and thioflavin-S-labelled fibrillar plaque load in both cortical hemispheres at 30 days post-injury. Table 4.1 gives the means ± the SEM for ipsilateral and contralateral hemispheres.

4.3.4 Plaque load in 6-month-old APP/PS1 mice 30 days post-LFPI (7-months-old at pathological analysis)

Aβ plaques deposition begins at 4 months of age in APP/PS1 mice and by 7 months of age, numerous Aβ plaques labelled with Aβ antibodies and thioflavin-S are usually present (Garcia-Alloza et al., 2006). Thus, 6-month-old APP/PS1 mice were subjected to LFPI and examined at 30 days post-injury (at 7 months of age) to assess the effects of TBI on the progression of Aβ plaque deposition.

No intra-neuronal Aβ labeling was observed in LFPI or sham treated mice at 30 days post-injury. Sham treated APP/PS1 mice had numerous MOAB-2 and thioflavin-S labelled Aβ plaques (Figures 4.3A and 4.4A), as expected for this age (Garcia-Alloza et al., 2006). LFPI treated mice had substantially fewer MOAB-2 labelled Aβ plaques, but a similar amount of thioflavin-S labelled fibrillar Aβ plaques compared to sham treated mice (Figures 4.3A and 4.4A).

ANOVA demonstrated a main effect of treatment for MOAB-2 with LFPI significantly decreasing the MOAB-2-labelled Aβ plaque load compared to sham treatment (2.02 ± 0.16% vs 3.04 ± 0.27%, both hemispheres, [$F(1,17) = 10.5$, $p<0.01$, partial η^2 0.38], Figure 4.3B). There was no significant main effect of hemisphere ($p>0.05$) and there was no treatment x hemisphere interaction ($p>0.05$) for MOAB-2-labelled Aβ plaque load. For thioflavin-S staining of plaques, there was no significant main effect of treatment (0.15 ± 0.02% vs 0.20 ± 0.02% both hemispheres, $p> 0.05$, Figure 4.4B) or hemisphere ($p> 0.05$) and

there was no significant treatment x hemisphere interaction ($p > 0.05$). Thus, LFPI caused a significant decrease in MOAB-2-labelled Aβ plaque load in both cortical hemispheres of the brain, however, did not significantly alter thioflavin-S-labelled fibrillar plaque load. Table 4.1 gives the means ± the SEM for ipsilateral and contralateral hemispheres.

Table 4.1 MOAB-2 and thioflavin-S plaque loads (means ± SEM).

Group	MOAB-2 plaque load (%)			Thioflavin-S plaque load (%)		
	Ipsilateral	**Contralateral**	**Bilaterally**	**Ipsilateral**	**Contralateral**	**Bilaterally**
3m LFPI	0.32 ± 0.03	0.26 ± 0.03	0.29 ± 0.02	0.062 ± 0.006	0.047 ± 0.009	0.055 ± 0.006
3m Sham	0.13 ± 0.02	0.12 ± 0.02	0.12 ± 0.01	0.022 ± 0.004	0.022 ± 0.005	0.022 ± 0.003
6m LFPI	1.98 ± 0.27	2.06 ± 0.18	2.02 ± 0.16	0.16 ± 0.02	0.15 ± 0.04	0.15 ± 0.02
6m Sham	0.16 ± 0.02	0.15 ± 0.04	3.04 ± 0.27	0.18 ± 0.01	0.22 ± 0.04	0.20 ± 0.02

3m, 3 months; 6m, 6 months.

4.3.5 Amyloid beta plaque dynamics in WT mice 30 days post-LFPI

Six-month-old WT mice were also examined for Aβ plaque deposition using the MOAB-2 antibody and thioflavin-S staining following LFPI. As MOAB-2 is a pan-specific Aβ antibody, which labels both mouse and human Aβ, (Youmans et al., 2012a) it will also detect endogenous mouse Aβ accumulations after LFPI. No Aβ labelling with either MOAB-2 or thioflavin-S was observed in WT mice at 30 days post-injury (Figure 4.5).

4.3.6 Astrocytic response at 30 days post-LFPI

The astrocytic response to LFPI was examined using an antibody to GFAP. Activated astrocytes surrounded Aβ plaques in APP/PS1 mice in both age cohorts (Figure 4.6A). For the 3-month-old cohort, there was no significant difference in the percent area occupied by GFAP labelling between injured and sham APP/PS1 mice at 30 days post-injury ($p>0.05$, Figure 4.6B). For the 6-month-old cohort at 30 days after LFPI, there was no main effect of treatment ($p>0.05$) or genotype (Figure 4.6B, $p>0.05$) on the percent area GFAP-positive. Thus, at 30 days post-injury, there was no difference in the percent area of GFAP-labelled astrocytes in injured mice compared to sham treated mice in any group. Table 4.2 summarises the means ± SEM for each group analysed.

Figure 4.3 LFPI effects total Aβ plaque load in APP/PS1 mice at 30 days post-injury. (A) Aβ immunohistochemistry with the MOAB-2 antibody. Right side is ipsilateral to the injury or sham site. Scale bar=1000μm. (B) There was a significant increase in total Aβ plaque load ($p<0.001$) in injured compared to sham 3-month-old APP/PS1 mice. (C) There was a significant decrease in total Aβ plaque load ($p<0.01$) in injured compared to sham 6-month-old APP/PS1 mice. Bars represent means ± standard error. *** denotes significance at $p<0.001$ for LFPI versus sham and ** denotes significance $p<0.01$ for LFPI versus sham. Ipsi = ipsilateral to the injury or sham site, Contra = contralateral to the injury or sham site.

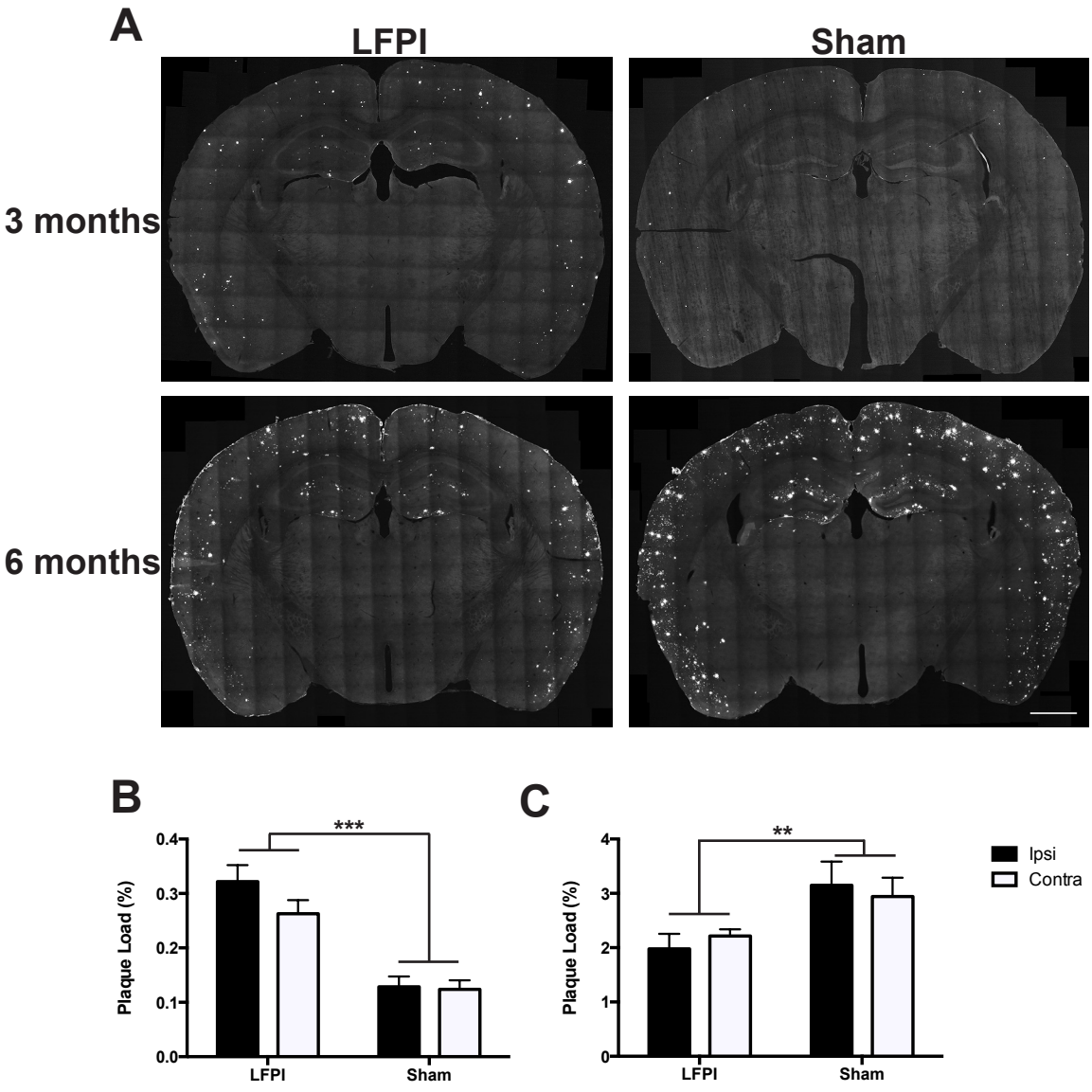
A
LFPI
Sham
3 months
6 months
B
***
Plaque Load (%)
0.4
0.3
0.2
0.1
0.0
LFPI
Sham
C
**
Plaque Load (%)
4
3
2
1
0
LFPI
Sham
Ipsi
Contra

Figure 4.4 Fibrillar Aβ plaque load is effected by LFPI in 3- but not 6-month-old APP/PS1 mice at 30 days post-injury. (A) Representive sections stained with thioflavin-S for fibrillar Aβ deposits. Right side is ipsilateral to the injury or sham site. Scale bar=1000μm. (B) LFPI caused a significant ($p<0.001$) increase in fibrillar Aβ plaque load in 3-month-old APP/PS1 mice at 30 days post-injury. (C) LFPI did not significantly ($p>0.05$) effect fibrillar Aβ plaque load in 6-month-old APP/PS1 mice at 30 days post-injury. Bars represent means ± standard error. *** denotes significance at $p<0.001$ for LFPI versus sham. Ipsi = ipsilateral to the injury or sham site, Contra = contralateral to the injury or sham site.

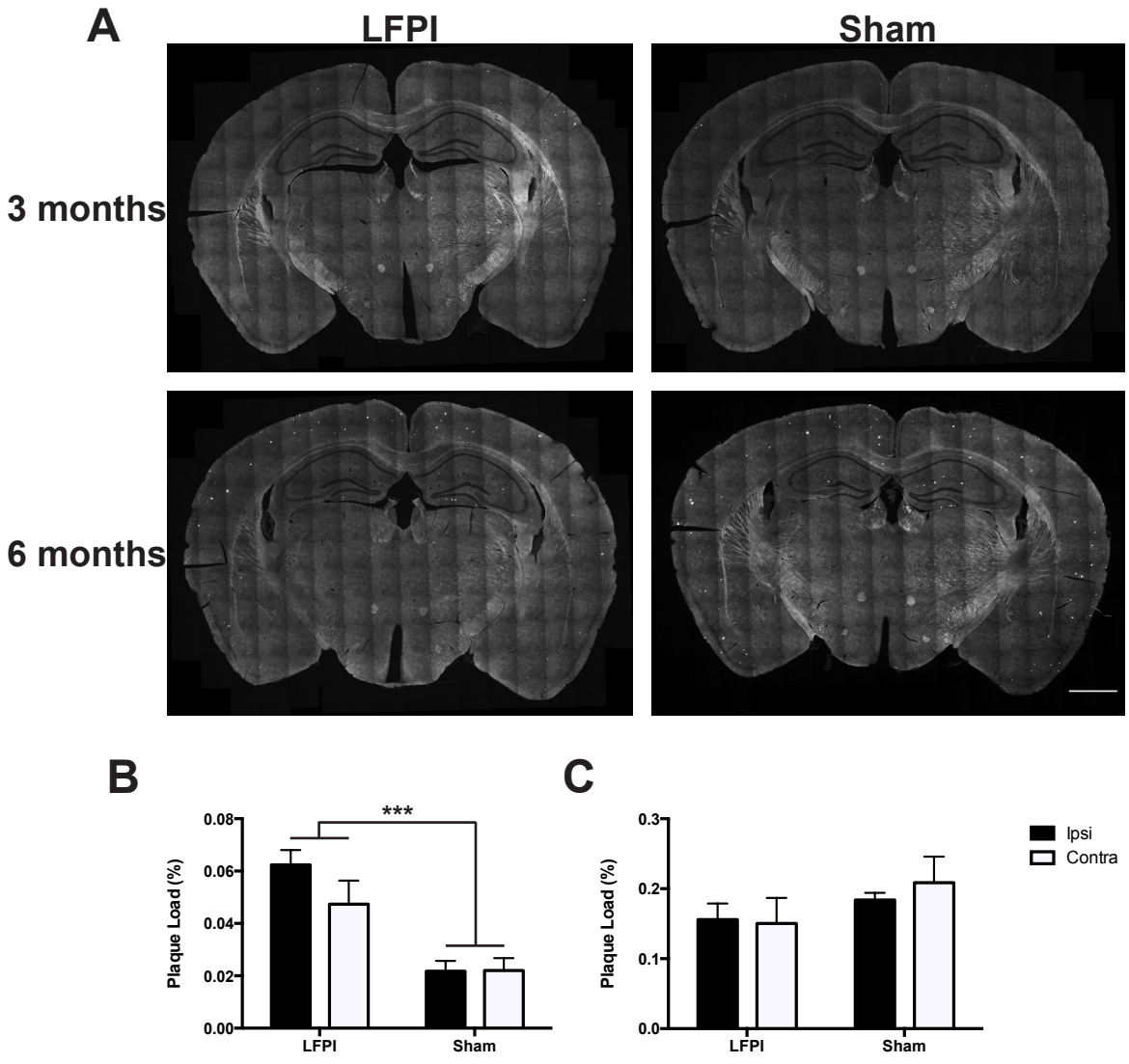
A
LFPI
Sham
3 months
6 months
B
***
Plaque Load (%)
0.08
0.06
0.04
0.02
0.00
LFPI
Sham
C
Plaque Load (%)
0.3
0.2
0.1
0.0
LFPI
Sham
Ipsi
Contra

Figure 4.5 LFPI does not cause Aβ plaque deposition in WT mice at 30 days post-injury. Aβ immunohistochemistry with the MOAB-2 antibody and thioflavin-S staining in injured and sham WT mice. Scale bar=1000μm.

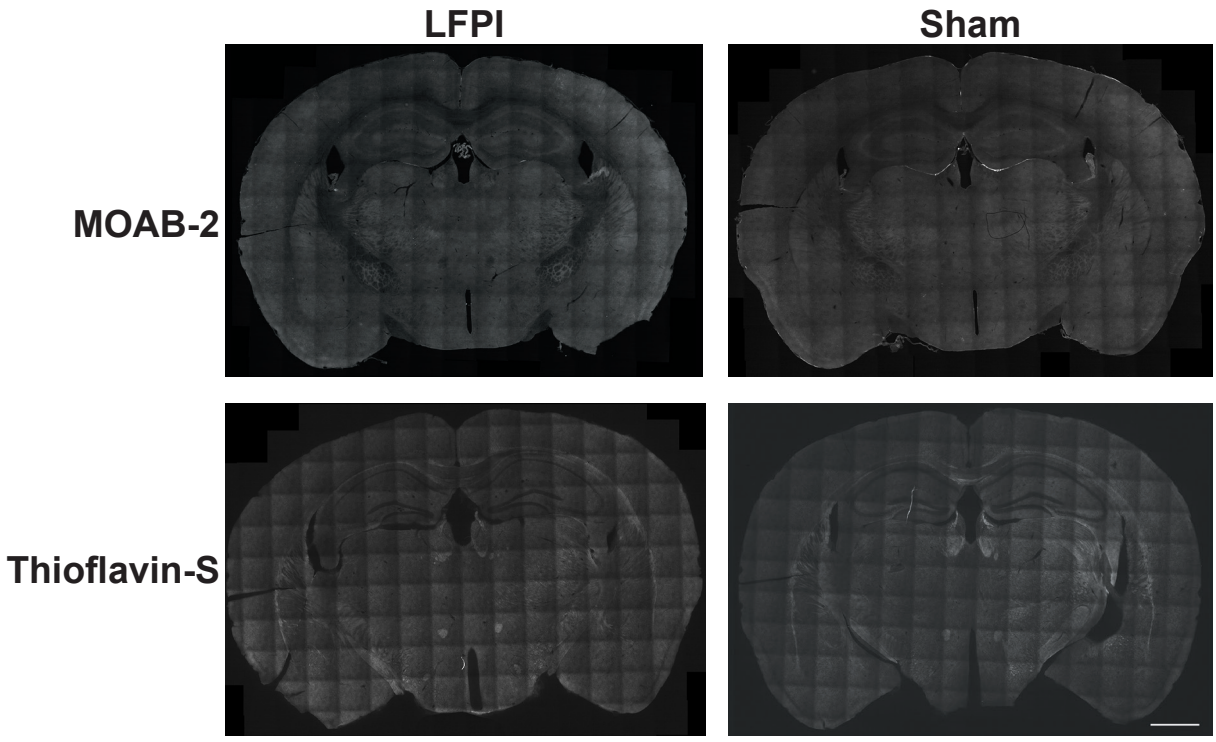
LFPI
Sham
MOAB-2
Thioflavin-S

Table 4.2 Percentage area covered by GFAP labelled astrocytes, and Iba-1 labelled microglia/macrophages.

Group	% area GFAP	% area Iba-1
3m APP/PS1 LFPI	28.3 ± 1.6	14.4 ± 1.0
3m APP/PS1 Sham	23.9 ± 3.5	12.5 ± 0.7
6m APP/PS1 LFPI	24.4 ± 3.0	15.5 ± 1.0
6m APP/PS1 sham	27.9 ± 2.5	16.4 ± 1.2
6m WT LFPI	24.2 ± 3.1	14.7 ± 1.3
6m WT Sham	19.3 ± 0.6	14.6 ± 1.4

3m, 3 months; 6m, 6 months.

4.3.7 Microglial/macrophage response at 30 days post-LFPI

The microglial/macrophage response to LFPI was examined using the Iba-1 antibody. Microglia surrounded Aβ plaques in both 3- and 6-month-old injured and sham mice (Figure 4.7A). In the 3-month-old cohort, there was no significant difference in the percent area covered by Iba-1-labelled microglia/macrophages in sections from injured and sham APP/PS1 mice at 30 days post-injury ($p>0.05$, Figure 4.7B). In the 6-month-old cohort, 30 days after LFPI, there were no significant main effects of treatment ($p>0.05$) or genotype ($p>0.05$) on the percent area Iba-1-labelled ($p>0.05$, Figure 4.7B). There was also no treatment x genotype interaction ($p>0.05$) for the percent area Iba-1-labelled. Therefore, at 30 days post-injury, there was no difference in the percent area of Iba-1-labelled microglia/macrophages in injured mice compared to sham treated mice or in APP/PS1 mice versus WT mice. Table 4.2 summarises the means ± SEM for each group analysed.

4.3.8 Hyperphosphorylated tau at 30 days post-LFPI

The AT8 antibody against hyperphosphorylated tau was used to examine misprocessing of tau following LFPI. As previously reported in other transgenic mouse models of AD (Woodhouse et al., 2009), AT8-immunoreactivity was detected within a small subgroup of dystrophic neurites surrounding Aβ plaques in APP/PS1 mice (see Figure 3.5). No AT8 labelling was detected within neurons anywhere else in the cortex at 30 days post-injury in any group of mice (Figure 4.8).

Figure 4.6 There is no difference in the percent area of astrocytic labelling between injured and sham mice or APP/PS1 and WT mice at 30 days post-injury. (A) GFAP immunolabelling in the ipsilateral cortex. Scale bar=500μm. (B) There were no significant differences ($p<0.05$) in the percent area of GFAP immunolabelling between injured and sham treated mice or APP/PS1 and WT mice at 30 days post-injury. Bars represent means ± standard error.

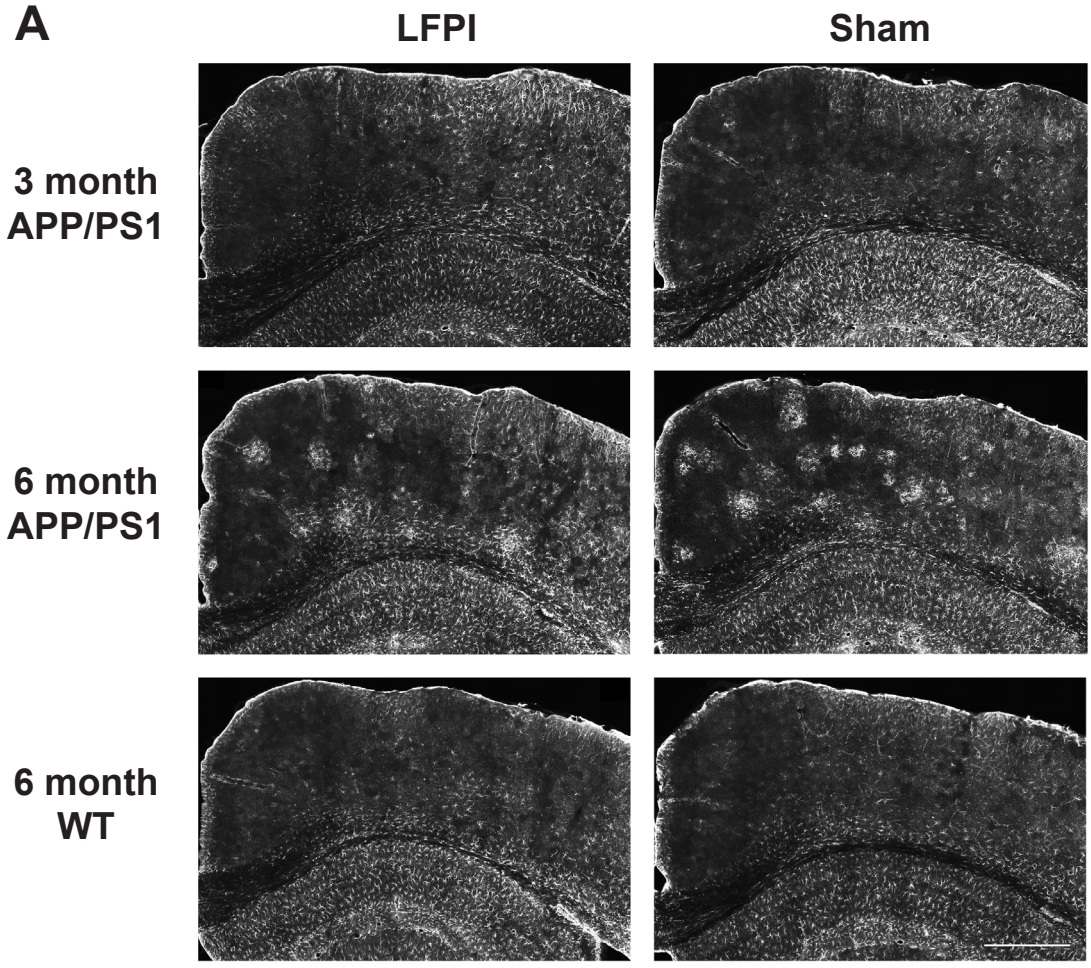
A
LFPI
Sham
3 month APP/PS1
6 month APP/PS1
6 month WT

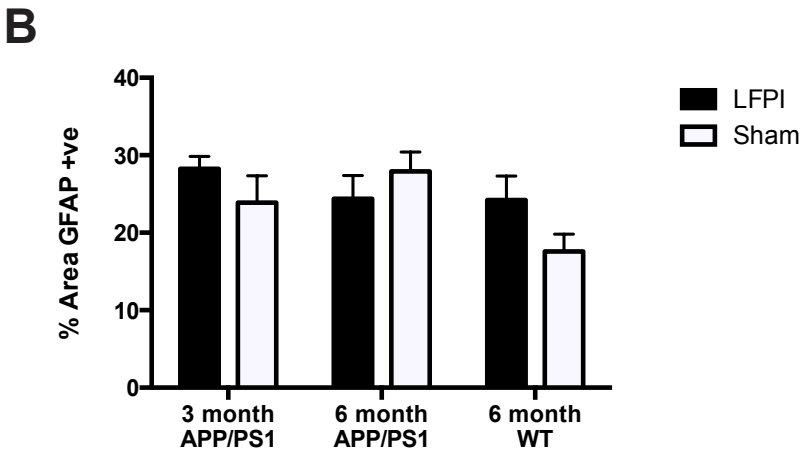
B
% Area GFAP +ve
40
30
20
10
0
3 month APP/PS1
6 month APP/PS1
6 month WT
LFPI
Sham

Figure 4.7 There is no difference in the percent area of microglial/macrophage labelling between injured and sham mice or APP/PS1 mice and WT mice at 30 days post-injury. (A) Iba-1 immunolabelling in the ipsilateral cortex. Scale bar=500μm. (B) There were no significant differences ($p<0.05$) in the percent area of Iba-1 immunolabelling between injured and sham treated mice or APP/PS1 and WT mice at 30 days post-injury. Bars represent means ± standard error.

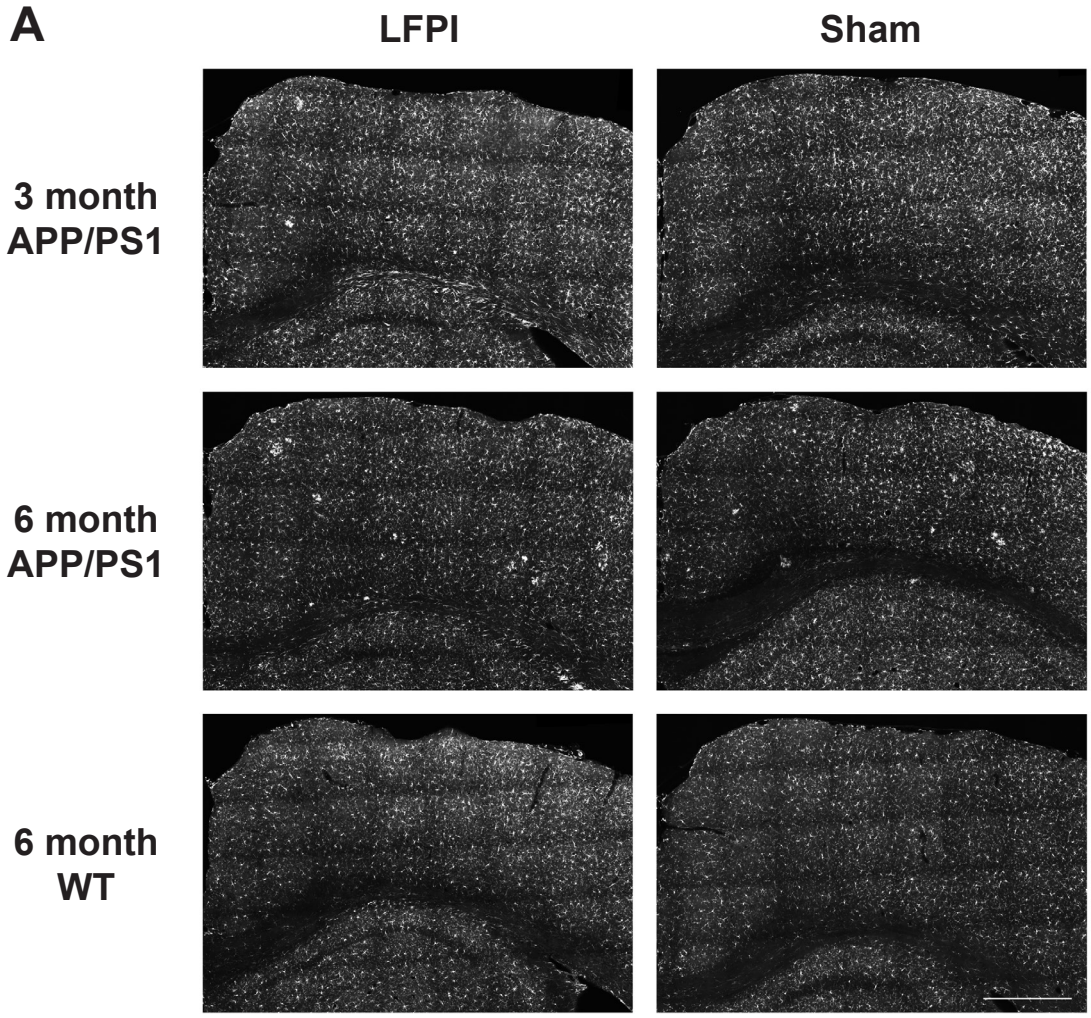
A
LFPI
Sham
3 month APP/PS1
6 month APP/PS1
6 month WT

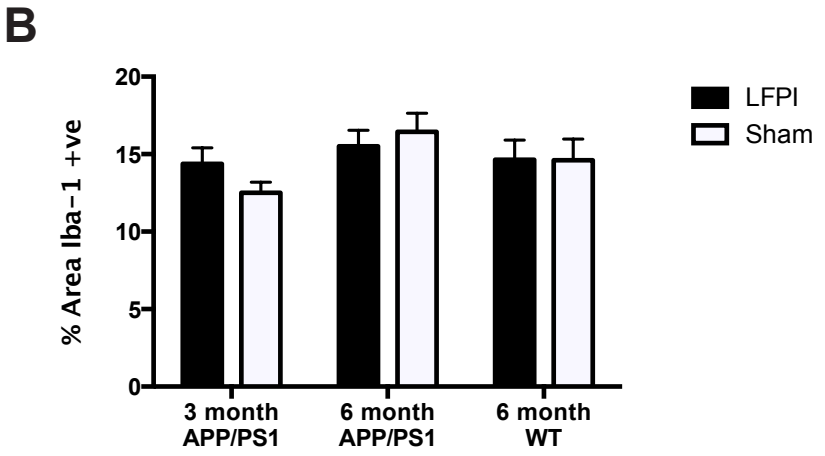
B
% Area Iba−1 +ve
20
15
10
5
0
3 month APP/PS1
6 month APP/PS1
6 month WT
LFPI
Sham

Figure 4.8 LFPI does not induce hyperphosphorylated tau at 30 days post-injury in APP/PS1 or WT mice. AT8 immunolabelling in the ipsilateral cortex. No immunolabelling was observed except in dystrophic neurites surrounding plaques (data not shown, see figure 3.5). Scale bar = 50μm.

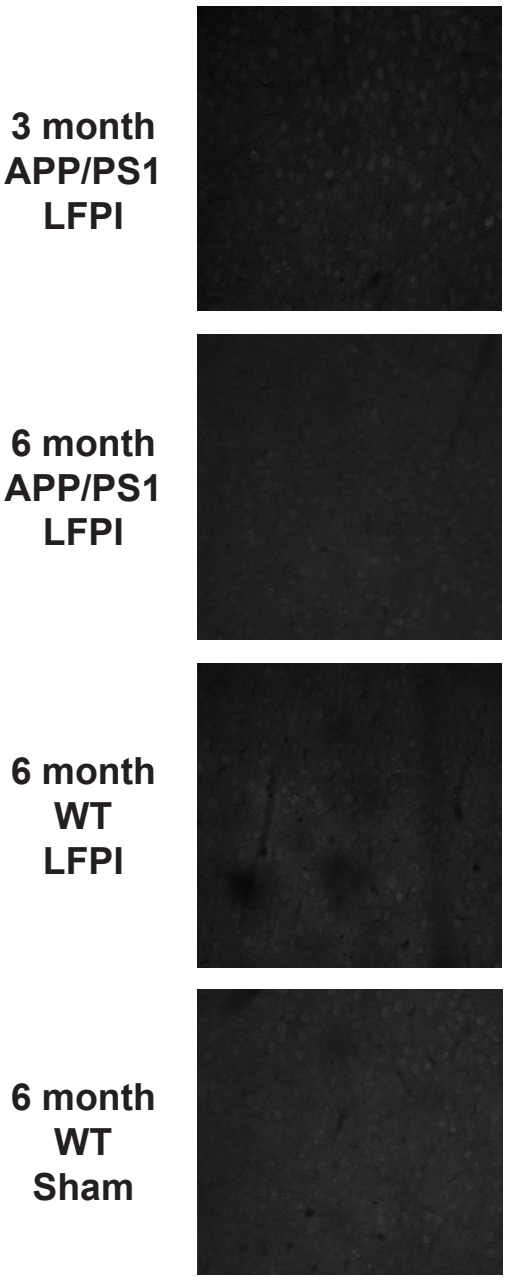
3 month
APP/PS1
LFPI
6 month
APP/PS1
LFPI
6 month
WT
LFPI
6 month
WT
Sham

4.3.9 Neurofilament changes at 30 days post-LFPI

Changes to neurites at 30 days after LFPI were examined by using the SMI-312 and SMI-32 antibodies. SMI-312 is an antibody cocktail containing antibodies that bind to a variety of phosphorylated neurofilament epitopes, principally labelling axons, whereas SMI-32 labels a non-phosphorylated epitope on neurofilament H and, thus, visualizes neuronal cell bodies, dendrites and some axons (Sternberger and Sternberger, 1983, Goldstein et al., 1983). Besides Aβ plaque-associated dystrophic neurites, no neuritic pathology was visualized with these markers at 30 days post-injury in any group of mice (Figure 4.9).

Figure 4.9 No neurofilament-positive neuritic pathology was observed at 30 days after LFPI in APP/PS1 or WT mice. SMI-312 and SMI-32 immunolabelling in the ipsilateral cortex. No neuritic pathology was observed except dystrophic neurites surrounding plaques (data not shown). Scale bar = 50μm.

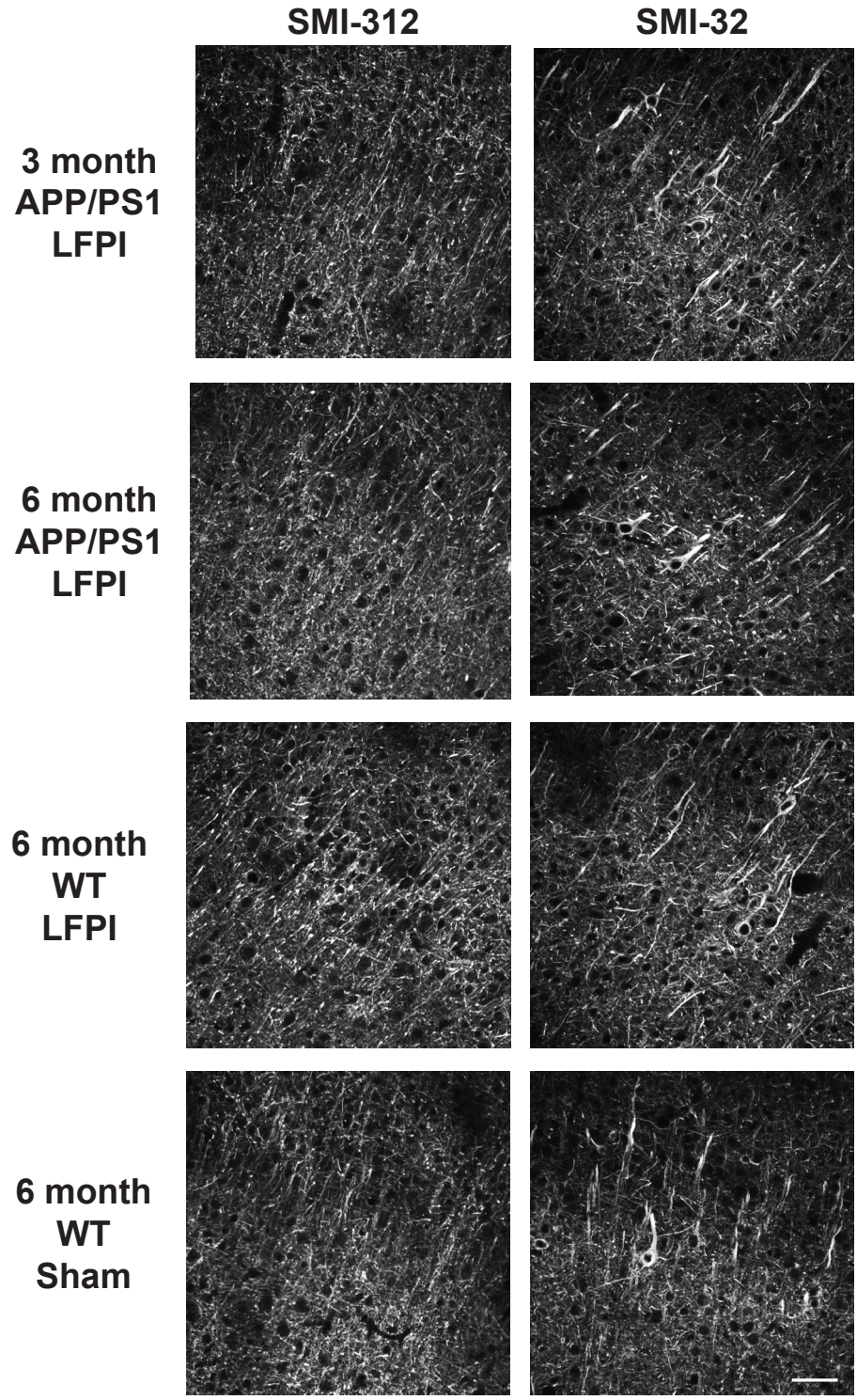
SMI-312
SMI-32
3 month APP/PS1 LFPI
6 month APP/PS1 LFPI
6 month WT LFPI
6 month WT Sham

4.4 Discussion

Understanding the pathological mechanism underlying the relationship between TBI and Aβ plaque deposition may lead to a better understanding of sporadic AD and direct the development of therapeutic interventions. The current study sought to investigate whether, and how, Aβ plaque dynamics are altered after LFPI as previous studies in transgenic models have reported conflicting results (Uryu et al., 2002, Nakagawa et al., 1999, Nakagawa et al., 2000, Smith et al., 1998, Collins et al., 2015). This study demonstrated both increased and decreased Aβ plaque deposition in APP/PS1 mice depending on the stage of Aβ deposition at the time of TBI. In 3-month-old pre-plaque APP/PS1 mice, injury accelerated total and fibrillar Aβ deposition in the cortex bilaterally after LFPI. However, in 6-month-old APP/PS1 mice with established amyloidosis, LFPI resulted in a bilateral decrease in total, but not fibrillar, Aβ plaque load in the cortex after LFPI. Hence, this study indicates that the stage of amyloidosis in the transgenic AD mouse model at the time of TBI may be a factor in determining the response of the brain to injury, including subsequent Aβ dynamics.

Comparisons between this and previous animal studies are difficult to make due to many differing experimental factors including: the time points analysed after injury, the AD transgenic mouse model used, the injury model and severity used and the area of the brain analysed for Aβ plaque deposition. The current data does, however, replicate many of the findings in previous literature. First, the current study supports the results of Uryu et al. (2002), which also show an increase in Aβ plaque load in AD transgenic mice injured prior to the development of amyloidosis. Second, in transgenic mice with established amyloidosis, our results support those of Nakagawa et al. (2000) showing a decrease in Aβ plaque load after injury. Third, as previously reported in numerous other studies, no plaques were observed in WT mice after TBI (Bramlett et al., 1997, Ciallella et al., 2002, Iwata et al., 2002, Masumura et al., 2000, Pierce et al., 1996) indicating that, in these models, the human APP isoform, possibly requiring mutation and overexpression, is still a requirement for brain amyloidosis.

The finding of increased Aβ plaque load in APP/PS1 mice injured prior to plaque development also supports epidemiological data showing accelerated AD onset in genetically predisposed individuals with a history of TBI (Nemetz et al., 1999) as well as post-mortem human data showing plaque deposition following TBI (Chen et al., 2009, DeKosky et al., 2007, Ikonomovic et al., 2004, Johnson et al., 2012, Nicoll et al., 1995, Roberts et al., 1991, Roberts et al., 1994, Smith et al., 2003, Uryu et al., 2007).

A potential mechanism for the increase in Aβ plaque deposition reported in the current study may be TBI-induced DAI. DAI is a significant pathology in TBI and is characterized by axonal swellings, which occur due to injury-induced damage to the axonal cytoskeleton, causing transport deficits and subsequent accumulation of cargoes (Tang-Schomer et al., 2012, Tang-Schomer et al., 2010). APP undergoes fast axonal transport (Koo et al., 1990) and its accumulation after TBI is a pathological hallmark of DAI (Gentleman et al., 1993, Otsuka et al., 1991, Sherriff et al., 1994). This study and other have shown the accumulation of APP's cleavage product Aβ within diffusely injured axons after experimental TBI in transgenic AD mouse models (Abrahamson et al., 2006, Tran et al., 2011a, Tran et al., 2011b) and in human TBI cases (Chen et al., 2009, Smith et al., 2003, Uryu et al., 2007). Furthermore, a study of TBI in swine demonstrated injury-induced plaques in the white matter tracts of pigs with the most extensive axonal pathology (Smith et al., 1999).

Further evidence for axonal transport deficits leading to Aβ plaque deposition comes from a study by Stokin et al. (2005) demonstrating that experimentally-induced interruption of axonal transport by down-regulation of kinesin-I results in more axonal swellings and increased Aβ deposition in the brains of transgenic AD mice. Furthermore, the study also demonstrated axonal swellings, morphologically similar to those seen in axonal injury, in AD transgenic mouse models prior to Aβ plaque deposition and in areas of the human brain devoid of Aβ plaques in early AD (Stokin et al., 2005). Thus, interrupted axonal transport and intracellular accumulation of Aβ may be early pathogenic events in the development of plaques.

The release of Aβ from axonal swellings may occur by the normal route, which is endosome recycling to the cell surface (Yamazaki et al., 1996, Koo et al., 1996, Koo and Squazzo, 1994) or by axonal disconnection or lysis. Intracellular Aβ42 accumulation is suggested to be neurotoxic to neurons (Kienlen-Campard et al., 2002), and thus following TBI may result in neuronal cell death, expulsion of Aβ and plaque formation.

The increase in cortical Aβ plaque load reported in this study was bilateral, which may be explained by the commissural connections between the two cerebral hemispheres. Commissural axons projecting into both hemispheres would be injured within the white matter tracts by LFPI, and thus if axonal transport deficits cause increased Aβ deposition, both hemispheres would show increased plaque load.

Alternatively, the bilateral changes in Aβ plaque load after TBI may be due to disruption in normal neuronal activity within the cortex. It has been shown previously that unilateral ablation of the olfactory epithelium and thus removal of peripheral sensory input, results in decreased Aβ plaque load in the olfactory bulb and cortex, bilaterally in APP/PS1 mice (Bibari et al., 2013). Similarly, 28 days of unilateral vibrissae deprivation in APP/PS1 mice has been shown to reduce Aβ plaque growth and formation in the barrel cortex (Bero et al., 2011). Thus LFPI may have caused enhanced or reduced cortical neuronal activity, resulting in increased or decreased Aβ plaque deposition at 30 days post-injury.

In contrast to the increase in Aβ plaque deposition observed in injured 3-month-old mice, this study also demonstrated a significant reduction in cortical Aβ plaque load bilaterally in injured 6-month-old mice compared to their uninjured counterparts.

A reduction in Aβ plaque load in brain-injured mice may potentially be due to either decreased deposition or increased clearance. A possible mechanism for increased Aβ plaque clearance after TBI is via increases in activated glia. The brain possesses two types of microglia, resident microglia and newly differentiated microglia derived from bone marrow stem cells (reviewed in

Soulet and Rivest, 2008). Following TBI, resident microglia become activated and migrate to the site of injury (Davalos et al., 2005). Similarly, neurological insults have been shown to induce the migration of bone marrow derived macrophages (BMDM) into the brain, which differentiate into microglia (Priller et al., 2001).

In AD, activated microglia surround Aβ plaques (reviewed in Malm et al., 2015) and in transgenic AD mouse models, many of these cells have been demonstrated to be BMDM (Simard et al., 2006), which are chemoattracted to Aβ40/42, have a specific immune reaction to Aβ and possess the ability to phagocytose Aβ plaques (Simard et al., 2006). Depletion of BMDM results in increased Aβ plaque deposition in the APP/PS1 mouse model of AD (Simard et al., 2006) and local inflammation induced by lipopolysaccharide injections into the hippocampus increases the infiltration of these cells while decreasing the Aβ plaque burden (Malm et al., 2005). Thus, following TBI, phagocytic BMDM recruited into the brain due to injury-induced inflammation may phagocytose existing Aβ plaques leading to an overall reduction in plaque load in 6-month-old APP/PS1 mice. In plaque-free 3-month-old APP/PS1 mice, Aβ plaques are not present for the BMDMs to phagocytose. Instead these cells will only have the TBI-induced damage to responds to, where they have been shown to have both beneficial and detrimental effects (reviwed in Loane and Byrnes, 2010). Detrimental effects include inducing an inflammatory environment, which has been suggested to enhance Aβ plaque formation (reviewed in Streit, 2004a).

Astrocytes like microglia and BMDM have also been shown to phagocytose Aβ (Funato et al., 1998, Wyss-Coray et al., 2003a), as well as be detrimental in AD due to the release of pro-inflammatory molecules (reviewed in Verkhratsky et al., 2010). Both the microglial and astrocytic responses were measured at 30 days after injury and no differences in the percent area of immuno-labelling for either cell type was found. At this protracted time point, an earlier difference may not be apparent or the sample size may have been inadequate to detect a significant result. Thus, an analysis of the glial responses in APP/PS1 mice throughout the time course after TBI should be the focus of future studies. There may also have been morphological or phenotypical differences in the microglia or astrocytes of

injured mice compared to sham mice, or APP/PS1 mice compared to WT mice. This limitation should be addressed in future studies examining the morphology of glial cells, and assessing the contribution of BMDM to the glial response. One phenotypical difference in astrocytes that may affect Aβ dynamics after TBI is the expression of AQP4. AQP4 is an integral part of the glymphatic system and is expressed perivascularily on astrocytic endfeet where it plays an important role in the clearance of solutes, including Aβ (Iliff et al., 2012). However, following TBI, AQP4 expression mislocalises from the perivascular astrocytic endfeet to the soma (Ren et al., 2013). This may result in inefficient clearance of Aβ following TBI, and the development of plaques. Other clearance mechanisms that may be affected following TBI include changes in the expression and/or activity of neprilysin (Chen et al., 2009, Iwata et al., 2000, Johnson et al., 2009) and alterations to the newly discovered cerebral lymphatic system (Louveau et al., 2015), both of which warrant further investigation.

As WT rodents do not form Aβ with aging (Selkoe, 1989) or after TBI (Bramlett et al., 1997, Ciallella et al., 2002, Iwata et al., 2002, Masumura et al., 2000, Pierce et al., 1996), the following study used the APP/PS1 mouse model of AD. This transgenic mouse model expresses two familial AD mutations and develops Aβ plaques at a young age (Jankowsky et al., 2001). As the majority of human TBI sufferers are not genetically predisposed to developing AD, this limitation must be taken into account when interpreting the results of this study. Furthermore, although the LFPI is a clinically relevant model, it does not recapitulate all of the features of human TBI (Xiong et al., 2013). For example the need for a craniotomy limits the formation of raised intracranial pressure (Albert-Weissenberger and Siren, 2010) following TBI and the effect of such factors on Aβ plaque deposition and tau hyperphosphorylation are unknown. Although the current study did not demonstrate tau hyperphosphorylation as reported in previous studies of TBI (Goldstein et al., 2012, Smith et al., 1999) it is possible that at more acute or chronic time points or using different phosphorylated-tau antibodies this pathology is present.

In conclusion, this study demonstrated that experimental TBI in the APP/PS1 mouse model of AD can modulate Aβ plaque deposition in the cortex bilaterally

at 30 days post-injury, but that the effect of injury is dependent on the stage of amyloidosis at the time of TBI.

5 The effect of alterations to the neurofilament cytoskeleton on the axonal response to diffuse traumatic brain injury

5.1 Introduction

TBI causes straining and shearing forces on the brain, which results in DAI (Adams et al., 1982, Gennarelli et al., 1982, Strich, 1956, Strich and Oxon, 1961). DAI is characterized by neurite swellings representing impaired axonal transport as well as neuritic bulbs representing axonal disconnection (Hanell et al., 2014, Tang-Schomer et al., 2012, Tang-Schomer et al., 2010). The previous chapter identified axonal transport deficits using APP immunohistochemistry at 24 hours following LFPI. Furthermore, Aβ was shown to co-accumulate with APP in diffusely injured axons. The accumulation of APP and Aβ within injured axons may be a mechanism by which TBI leads to increased Aβ plaque deposition, as seen in the previous chapter, and thus increases the risk of developing AD.

The impairment of axonal transport and disconnection of axons following TBI is in part due to damage to the axonal cytoskeleton (Smith and Meaney, 2000, Tang-Schomer et al., 2012, Tang-Schomer et al., 2010). The axonal cytoskeleton is comprised of microtubules, actin filaments and NFs. Following TBI, breakage, disorganization and disassembly of microtubules causes interruption to axonal transport resulting in the accumulation of transported cargoes and thus axonal swellings (Tang-Schomer et al., 2012, Tang-Schomer et al., 2010). TBI may also cause degradation of NFs due to the activation of proteases, including calpain (Buki et al., 2003, Ma et al., 2013) as well as a reduction in the interfilament spacing of NFs, termed NF compaction (Pettus et al., 1994, Povlishock et al., 1997). NF compaction has been hypothesized to be part of the same evolving axonal pathology as microtubule disassembly, ultimately leading to axonal transport deficits (Pettus et al., 1994, Povlishock and Pettus, 1996), but recent evidence suggests it occurs independently and is a separate injury phenotype (Marmarou et al., 2005, Stone et al., 2001).

NFs in the central nervous system are comprised of four subunits, NF heavy (NFH), NF medium (NFM), NF light (NFL) and alpha-internexin, which co-polymerise into obligate heteropolymers forming intermediate filaments (reviewed in Yuan et al., 2012). NFs are exceedingly abundant in many axons and are expressed in a subset of neurons in the brain (Vickers and Costa, 1992, Kirkcaldie et al., 2002). The genetic deletion of the NFL protein has been shown to significantly alter the expression and distribution of the other NF subunits throughout the cortex, however cortical structure and cytoarchitecture remain apparently normal (Liu et al., 2013).

In AD, the accumulation of NFs in dystrophic neurites is an early neuronal change associated with Aβ plaque formation (Vickers et al., 1996, Masliah et al., 1993, Dickson et al., 1999) and neurons expressing NFs are selectively vulnerable to tau neurofibrillary tangle formation and degeneration (Mitew et al., 2013b, Vickers and Costa, 1992, Vickers et al., 1994). Furthermore, the deletion of NFL in the APP/PS1 mouse model of AD has been shown to result in increased Aβ plaque deposition and enhanced dystrophic neurite formation (Fernandez-Martos et al., 2015). Thus, these studies demonstrate that the NF network is important in the neuronal and axonal responses to AD-associated pathology and perhaps etiology.

Axons lacking NFL show reduced APP accumulation in damaged neurites and attenuated regeneration following *in vitro* localized axotomy (Blizzard et al., 2013). However, the exact effect of ablating the NF network on the axonal response to diffuse TBI *in vivo* remains unknown. This chapter explores whether the deletion of NFL affects axonal transport deficits following TBI, as shown by APP immunohistochemistry. To this end, mice with homozygous deletion of NFL (NFLKO) and WT mice (NFLWT) were subjected to LFPI and changes in the accumulation and expression of APP were examined by immunohistochemical and biochemical assays.

5.2 Materials and Methods

5.2.1 Mice

Male transgenic mice harbouring a disruption of the NFL gene (C57BL/6J×129Sv.NFL$^{-/-}$) were a gift from Dr Jean-Pierre Julien (Université Laval, Canada) and were maintained as a homozygous colony (Zhu et al., 1997) by Dr Mala Rao (Nathan Kline Institute, New York). As most antibodies used to label axons by immunohistochemistry are directed against NF proteins, and this project was part of a larger study, the C57BL/6×129Sv.NFL$^{-/-}$ mice were crossed with YFPH transgenic mice (Jackson Laboratory, USA, Strain B6.Cg-Tg(Thy1-YFP$^{+/-}$)HJrs/J, Stock No. 003782) to obtain an F1 generation (NFL$^{+/-}$.Thy1-YFPH$^{+/-}$ and NFL$^{+/-}$.Thy1-YFPH$^{-/-}$). The F1 generation was then crossed to obtain transgenic mice with a disruption of the NFL gene and neuronal YFP expression (C57BL/6×129Sv.NFL$^{-/-}$.Thy1-YFPH$^{+/-}$) and with normal NFL gene expression and neuronal YFP expression (NFL$^{+/+-}$.Thy1-YFPH$^{+/-}$). In the studies included in this thesis both mice expressing neuronal YFP (YFPH positive, Thy1-YFPH$^{+/-}$) and not expressing neuronal YFP (YFPH negative, Thy1-YFPH$^{-/-}$) were used. Therefore, the mice used in this study were NFLKO mice (either NFL$^{-/-}$.Thy1-YFPH$^{+/-}$ (YFPH positive) or NFL$^{-/-}$.Thy1-YFPH$^{-/-}$ (YFPH negative)) and NFLWT mice (either NFL$^{+/+}$.Thy1-YFPH$^{+/-}$ or NFL$^{+/+}$.Thy1-YFPH$^{-/-}$). All experimental procedures were undertaken on mice between the ages of 2-6 months and, due to time constraints on breeding, both male and female mice were utilized for some experiments. Table 5.1 outlines the genders and genotypes of the mice used in each set of experiments.

5.2.2 Genotyping

Mice were genotyped as specified in the Materials and Methods section 2.2. Specific primers to the genes YFP, NFL, neomycin phosphotransferase (present within the pMC1neoPoly A vector indicating deletion of NFL) and Tcrd (internal control) were used to determine the genotypes of mice used. Refer to Table 5.2 for primer sequences and PCR product sizes.

Table 5.1 Genotypes of the mice used for experiments.

Experiment	**NFL genotype**	**Gender**	**YFPH genotype**	**Number**
LFPI Immunohistochemistry	NFLKO	male	positive negative **Total**	6 - **6**
	NFLWT	male	positive negative **Total**	2 4 **6**
Sham Immunohistochemistry	NFLKO	male	positive negative **Total**	3 - **3**
	NFLWT	male	positive negative **Total**	4 - **4**
LFPI Western Blot	NFLKO	male female	positive negative positive negative **Total**	1 2 1 2 **6**
	NFLWT	male female	positive negative positive negative **Total**	2 1 1 2 **6**
Sham Western Blot	NFLKO	male female	positive negative positive negative **Total**	2 1 2 1 **6**
	NFLWT	male female	positive negative positive negative **Total**	2 1 2 1 **6**

Table 5.2 Genotyping PCR primers.

Gene	Primer sequence	Product Size (bp)
YFP	forward 5'- TCTGAGTGGCAAAGGACCTTAGG-3' reverse 5'- CGCTGAACTTGTGGCCGTTTACG-3'	300
NFL	forward 5'-CAGCTTCATCGAGCGCGTGC-3' reverse 5'-CGTCGGTGTTCTTGGCGGC-3'	589
Neo Insert	forward 5'-CTGAATGAACTGCAGGACGAG-3' reverse 5'-GGCAAGCAGGCATCGCCATG-3'	413
Tcrd	forward 5'- CAA ATGTTGCTTGTCTGGTG3'-3' reverse 5'- GTCAGTCGAGTGCACAGTTT-3'	200

5.2.3 In vivo diffuse traumatic brain injury

LFPI was performed as outlined in the Materials and Methods section 2.4. A mild injury severity of 1.25-1.35atm was used. Surgeries were performed by two trained individuals.

5.2.4 Tissue preparation

At 3 days post-injury, mice were terminally anaesthetized, transcardially perfused and tissue was prepared for either immunohistochemistry or Western blotting as outlined in the Materials and Methods section 2.4. For immunohistochemical studies serial 50μm coronal sections were cut on a vibratome (Leica VT1000).

5.2.5 Immunohistochemistry

Immunohistochemistry was performed as outlined in Materials and Methods, section 2.6.1. To detect DAI, a polyclonal rabbit anti-APP antibody was used followed by an Alexa 594-conjugated goat anti-rabbit IgG secondary antibody (refer to Table 2.1 in the Materials and Methods for antibody dilutions and details).

5.2.6 Protein extraction and Western blotting

Protein extraction and Western blotting was performed as outlined in the Materials and Methods section 2.7. For each sample, 20μg of protein was loaded onto the gel. The expression of APP was normalized to the loading control GAPDH and ImageJ software was used to measure the integrated intensity of bands (refer to Table 2.1 in the Materials and Methods section for antibody concentrations). Western blotting and quantification was performed blinded to treatment and genotype.

5.2.7 Confocal microscopy and quantitation

Confocal microscopy was performed on a Perkin-Elmer Ultraview VOX confocal imaging system using Volocity 6.3 software for image capture and stitching (10% overlap, no corrections). APP accumulations within the white matter tracts were imaged using a 20x objective. Analysis was performed on the deep cortical white matter tracts, including the cingulum, from the midline to the end of the lateral ventricle/hippocampus on a single plane between bregma – 0.34 and bregma – 1.94 for 3 sections per mouse. APP-positive axonal profiles within the region of interest were counted manually using ImageJ. The region of interest was then measured using ImageJ, and counts expressed as the number of APP-positive axonal profiles/mm^2. Confocal microscopy and analysis were performed blinded to genotype.

5.2.8 Statistical analysis

Data were analysed using SPSS (Version 19, IBM). For axonal profile counts, Student's two-tailed t-test was used to compare injured NLFKO to injured NFLWT mice. For the analyses of Western blot data, Student's two-tailed t-test showed no sex difference in any of the groups, and thus male and female data was pooled for ANOVA analysis. An ANOVA with the factor variables of treatment (LFPI or sham) and genotype (NFLKO or NFLWT) as well as a full factorial ANOVA looking at the interaction between these two these two factors was performed. All data are expressed as means ± standard error of the mean (SEM) with significance set at $p < 0.05$.

5.3 Results

5.3.1 LFPI characterisation

The parameters of this LFPI model did not cause obvious cortical loss in NFLKO or NFLWT mice. The mean impact pressure pulses for each group were 1.33 ± 0.03atm for the NFLKO mice and 1.31±0.02atm for the NFLWT mice, and were not significantly different ($p>0.05$, Figure 5.1). This injury did not induce prolonged unconsciousness, with the animals able to right themselves immediately following the injury. APP-positive axonal profiles were observed in the corpus callosum, cingulum, external capsule and hippocampus (Figure 5.2). APP-positive axonal profiles appeared most concentrated in the corpus callosum adjacent to the lateral ventricle, the cingulum and the external capsule (Figure 5.2). APP-positive axonal profiles were not seen in sham treated NFLKO or NFLWT mice (Figure 5.2).

5.3.2 NFL deletion affects the number of APP-positive axonal profiles in white matter tracts at 3 days post-injury.

It is well established in the literature that the accumulation of APP within axons is indicative of DAI (Gentleman et al., 1993, Tang-Schomer et al., 2012). However, it has been shown that axonal accumulations of APP rarely co-localise with intra-axonal NF compaction suggesting they are separate TBI-induced pathologies (Marmarou et al., 2005, Stone et al., 2001) and thus, the role of NFs in DAI and APP accumulation remains unknown. Therefore, the effect of NFL deletion on the axonal response to injury was examined by APP immunohistochemistry. The number of APP-positive axonal profiles per mm^2 within the corpus callosum, cingulum and external capsule was counted. Following LFPI, there were significantly more APP-positive axonal profiles/mm^2 in NFLKO mice than in NFLWT mice (328.3 ± 46.1/mm^2 vs 182.5 ± 42.7mm^2, $p<0.05$, Figures 5.3A and B).

Figure 5.1 Average injury severity as determined by the fluid pressure pulse delivered in atm, did not vary between groups. There was no signficant difference ($p>0.05$) in the average pressure pulse delivered between any of the injured groups. Bars represent means ± standard error.

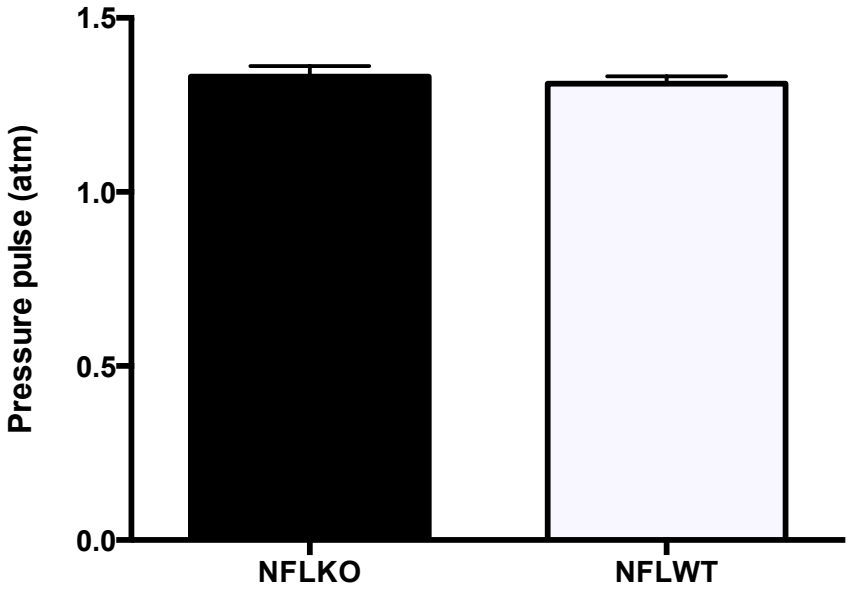
Pressure pulse (atm)
1.5
1.0
0.5
0.0
NFLKO
NFLWT

Figure 5.2 APP-positive axon pathology in NFLKO and NFLWT mice at 3 days post-LFPI. APP immunohistochemistry in the white matter tracts demonstrates APP-positive axonal profiles in NFLKO and NFLWT mice after LFPI. APP-positive axonal profiles are not seen in the white matter tracts of sham treated NFLKO and NFLWT mice. Scale bar=100μm.

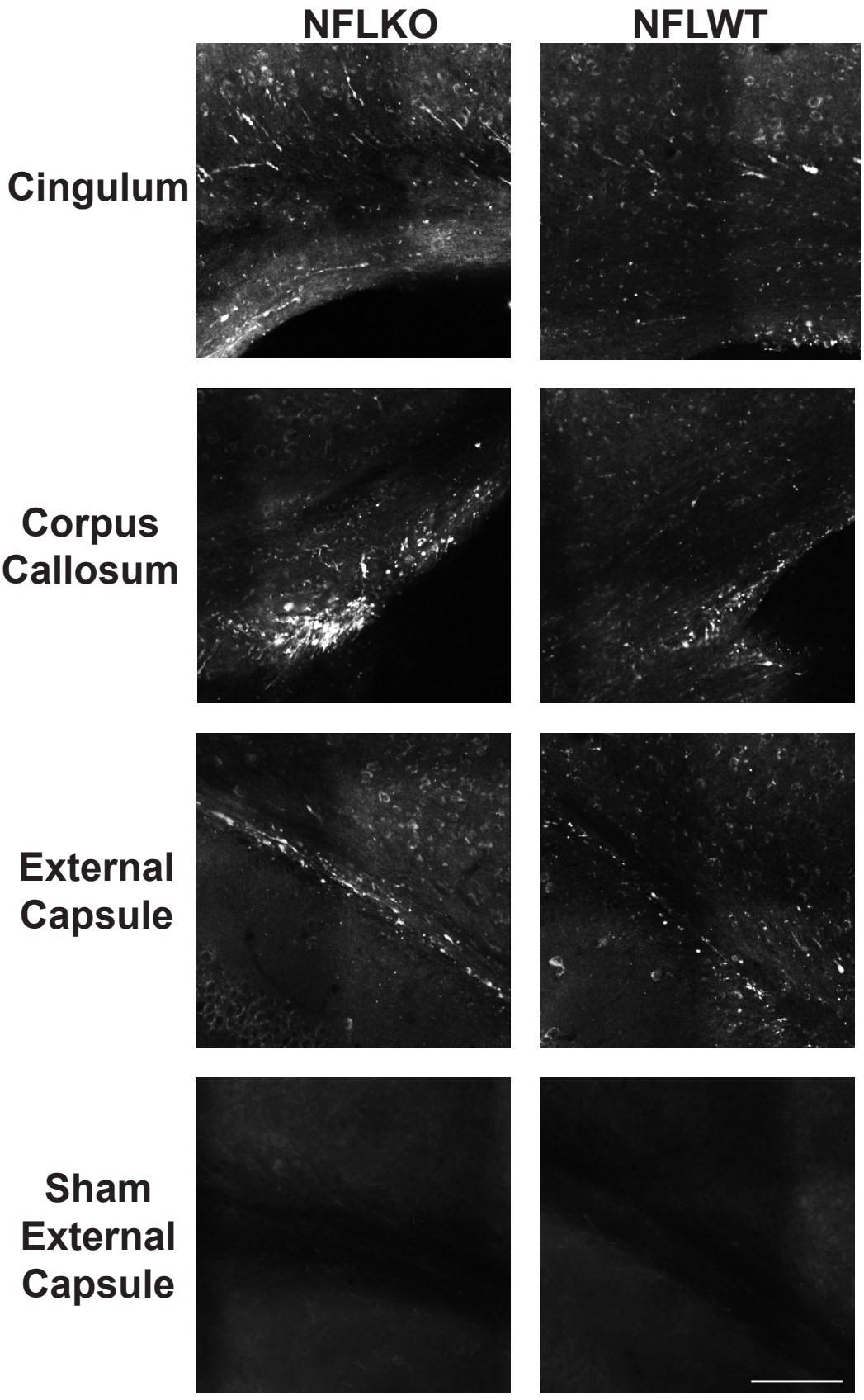
NFLKO
NFLWT
Cingulum
Corpus Callosum
External Capsule
Sham External Capsule

Figure 5.3 NFLKO mice have more APP-positive axonal profiles in the white matter tracts compared to NFLWT mice at 3 days post-injury. (A) Representive sections labelled with APP. Yellow arrows indicate APP-positive axonal profiles. Scale bar=50μm. (B) LFPI caused significantly ($p<0.05$) more APP-positive axonal profiles in NFLKO mice at 3 days post-injury. (C) Bars represent means ± standard error. * denotes significance at $p<0.05$ for NFLKO versus NFLWT.

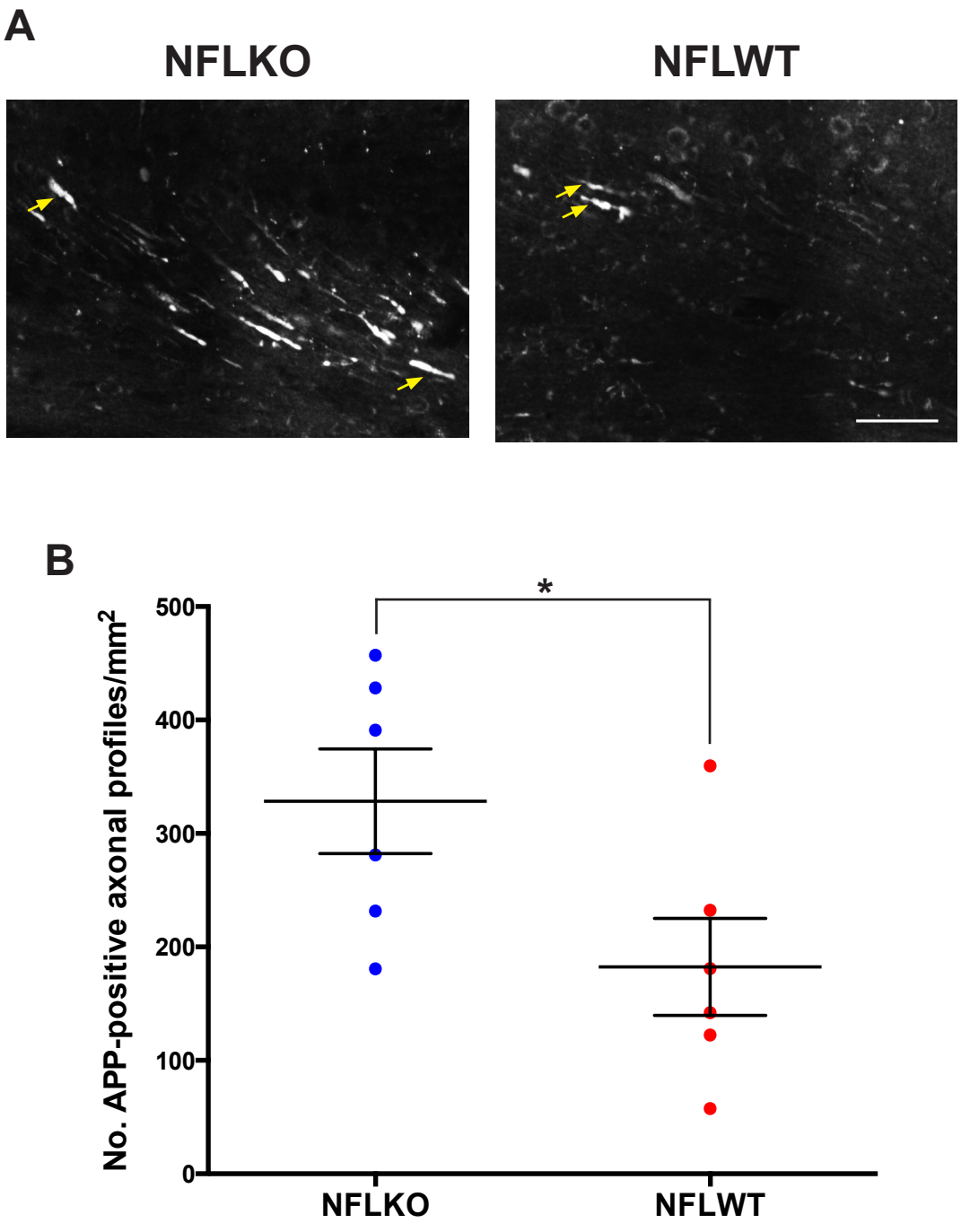
A
NFLKO
NFLWT
B
No. APP-positive axonal profiles/mm2
500
400
300
200
100
0
*
NFLKO
NFLWT

5.3.3 NFL deletion does not alter the expression of APP within the cortex and underlying white matter tracts in injured or sham mice.

To examine whether the deletion of NFL effects the expression of APP in injured and sham mice, Western blot analysis was performed. Ipsilateral cortical tissue including underlying white matter was dissected from injured and sham treated NFLKO and NFLWT mice. This analysis was performed on 3 male and 3 female mice from each genotype for each treatment. There was no significant effect ($p>0.05$) of gender for any group and thus the male and female mice were pooled together for further analyses. There was no significant effect of either treatment ($p>0.05$) or genotype ($p>0.05$) on APP protein levels at 3 days post-injury (Figures 5.4A and B), nor any interaction between these factors ($p>0.05$). Thus, NFL deletion does not affect the expression of APP within the cortex and underlying white matter tracts in either sham-treated or LFPI-treated mice.

Figure 5.4 NFL deletion does not effect APP expression at 3 days post-injury. (A) Representive Western blots for APP and the house keeping gene GAPDH. (B) There was no significant differences in APP expression between NFLKO or NFLWT mice with either injury or sham treatment ($p>0.05$). Bars represent means ± standard error.

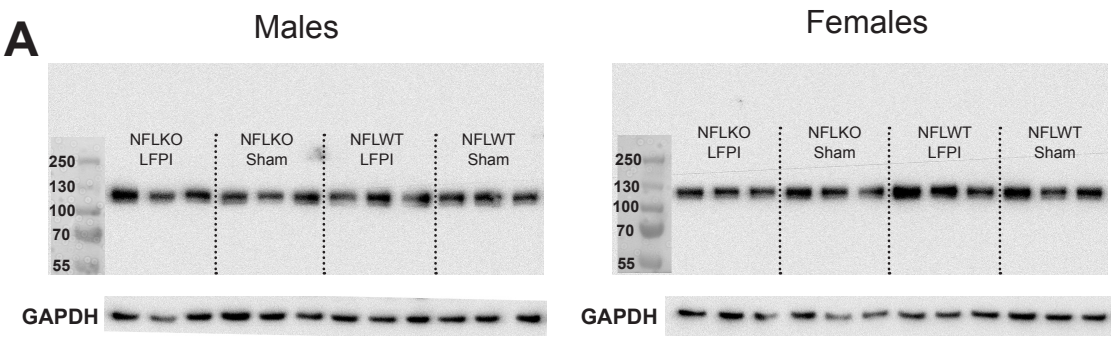
A
Males
Females
NFLKO LFPI
NFLKO Sham
NFLWT LFPI
NFLWT Sham
250
130
100
70
55
GAPDH

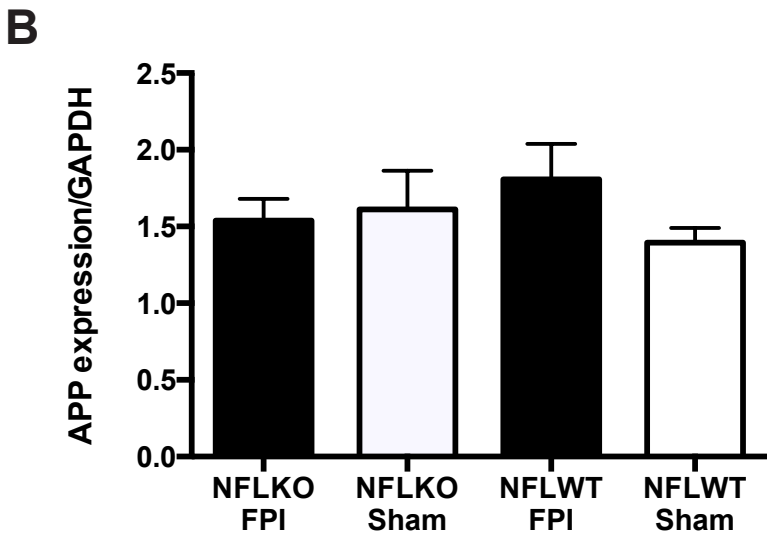
B
APP expression/GAPDH
2.5
2.0
1.5
1.0
0.5
0.0
NFLKO FPI
NFLKO Sham
NFLWT FPI
NFLWT Sham

5.4 Discussion

DAI is one of the most common and significant pathological changes produced by TBI, and has been proposed to be responsible for a substantial proportion of subsequent morbidity (Johnson et al., 2013b). Axons are particularly vulnerable to mechanical injury in brain trauma due to their highly structured arrangement in the white matter tracts and their viscoelastic properties (Smith and Meaney, 2000). During TBI, inertial forces on the head result in rapid stretching of axons (Adams et al., 1982, Gennarelli et al., 1982, Strich, 1956, Strich and Oxon, 1961) culminating in damage to the axonal cytoskeleton and impaired axonal transport (Tang-Schomer et al., 2012, Tang-Schomer et al., 2010). Impaired axonal transport due to the breakage and disassembly of microtubules causes accumulation of transported cargoes (Tang-Schomer et al., 2012, Tang-Schomer et al., 2010), however, the role of NFs in DAI is unclear. Thus, this study sought to determine the effect of NFL deletion on the axonal response to TBI.

APP accumulation is a pathological hallmark of DAI (Gentleman et al., 1993, Tang-Schomer et al., 2012) because it is rapidly transported by kinesin-I (Kamal et al., 2000). Therefore, this study immunolabelled APP to explore the effect of NFL deletion on axonal transport after LFPI, finding that NFLKO mice have more APP-positive axonal profiles in the white matter tracts after LFPI than do NFLWT mice. This increase was not due to higher levels or enhanced upregulation of APP, since biochemical analyses showed no differences in APP levels between NFLKO and NFLWT mice either with or without LFPI.

The increase in APP-positive axonal pathology in NFLKO mice may suggest that axons lacking a complete NF network are more mechanically vulnerable to the stretching caused by TBI, leading to enhanced microtubule breakage and APP accumulation. In support of this notion, previous evidence has shown that NFs can stretch more than three-fold, and may function as mechanical shock absorbers within axons (Kreplak et al., 2005). Furthermore, studies have demonstrated that APP accumulation and NF compaction primarily occur independently and are thus distinct TBI-induced pathologies (Marmarou et al., 2005, Stone et al., 2001). However, the results of the current study demonstrating

enhanced axonal APP accumulation following LFPI in NFL deplete neurons suggests the two pathologies may be linked. For example, NFs may protect microtubules from TBI-induced DAI and thus APP accumulation, but undergo compaction in the process and hence the pathologies are observed in separate axons/ axonal regions.

The deletion of NFL has also been shown to increase the rate of fast anterograde and retrograde axonal transport of mitochondria and lysosomes *in vitro* (Perrot and Julien, 2009). Thus, the rate of APP axonal transport may also be increased due to NFL deletion, causing more rapid APP accumulation at points of axonal disruption following LFPI.

Although the increase in APP-positive profiles in NFLKO mice may be due to differences in initial axonal damage or impaired axon transport, they may also be caused by an altered ability to repair cytoskeletal damage after injury. Axonal swellings occur where the cytoskeleton is disrupted (Tang-Schomer et al., 2012, Tang-Schomer et al., 2010), but if they do not grow to the point of disconnection then the damaged cytoskeleton may be repaired, and this ability may differ between NFL deficient and replete axons. As APP has been shown to begin accumulating in axons within hours after TBI (Pierce et al., 1996, Ciallella et al., 2002, Sherriff et al., 1994) future studies should look at more acute time points to assess initial axonal damage and APP accumulation.

In contrast to the current study, *in vitro* axotomy of NFLKO neurons resulted in reduced APP accumulation in damaged neurites compared to NFLWT neurons (Blizzard et al., 2013), but the primary axotomy used in this study would be expected to differ from the DAI of the current study, culminating in impaired axonal transport.

Impaired axonal transport is an early pathological alteration in AD, and evidence suggests that it may acutely and chronically facilitate the development of Aβ plaques and thus AD (Stokin et al., 2005). A recent study has demonstrated that NFL deletion results in increased Aβ plaque deposition in APP/PS1 mice (Fernandez-Martos et al., 2015). Data from this thesis has shown the co-

accumulation of APP with Aβ in diffusely injured axons and increased Aβ plaque deposition after LFPI in APP/PS1 mice. Thus, these data in combination with the current study demonstrating enhanced APP accumulation after LFPI in NLFKO mice suggest that increased axonal transport deficits may underlie the enhanced Aβ plaque deposition shown in NFLKO APP/PS1 mice in the previous study.

A limitation of this study is the sole use of APP as a marker for axonal damage. Most antibodies used to label axons by immunohistochemistry are directed against NF proteins, but they could not be used in this study because the NFLKO mice have altered expression of the other NF subunits (Liu et al., 2013). Hence, to visualize axons the NFLKO mice were crossed with mice expressing yellow fluorescent protein (YFP) in a subset of cortical layer V pyramidal neurons (Feng et al., 2000). However, due to low breeding yields, insufficient YFP×NFLKO mice were available. Thus, a mixture of YFP positive and negative mice were utilized in these experiments, and the analysis was restricted to APP as a marker of axonal damage.

The number of YFP positive and negative mice used in this study was not large enough to test if YFP expression had an effect on the axonal response to injury. However, the proportion of axons expressing YFP is so low that axonal swellings were rarely both APP and YFP positive (Hanell et al., 2014); thus it is unlikely that YFP expression altered the number of APP-positive axonal profiles. Nonetheless, this is a limitation of the study, which should be addressed in future studies. Further experiments analyzing both YFP- and APP-positive axonal injury will give a more complete understanding of how perturbation of the NF cytoskeleton affects the axonal response after TBI.

The biochemical analyses in this study utilised both male and female mice, which was also due to the time constraints of breeding. Previous studies have shown that sex hormones can affect certain aspects of the response to TBI (reviewed in Marklund and Hillered, 2011), however the results of the current study show no effect of gender on APP levels in either NFLKO or NFLWT

mice. Furthermore, the use of both genders may be viewed as a strength, as it increases the generalizability of the results (Prendergast et al., 2014).

In conclusion, this study highlights the importance of intermediate filaments in the axonal response to TBI, particularly their role in impaired axonal transport. This thesis has demonstrated that TBI results in intra-axonal APP and Aβ accumulation and has shown that diffuse TBI can accelerate Aβ plaque deposition. The current study has shown that altering the axonal NF cytoskeleton exacerbates impaired axonal transport following LFPI as indicated by increased axonal APP accumulations. Thus, these results suggest, there is a direct relationship between NF networks and APP transport and/or processing. As axonal transport deficits are implicated in much of the morbidity following TBI (Johnson et al., 2013a), including Aβ plaque deposition (Johnson et al., 2010), NFs may be a good therapeutic target for the treatment of TBI and the ensuing neurodegenerative cascade.

6 Discussion

TBI is an important health problem worldwide, resulting in significant morbidity, disability and death (Maas et al., 2008, Roozenbeek et al., 2013). In high-income countries TBI is the leading cause of disability and mortality in young people and poses a substantial economic burden due to the costs associated with ongoing care for people with cognitive deficits (Maas et al., 2008, Roozenbeek et al., 2013).

TBI can cause persistent neurodegeneration within the brain many years after the initial insult (reviewed in Faden and Loane, 2015) and currently there are no effective therapeutics to intervene in the process. TBI is a risk factor for AD (Fleminger et al., 2003, French et al., 1985, Graves et al., 1990, Guo et al., 2000, Heyman et al., 1984, Kondo et al., 1994, Mayeux et al., 1993, Mortimer et al., 1991, O'Meara et al., 1997, Plassman et al., 2000, Rasmusson et al., 1995, Schofield et al., 1997, Sullivan et al., 1987, Wang et al., 2012) and repetitive TBI can result in the development of CTE, a disease with many AD-like features (Corsellis et al., 1973, Martland, 1928, McKee et al., 2009). Currently, there is no cure for AD or CTE and existing therapies are of little efficacy, thus efforts to prevent disease development are of the upmost importance.

To develop therapies for AD, we first must understand its etiology. Uncovering the molecular mechanisms underlying the relationship between TBI and AD may lead to interventions to prevent both ongoing neurodegeneration after TBI and the development of AD.

Aβ plaques are one of the pathological hallmarks of AD (Braak and Braak, 1991) and are associated with many of the neurodegenerative changes underlying the disease (Mitew et al., 2013a, Mitew et al., 2010, Dickson and Vickers, 2001, Hardy and Allsop, 1991, Kuchibhotla et al., 2008, Vickers et al., 1996). Aβ plaques also occur in approximately 50% of CTE cases and these cases were shown to be a more aggressive, distinct subtype of the disease with a worse clinical outcome (Stein et al., 2015). Mutations in the APP gene that result in

enhanced genesis of the Aβ peptide cause familial AD (Bagyinszky et al., 2014, Goate et al., 1991). Therefore, one mechanism by which TBI may lead to the development of AD is through altering Aβ dynamics.

As previously discussed, studies have shown the presence of Aβ plaques in surgically excised and post-mortem brain tissue from severe TBI cases (Roberts et al., 1991, Roberts et al., 1994, DeKosky et al., 2007, Ikonomovic et al., 2004). However, whether mild and moderate TBI leads to the development of Aβ plaques and whether these plaques persist after injury remains unclear. Animal models of experimental TBI have also been used to explore the relationship between TBI and Aβ plaque dynamics. However, the results of these studies have been conflicting with evidence for increased (Uryu et al., 2002), decreased (Nakagawa et al., 1999, Nakagawa et al., 2000) and unchanged (Smith et al., 1998) Aβ plaque deposition after TBI. Therefore, the central aim of this thesis was to determine the effects of TBI on Aβ plaque dynamics.

Beta-amyloid deposition following traumatic brain injury

This thesis utilized two models of TBI to investigate the effects of different types of injury on Aβ plaque deposition. The first model was a focal penetrative brain injury to the somatosensory cortex, which causes localized inflammation, neovascularization, tissue remodeling and glial scar formation, without widespread secondary pathology (Blizzard et al., 2011, King et al., 2001). The second model was the LFPI model, which induces both focal and diffuse TBI (Alder et al., 2011, Xiong et al., 2013) allowing the effects of widespread injury with secondary pathological changes, on Aβ plaque deposition to be examined.

Focal cortical TBI did not alter Aβ plaque load at 24 hours or 7 days post-injury in APP/PS1 mice injured either prior to amyloidosis (3-months of age) or during plaque deposition (9-months of age). Although it is possible that Aβ plaque deposition may have been altered at a more protracted time point after injury, this is unlikely since by 7 days post-injury substantial tissue remodeling and glial scar formation has occurred and the lesion is resolving (this study, Blizzard et al., 2011). Therefore, the results of this study indicate that focal brain injury is unlikely to affect the onset or progression of Aβ plaque deposition post-injury.

In contrast to the focal brain injury model used in aim 1, the LFPI model of diffuse TBI used in aim 2, did alter Aβ plaque deposition post-injury. The results demonstrated that diffuse TBI altered Aβ plaque deposition in the cortex bilaterally at 30 days post-injury, dependent on the stage of amyloidosis at the time of injury. LFPI prior to the onset of amyloidosis (at 3-months of age) accelerated plaque deposition, whereas LFPI during amyloidosis (at 6-months of age) reduced plaque deposition.

Total Aβ plaque load, but not fibrillar plaque load was reduced in 6-month-old APP/PS1 mice after LFPI. Whether or not LFPI caused reduced deposition or enhanced clearance of Aβ plaques remains to be elucidated. Studies suggest that non-fibrillar/diffuse Aβ is more readily cleared than fibrillar Aβ (Wang et al., 2011, Levites et al., 2006). Thus, the reduction in total, but not fibrillar Aβ plaque load seen in the current study may be due to the clearance of existing or newly formed diffuse Aβ plaques. Future experiments should investigate the mechanism/s by which LFPI caused a reduction in Aβ plaque load including removal by glia, the recruitment of BMDM, changes to the glymphatic clearance of Aβ and the activation of Aβ-degrading enzymes such as neprilysin. This may lead to the development of new therapeutics for AD, with the ability to remove or reduce the deposition of Aβ plaques in the brain. Furthermore, as the LFPI causes both acute and chronic pathological alterations to the brain post-injury (Spain et al., 2010, Thompson et al., 2005), a limitation of this study is Aβ plaque load after LFPI was only evaluated at the time point of 30 days post-injury. Future studies should address this limitation by examining changes in A β plaque load at more acute and chronic time points after LFPI.

The differing effects of the two injury models on Aβ plaque deposition may be due to the more widespread and evolving secondary pathology induced by the LFPI model (Alder et al., 2011, Xiong et al., 2013) in comparison to the focal brain injury model (Blizzard et al., 2011). Previous studies on transgenic mouse models of AD demonstrating changes in Aβ plaque deposition post-injury (Nakagawa et al., 1999, Nakagawa et al., 2000, Uryu et al., 2002) have utilized

the CCI model of TBI, which like the LFPI model, induces both focal and diffuse brain damage (reviewed in Xiong et al., 2013). One major difference between focal and diffuse TBI is the presence of DAI in the latter (Adams et al., 1982, Gennarelli et al., 1982, Strich, 1956, Strich and Oxon, 1961), which may be integral in TBI-induced changes in Aβ plaque deposition and will be discussed below. Thus, this thesis and previous literature (Nakagawa et al., 1999, Nakagawa et al., 2000, Uryu et al., 2002) support the notion that diffuse brain injury may be necessary for the modulation of Aβ plaque deposition post-TBI.

Axonal injury and its role in traumatic brain injury-induced Alzheimer's disease risk

No intra-axonal accumulations of Aβ were seen following the focal cortical brain injury utilized in aim 1. However, LFPI prior to amyloidosis caused the co-accumulation of Aβ with APP in diffusely injured axons. The accumulation of APP following TBI is due to damage to the axonal cytoskeleton resulting in impaired axonal transport (Tang-Schomer et al., 2012, Tang-Schomer et al., 2010). The co-accumulation of Aβ may be due to aberrant generation of Aβ at sites of impaired axonal transport as studies have demonstrated that it co-accumulates with its amyloidogenic processing enzymes as well as Aβ (Chen et al., 2009, Uryu et al., 2007). Intra-axonal accumulations of Aβ may seed plaque formation due to its localized release into the brain parenchyma. Thus, the increase in Aβ plaque deposition demonstrated in mice subjected to LFPI prior to amyloidosis, in the current study, may be due to TBI-induced impaired axonal transport. In support of this hypothesis, it has been shown that impairment of axonal transport by the inhibition of kinesin-I results in enhanced Aβ plaque deposition in a mouse model of AD (Stokin et al., 2005). Furthermore, axonal swellings morphologically similar to those seen following TBI have been demonstrated in early AD and in transgenic mouse models of AD (Stokin et al., 2005). Together, these data indicate that impaired axonal transport may be an initiating factor in the development of Aβ plaques.

As mentioned previously TBI induces damage to components of the axonal cytoskeleton. Following TBI, microtubules undergo breakage, disassembly and disorganization (Tang-Schomer et al., 2012, Tang-Schomer et al., 2010) and NFs

are shown to accumulate within axonal swellings (Chen et al., 1999) as well as undergo degradation (Buki et al., 2003, Ma et al., 2013) and compaction (Pettus et al., 1994, Povlishock et al., 1997). In AD the accumulation of NFs is an early neuronal change associated with Aβ plaque formation (Vickers et al., 1996, Masliah et al., 1993, Dickson et al., 1999). Additionally, a study from the same laboratory group has shown that altering the axonal cytoskeleton by deletion of NFL resulted in enhanced Aβ plaque deposition and exacerbated the development of a subset of dystrophic neurites in the APP/PS1 mouse model of AD (Fernandez-Martos et al., 2015). Thus, these studies demonstrate that the NF network is important in the axonal responses to TBI and AD-associated neurodegeneration. Therefore, the third aim of this thesis was to examine the effect of altering the NF cytoskeleton on the axonal response to TBI.

The results of this thesis demonstrated that the deletion of NFL caused increased APP accumulation in axons of the white matter tracts after LFPI, yet no overall increase in the expression of APP. This indicates that altering the NF cytoskeleton does affect TBI-induced impaired axonal transport. NFs are suggested to perform as mechanical shock absorbers within axons (Kreplak et al., 2005) and thus the deletion of NFL, which also results in reduced expression of the other NF triplet proteins (Liu et al., 2013), may result in axons that are more vulnerable to the tensile forces imparted by TBI leading to more microtubule damage.

However, whether the increased amount of intra-axonal APP accumulations demonstrated was directly due to the reduction in NF content remains unknown. Studies have demonstrated that the deletion of NFL causes increased β-tubulin expression (Liu et al., 2013) as well as enhanced axonal transport rates (Perrot and Julien, 2009), which both may play a role in APP accumulation after TBI. Thus future studies should investigate the mechanism/s by which NFL deletion caused increased axonal pathology. This may elucidate new therapeutic targets for attenuating axonal damage, axonal APP and Aβ accumulation and ongoing neurodegeneration after TBI.

The glial response to traumatic brain injury in the setting of Alzheimer's disease-related pathology

The studies included in this thesis also investigated whether the brains response to TBI was enhanced or reduced in the setting of AD-related pathology. Following focal cortical brain injury there were no significant differences in the recruitment of activated microglia and astrocytes to the injury site between APP/PS1 and WT mice. These data were also supported by the results of the LFPI study, demonstrating no significant differences in the microglial or astrocytic responses between APP/PS1 and WT mice after injury. Therefore, these data indicate that microglia and astrocytes retain the ability to respond to traumatic insults despite the presence of AD-related neuroinflammation.

At 30 days post-LFPI there was also no difference in the percent area occupied by microglia or astrocytes in sections of the cortex from injured versus sham-treated APP/PS1 mice. There were however, changes in Aβ plaque deposition, which differed dependent on the stage of amyloidosis at the time of injury. It is possible that following LFPI there were differences in the phenotypes of microglial and/or astrocytes resulting in differential modulation of Aβ plaque deposition post-injury. Furthermore, changes in glial cells may have been apparent at early time-points post-injury. These limitations should be addressed in future studies to more fully understand the role of glial cells in Aβ plaque formation and removal following TBI.

Synaptic changes following traumatic brain injury in the setting of Alzheimer's disease-related pathology

Synaptic changes after focal cortical brain injury were also investigated in the setting of amyloidosis. The loss and recovery of synaptophysin immunoreactivity after focal cortical brain injury did not differ between APP/PS1 and wild-type mice suggesting that the synaptophysin loss seen in the APP/PS1 mouse model (Mitew et al., 2013a) occurs via specific AD-related neuropathological mechanisms. Additionally, these data indicate synaptic plasticity may still be able to occur in the brain despite the presence of AD-related pathology.

Synaptic alterations and cognitive deficits were not quantified following LFPI in this thesis. Although alterations in Aβ plaque deposition were seen following LFPI, whether these changes were associated with altered cognitive decline or synaptic plasticity was not elucidated. Previous studies have shown that Aβ plaque load does not correlate well will cognitive deficits in AD, however synaptic loss does (reviewed in Arendt, 2009). As synaptic loss and cognitive changes occur in both AD (Mitew et al., 2013a, reviewed in Arendt, 2009) and TBI (McAllister, 2011, Gao and Chen, 2011, Ding et al., 2009) future studies should quantify synaptic changes and cognition after TBI in mice at different stages of amyloidosis. This will provide important information on the interactions between AD-related synaptic alterations, TBI-induced synaptic changes and cognitive deficits after injury.

Transgenic mouse models of Alzheimer's disease in traumatic brain injury research

The main limitation that must be taken into account when interpreting the results of this thesis is the use of a transgenic mouse model of AD. The results of the studies in this thesis give evidence for altered Aβ plaque deposition following TBI on the background of genetic susceptibility. Although most people do not have dominant AD causing mutations, many do develop Aβ plaques, and AD with ageing. WT mice however, do not form Aβ plaques with ageing (Selkoe, 1989) or following TBI (Bramlett et al., 1997, Ciallella et al., 2002, Iwata et al., 2002, Masumura et al., 2000, Pierce et al., 1996) and thus transgenic AD mouse models are necessary for examining the role of TBI in Aβ plaque formation. As the aim of this thesis was to uncover the effects of TBI on AD pathology and APP and Aβ dynamics, not AD in its entirety, the APP/PS1 mouse of AD amyloidosis is an appropriate model. AD mouse models will continue to be a useful tool in investigating the mechanistic links between TBI and the development of AD-related pathology.

Conclusion

In conclusion, this thesis has expanded our knowledge of the effects of TBI on Aβ plaque dynamics, strongly suggesting that diffuse, but not focal TBI can alter the onset and progression of Aβ plaque deposition after injury. The results indicate that the stage of amyloidosis at the time of TBI effects whether or not Aβ plaque deposition increases or decreases and gives evidence supporting the role of the impaired axonal transport in the genesis of Aβ plaques. It indicates that the brain can respond to traumatic insults despite AD-related neuropathology and highlights the role of the NF network in axonal injury and impaired axonal transport, providing a potential therapeutic target to prevent TBI-induced neurodegeneration.

6.1 Summary of the main findings of this thesis

- Focal cortical TBI does not affect the onset or progression of Aβ plaque deposition in the APP/PS1 mouse model of AD prior to the onset of or during amyloidosis.
- Diffuse TBI causes the intra-neuronal and intra-axonal accumulation of APP and Aβ acutely after injury in APP/PS1 mice, whereas focal cortical TBI does not.
- Diffuse TBI accelerates the onset of amyloidosis in the APP/PS1 mouse model of AD as LFPI prior to amyloidosis caused an increase in fibrillar and total Aβ plaque deposition at 30 days post-injury.
- Diffuse TBI during amyloidosis in APP/PS1 mice causes regression or slows progression of Aβ plaque deposition as LFPI caused a reduction in total Aβ plaque deposition at 30 days after injury.
- Despite the background of AD-related neurodegeneration, APP/PS1 and WT mice have the same inflammatory response to focal cortical and diffuse TBI.
- APP/PS1 and WT mice exhibit a similar synaptic response and equivalent levels of neuritic dystrophy following TBI.

- The deletion of NFL results in enhanced axonal transport deficits as indicated by intra-axonal APP accumulation after LFPI.

7 References

ABRAHAMSON, E. E., IKONOMOVIC, M. D., CIALLELLA, J. R., HOPE, C. E., PALJUG, W. R., ISANSKI, B. A., FLOOD, D. G., CLARK, R. S. & DEKOSKY, S. T. 2006. Caspase inhibition therapy abolishes brain trauma-induced increases in Abeta peptide: implications for clinical outcome. *Experimental neurology,* 197**,** 437-50.

ADAMS, J. H., DOYLE, D., FORD, I., GENNARELLI, T. A., GRAHAM, D. I. & MCLELLAN, D. R. 1989. Diffuse axonal injury in head injury: definition, diagnosis and grading. *Histopathology,* 15**,** 49-59.

ADAMS, J. H., GRAHAM, D. I., GENNARELLI, T. A. & MAXWELL, W. L. 1991. Diffuse axonal injury in non-missile head injury. *Journal of neurology, neurosurgery, and psychiatry,* 54**,** 481-3.

ADAMS, J. H., GRAHAM, D. I., MURRAY, L. S. & SCOTT, G. 1982. Diffuse axonal injury due to nonmissile head injury in humans: an analysis of 45 cases. *Annals of neurology,* 12**,** 557-63.

AKIYAMA, H., KONDO, H., IKEDA, K., KATO, M. & MCGEER, P. L. 2001. Immunohistochemical localization of neprilysin in the human cerebral cortex: inverse association with vulnerability to amyloid beta-protein (Abeta) deposition. *Brain research,* 902**,** 277-81.

AL-SARRAJ, S. T., HORTOBAGYI, T. & WISE, S. 2004. Beta amyloid precursor protein (Beta APP) immunohistochemistry detects axonal injury in less than 60 minutes after human brain trauma. *Journal of neuropathology and experimental neurology,* 63**,** 534.

ALBERT-WEISSENBERGER, C. & SIREN, A. L. 2010. Experimental traumatic brain injury. *Experimental & translational stroke medicine,* 2**,** 16.

ALDER, J., FUJIOKA, W., LIFSHITZ, J., CROCKETT, D. P. & THAKKER-VARIA, S. 2011. Lateral fluid percussion: model of traumatic brain injury in mice. *Journal of visualized experiments : JoVE*.

AMADUCCI, L. A., FRATIGLIONI, L., ROCCA, W. A., FIESCHI, C., LIVREA, P., PEDONE, D., BRACCO, L., LIPPI, A., GANDOLFO, C., BINO, G. & ET AL. 1986. Risk factors for clinically diagnosed

Alzheimer's disease: a case-control study of an Italian population. *Neurology,* 36**,** 922-31.

ANDRIESSEN, T. M., JACOBS, B. & VOS, P. E. 2010. Clinical characteristics and pathophysiological mechanisms of focal and diffuse traumatic brain injury. *Journal of cellular and molecular medicine,* 14**,** 2381-92.

ARENDT, T. 2009. Synaptic degeneration in Alzheimer's disease. *Acta neuropathologica,* 118**,** 167-79.

BAGULEY, I. J., NOTT, M. T., HOWLE, A. A., SIMPSON, G. K., BROWNE, S., KING, A. C., COTTER, R. E. & HODGKINSON, A. 2012. Late mortality after severe traumatic brain injury in New South Wales: a multicentre study. *The Medical journal of Australia,* 196**,** 40-5.

BAGYINSZKY, E., YOUN, Y. C., AN, S. S. & KIM, S. 2014. The genetics of Alzheimer's disease. *Clinical interventions in aging,* 9**,** 535-51.

BERO, A. W., YAN, P., ROH, J. H., CIRRITO, J. R., STEWART, F. R., RAICHLE, M. E., LEE, J. M. & HOLTZMAN, D. M. 2011. Neuronal activity regulates the regional vulnerability to amyloid-beta deposition. *Nature neuroscience,* 14**,** 750-6.

BERTRAM, L. & TANZI, R. E. 2008. Thirty years of Alzheimer's disease genetics: the implications of systematic meta-analyses. *Nature reviews. Neuroscience,* 9**,** 768-78.

BIBARI, O., LEE, S., DICKSON, T. C., MITEW, S., VICKERS, J. C. & CHUAH, M. I. 2013. Denervation of the olfactory bulb leads to decreased Abeta plaque load in a transgenic mouse model of Alzheimer' s disease. *Current Alzheimer research,* 10**,** 688-96.

BILLINGS, L. M., ODDO, S., GREEN, K. N., MCGAUGH, J. L. & LAFERLA, F. M. 2005. Intraneuronal Abeta causes the onset of early Alzheimer's disease-related cognitive deficits in transgenic mice. *Neuron,* 45**,** 675-88.

BLASKO, I., BEER, R., BIGL, M., APELT, J., FRANZ, G., RUDZKI, D., RANSMAYR, G., KAMPFL, A. & SCHLIEBS, R. 2004. Experimental traumatic brain injury in rats stimulates the expression, production and activity of Alzheimer's disease beta-secretase (BACE-1). *Journal of neural transmission,* 111**,** 523-36.

BLIZZARD, C. A., CHUCKOWREE, J. A., KING, A. E., HOSIE, K. A., MCCORMACK, G. H., CHAPMAN, J. A., VICKERS, J. C. &

DICKSON, T. C. 2011. Focal damage to the adult rat neocortex induces wound healing accompanied by axonal sprouting and dendritic structural plasticity. *Cerebral cortex,* 21**,** 281-91.

BLIZZARD, C. A., KING, A. E., VICKERS, J. & DICKSON, T. 2013. Cortical murine neurons lacking the neurofilament light chain protein have an attenuated response to injury in vitro. *Journal of neurotrauma,* 30**,** 1908-18.

BLUMBERGS, P. C., SCOTT, G., MANAVIS, J., WAINWRIGHT, H., SIMPSON, D. A. & MCLEAN, A. J. 1994. Staining of amyloid precursor protein to study axonal damage in mild head injury. *Lancet,* 344**,** 1055-6.

BRAAK, H. & BRAAK, E. 1991. Neuropathological stageing of Alzheimer-related changes. *Acta neuropathologica,* 82**,** 239-59.

BRAMLETT, H. M., KRAYDIEH, S., GREEN, E. J. & DIETRICH, W. D. 1997. Temporal and regional patterns of axonal damage following traumatic brain injury: a beta-amyloid precursor protein immunocytochemical study in rats. *Journal of neuropathology and experimental neurology,* 56**,** 1132-41.

BROE, G. A., HENDERSON, A. S., CREASEY, H., MCCUSKER, E., KORTEN, A. E., JORM, A. F., LONGLEY, W. & ANTHONY, J. C. 1990. A case-control study of Alzheimer's disease in Australia. *Neurology,* 40**,** 1698-707.

BUKI, A., FARKAS, O., DOCZI, T. & POVLISHOCK, J. T. 2003. Preinjury administration of the calpain inhibitor MDL-28170 attenuates traumatically induced axonal injury. *Journal of neurotrauma,* 20**,** 261-8.

BUTTON, K. S., IOANNIDIS, J. P., MOKRYSZ, C., NOSEK, B. A., FLINT, J., ROBINSON, E. S. & MUNAFO, M. R. 2013. Power failure: why small sample size undermines the reliability of neuroscience. *Nature reviews. Neuroscience,* 14**,** 365-76.

CACCAMO, A., ODDO, S., SUGARMAN, M. C., AKBARI, Y. & LAFERLA, F. M. 2005. Age- and region-dependent alterations in Abeta-degrading enzymes: implications for Abeta-induced disorders. *Neurobiology of aging,* 26**,** 645-54.

CALHOUN, M. E., JUCKER, M., MARTIN, L. J., THINAKARAN, G., PRICE, D. L. & MOUTON, P. R. 1996. Comparative evaluation of

synaptophysin-based methods for quantification of synapses. *Journal of neurocytology,* 25**,** 821-8.

CARBONELL, W. S., MURASE, S., HORWITZ, A. F. & MANDELL, J. W. 2005. Migration of perilesional microglia after focal brain injury and modulation by CC chemokine receptor 5: an in situ time-lapse confocal imaging study. *Journal of neuroscience,* 25**,** 7040-7.

CHANDRA, V., KOKMEN, E., SCHOENBERG, B. S. & BEARD, C. M. 1989. Head trauma with loss of consciousness as a risk factor for Alzheimer's disease. *Neurology,* 39**,** 1576-8.

CHEN, X. H., JOHNSON, V. E., URYU, K., TROJANOWSKI, J. Q. & SMITH, D. H. 2009. A lack of amyloid beta plaques despite persistent accumulation of amyloid beta in axons of long-term survivors of traumatic brain injury. *Brain pathology,* 19**,** 214-23.

CHEN, X. H., MEANEY, D. F., XU, B. N., NONAKA, M., MCINTOSH, T. K., WOLF, J. A., SAATMAN, K. E. & SMITH, D. H. 1999. Evolution of neurofilament subtype accumulation in axons following diffuse brain injury in the pig. *Journal of neuropathology and experimental neurology,* 58**,** 588-96.

CHEN, X. H., SIMAN, R., IWATA, A., MEANEY, D. F., TROJANOWSKI, J. Q. & SMITH, D. H. 2004. Long-term accumulation of amyloid-beta, beta-secretase, presenilin-1, and caspase-3 in damaged axons following brain trauma. *The American journal of pathology,* 165**,** 357-71.

CHUNG, R. S., ADLARD, P. A., DITTMANN, J., VICKERS, J. C., CHUAH, M. I. & WEST, A. K. 2004. Neuron-glia communication: metallothionein expression is specifically up-regulated by astrocytes in response to neuronal injury. *Journal of neurochemistry,* 88**,** 454-61.

CHUNG, R. S., FUNG, S. J., LEUNG, Y. K., WALKER, A. K., MCCORMACK, G. H., CHUAH, M. I., VICKERS, J. C. & WEST, A. K. 2007. Metallothionein expression by NG2 glial cells following CNS injury. *Cellular and molecular life sciences : CMLS,* 64**,** 2716-22.

CHUNG, R. S., PENKOWA, M., DITTMANN, J., KING, C. E., BARTLETT, C., ASMUSSEN, J. W., HIDALGO, J., CARRASCO, J., LEUNG, Y. K., WALKER, A. K., FUNG, S. J., DUNLOP, S. A., FITZGERALD, M., BEAZLEY, L. D., CHUAH, M. I., VICKERS, J. C. & WEST, A. K.

2008. Redefining the role of metallothionein within the injured brain: extracellular metallothioneins play an important role in the astrocyte-neuron response to injury. *The Journal of biological chemistry,* 283**,** 15349-58.

CHUNG, R. S., VICKERS, J. C., CHUAH, M. I. & WEST, A. K. 2003. Metallothionein-IIA promotes initial neurite elongation and postinjury reactive neurite growth and facilitates healing after focal cortical brain injury. *The Journal of neuroscience,* 23**,** 3336-42.

CIALLELLA, J. R., IKONOMOVIC, M. D., PALJUG, W. R., WILBUR, Y. I., DIXON, C. E., KOCHANEK, P. M., MARION, D. W. & DEKOSKY, S. T. 2002. Changes in expression of amyloid precursor protein and interleukin-1beta after experimental traumatic brain injury in rats. *Journal of neurotrauma,* 19**,** 1555-67.

COLLINS, J. M., KING, A. E., WOODHOUSE, A., KIRKCALDIE, M. T. & VICKERS, J. C. 2015. The effect of focal brain injury on beta-amyloid plaque deposition, inflammation and synapses in the APP/PS1 mouse model of Alzheimer's disease. *Experimental neurology,* 267**,** 219-29.

CORSELLIS, J. A., BRUTON, C. J. & FREEMAN-BROWNE, D. 1973. The aftermath of boxing. *Psychological medicine,* 3**,** 270-303.

DAVALOS, D., GRUTZENDLER, J., YANG, G., KIM, J. V., ZUO, Y., JUNG, S., LITTMAN, D. R., DUSTIN, M. L. & GAN, W. B. 2005. ATP mediates rapid microglial response to local brain injury in vivo. *Nature neuroscience,* 8**,** 752-8.

DEKOSKY, S. T., ABRAHAMSON, E. E., CIALLELLA, J. R., PALJUG, W. R., WISNIEWSKI, S. R., CLARK, R. S. & IKONOMOVIC, M. D. 2007. Association of increased cortical soluble abeta42 levels with diffuse plaques after severe brain injury in humans. *Archives of neurology,* 64**,** 541-4.

DICKSON, T. C., KING, C. E., MCCORMACK, G. H. & VICKERS, J. C. 1999. Neurochemical diversity of dystrophic neurites in the early and late stages of Alzheimer's disease. *Experimental neurology,* 156**,** 100-10.

DICKSON, T. C. & VICKERS, J. C. 2001. The morphological phenotype of beta-amyloid plaques and associated neuritic changes in Alzheimer's disease. *Neuroscience,* 105**,** 99-107.

DING, J. Y., KREIPKE, C. W., SCHAFER, P., SCHAFER, S., SPEIRS, S. L. & RAFOLS, J. A. 2009. Synapse loss regulated by matrix metalloproteinases in traumatic brain injury is associated with hypoxia inducible factor-1alpha expression. *Brain research,* 1268**,** 125-34.

DUFF, K., ECKMAN, C., ZEHR, C., YU, X., PRADA, C. M., PEREZ-TUR, J., HUTTON, M., BUEE, L., HARIGAYA, Y., YAGER, D., MORGAN, D., GORDON, M. N., HOLCOMB, L., REFOLO, L., ZENK, B., HARDY, J. & YOUNKIN, S. 1996. Increased amyloid-beta42(43) in brains of mice expressing mutant presenilin 1. *Nature,* 383**,** 710-3.

FADEN, A. I. & LOANE, D. J. 2015. Chronic neurodegeneration after traumatic brain injury: Alzheimer disease, chronic traumatic encephalopathy, or persistent neuroinflammation? *Neurotherapeutics,* 12**,** 143-50.

FEIGIN, V. L., THEADOM, A., BARKER-COLLO, S., STARKEY, N. J., MCPHERSON, K., KAHAN, M., DOWELL, A., BROWN, P., PARAG, V., KYDD, R., JONES, K., JONES, A. & AMERATUNGA, S. 2013. Incidence of traumatic brain injury in New Zealand: a population-based study. *Lancet neurology,* 12**,** 53-64.

FENG, G., MELLOR, R. H., BERNSTEIN, M., KELLER-PECK, C., NGUYEN, Q. T., WALLACE, M., NERBONNE, J. M., LICHTMAN, J. W. & SANES, J. R. 2000. Imaging neuronal subsets in transgenic mice expressing multiple spectral variants of GFP. *Neuron,* 28**,** 41-51.

FERNANDEZ-MARTOS, C. M., KING, A. E., ATKINSON, R. A., WOODHOUSE, A. & VICKERS, J. C. 2015. Neurofilament light gene deletion exacerbates amyloid, dystrophic neurite and synaptic pathology in the APP/PS1 transgenic model of Alzheimer's disease. *Neurobiology of Aging*.

FLEMINGER, S., OLIVER, D. L., LOVESTONE, S., RABE-HESKETH, S. & GIORA, A. 2003. Head injury as a risk factor for Alzheimer's disease: the evidence 10 years on; a partial replication. *Journal of neurology, neurosurgery, and psychiatry,* 74**,** 857-62.

FRATIGLIONI, L., AHLBOM, A., VIITANEN, M. & WINBLAD, B. 1993. Risk factors for late-onset Alzheimer's disease: a population-based, case-control study. *Annals of neurology,* 33**,** 258-66.

FRENCH, L. R., SCHUMAN, L. M., MORTIMER, J. A., HUTTON, J. T., BOATMAN, R. A. & CHRISTIANS, B. 1985. A case-control study of dementia of the Alzheimer type. *American journal of epidemiology,* 121**,** 414-21.

FUNATO, H., YOSHIMURA, M., YAMAZAKI, T., SAIDO, T. C., ITO, Y., YOKOFUJITA, J., OKEDA, R. & IHARA, Y. 1998. Astrocytes containing amyloid beta-protein (Abeta)-positive granules are associated with Abeta40-positive diffuse plaques in the aged human brain. *The American journal of pathology,* 152**,** 983-92.

GAO, X. & CHEN, J. 2011. Mild traumatic brain injury results in extensive neuronal degeneration in the cerebral cortex. *Journal of neuropathology and experimental neurology,* 70**,** 183-91.

GARCIA-ALLOZA, M., ROBBINS, E. M., ZHANG-NUNES, S. X., PURCELL, S. M., BETENSKY, R. A., RAJU, S., PRADA, C., GREENBERG, S. M., BACSKAI, B. J. & FROSCH, M. P. 2006. Characterization of amyloid deposition in the APPswe/PS1dE9 mouse model of Alzheimer disease. *Neurobiology of disease,* 24**,** 516-24.

GENNARELLI, T. A., THIBAULT, L. E., ADAMS, J. H., GRAHAM, D. I., THOMPSON, C. J. & MARCINCIN, R. P. 1982. Diffuse axonal injury and traumatic coma in the primate. *Annals of neurology,* 12**,** 564-74.

GENTLEMAN, S. M., LECLERCQ, P. D., MOYES, L., GRAHAM, D. I., SMITH, C., GRIFFIN, W. S. & NICOLL, J. A. 2004. Long-term intracerebral inflammatory response after traumatic brain injury. *Forensic science international,* 146**,** 97-104.

GENTLEMAN, S. M., NASH, M. J., SWEETING, C. J., GRAHAM, D. I. & ROBERTS, G. W. 1993. Beta-amyloid precursor protein (beta APP) as a marker for axonal injury after head injury. *Neuroscience letters,* 160**,** 139-44.

GOATE, A., CHARTIER-HARLIN, M. C., MULLAN, M., BROWN, J., CRAWFORD, F., FIDANI, L., GIUFFRA, L., HAYNES, A., IRVING, N., JAMES, L. & ET AL. 1991. Segregation of a missense mutation in the amyloid precursor protein gene with familial Alzheimer's disease. *Nature,* 349**,** 704-6.

GOLDSTEIN, L. E., FISHER, A. M., TAGGE, C. A., ZHANG, X. L., VELISEK, L., SULLIVAN, J. A., UPRETI, C., KRACHT, J. M., ERICSSON, M., WOJNAROWICZ, M. W., GOLETIANI, C. J., MAGLAKELIDZE, G. M., CASEY, N., MONCASTER, J. A., MINAEVA, O., MOIR, R. D., NOWINSKI, C. J., STERN, R. A., CANTU, R. C., GEILING, J., BLUSZTAJN, J. K., WOLOZIN, B. L., IKEZU, T., STEIN, T. D., BUDSON, A. E., KOWALL, N. W., CHARGIN, D., SHARON, A., SAMAN, S., HALL, G. F., MOSS, W. C., CLEVELAND, R. O., TANZI, R. E., STANTON, P. K. & MCKEE, A. C. 2012. Chronic traumatic encephalopathy in blast-exposed military veterans and a blast neurotrauma mouse model. *Science translational medicine,* 4**,** 134ra60.

GOLDSTEIN, M. E., STERNBERGER, L. A. & STERNBERGER, N. H. 1983. Microheterogeneity ("neurotypy") of neurofilament proteins. *Proceedings of the national academy of sciences of the United States of America,* 80**,** 3101-5.

GOURAS, G. K., TSAI, J., NASLUND, J., VINCENT, B., EDGAR, M., CHECLER, F., GREENFIELD, J. P., HAROUTUNIAN, V., BUXBAUM, J. D., XU, H., GREENGARD, P. & RELKIN, N. R. 2000. Intraneuronal Abeta42 accumulation in human brain. *The American journal of pathology,* 156**,** 15-20.

GRAVES, A. B., WHITE, E., KOEPSELL, T. D., REIFLER, B. V., VAN BELLE, G., LARSON, E. B. & RASKIND, M. 1990. The association between head trauma and Alzheimer's disease. *American journal of epidemiology,* 131**,** 491-501.

GUO, Z., CUPPLES, L. A., KURZ, A., AUERBACH, S. H., VOLICER, L., CHUI, H., GREEN, R. C., SADOVNICK, A. D., DUARA, R., DECARLI, C., JOHNSON, K., GO, R. C., GROWDON, J. H., HAINES, J. L., KUKULL, W. A. & FARRER, L. A. 2000. Head injury and the risk of AD in the MIRAGE study. *Neurology,* 54**,** 1316-23.

HALL, A. M. & ROBERSON, E. D. 2012. Mouse models of Alzheimer's disease. *Brain research bulletin,* 88**,** 3-12.

HANELL, A., GREER, J. E., MCGINN, M. J. & POVLISHOCK, J. T. 2014. Traumatic brain injury-induced axonal phenotypes react differently to treatment. *Acta neuropathologica,* 31**,** 42-55.

HARDY, J. & ALLSOP, D. 1991. Amyloid deposition as the central event in the aetiology of Alzheimer's disease. *Trends in pharmacological sciences,* 12**,** 383-8.

HARTMAN, R. E., LAURER, H., LONGHI, L., BALES, K. R., PAUL, S. M., MCINTOSH, T. K. & HOLTZMAN, D. M. 2002. Apolipoprotein E4 influences amyloid deposition but not cell loss after traumatic brain injury in a mouse model of Alzheimer's disease. *The Journal of neuroscience : the official journal of the Society for Neuroscience,* 22**,** 10083-7.

HELISALMI, S., HILTUNEN, M., VEPSALAINEN, S., IIVONEN, S., MANNERMAA, A., LEHTOVIRTA, M., KOIVISTO, A. M., ALAFUZOFF, I. & SOININEN, H. 2004. Polymorphisms in neprilysin gene affect the risk of Alzheimer's disease in Finnish patients. *Journal of neurology, neurosurgery, and psychiatry,* 75**,** 1746-8.

HEYMAN, A., WILKINSON, W. E., STAFFORD, J. A., HELMS, M. J., SIGMON, A. H. & WEINBERG, T. 1984. Alzheimer's disease: a study of epidemiological aspects. *Annals of neurology,* 15**,** 335-41.

HIGASHIDA, T., KREIPKE, C. W., RAFOLS, J. A., PENG, C., SCHAFER, S., SCHAFER, P., DING, J. Y., DORNBOS, D., 3RD, LI, X., GUTHIKONDA, M., ROSSI, N. F. & DING, Y. 2011. The role of hypoxia-inducible factor-1alpha, aquaporin-4, and matrix metalloproteinase-9 in blood-brain barrier disruption and brain edema after traumatic brain injury. *Journal of neurosurgery,* 114**,** 92-101.

HOLBOURN, A. H. S. 1943. Mechanics of head injuries. *The Lancet,* 242**,** 438-441.

HOLBOURN, A. H. S. 1945. Mechanics of brain injuries. *British Medical Bulletin* 3**,** 147-149.

HONG, Y. T., VEENITH, T., DEWAR, D., OUTTRIM, J. G., MANI, V., WILLIAMS, C., PIMLOTT, S., HUTCHINSON, P. J., TAVARES, A., CANALES, R., MATHIS, C. A., KLUNK, W. E., AIGBIRHIO, F. I., COLES, J. P., BARON, J. C., PICKARD, J. D., FRYER, T. D.,

STEWART, W. & MENON, D. K. 2014. Amyloid imaging with carbon 11-labeled Pittsburgh compound B for traumatic brain injury. *JAMA neurology,* 71**,** 23-31.

HYLIN, M. J., ORSI, S. A., ZHAO, J., BOCKHORST, K., PEREZ, A., MOORE, A. N. & DASH, P. K. 2013. Behavioral and histopathological alterations resulting from mild fluid percussion injury. *Journal of neurotrauma,* 30**,** 702-15.

IKONOMOVIC, M. D., URYU, K., ABRAHAMSON, E. E., CIALLELLA, J. R., TROJANOWSKI, J. Q., LEE, V. M., CLARK, R. S., MARION, D. W., WISNIEWSKI, S. R. & DEKOSKY, S. T. 2004. Alzheimer's pathology in human temporal cortex surgically excised after severe brain injury. *Experimental neurology,* 190**,** 192-203.

ILIFF, J. J., WANG, M., LIAO, Y., PLOGG, B. A., PENG, W., GUNDERSEN, G. A., BENVENISTE, H., VATES, G. E., DEANE, R., GOLDMAN, S. A., NAGELHUS, E. A. & NEDERGAARD, M. 2012. A paravascular pathway facilitates CSF flow through the brain parenchyma and the clearance of interstitial solutes, including amyloid beta. *Science translational medicine,* 4**,** 147ra111.

IWATA, A., CHEN, X. H., MCINTOSH, T. K., BROWNE, K. D. & SMITH, D. H. 2002. Long-term accumulation of amyloid-beta in axons following brain trauma without persistent upregulation of amyloid precursor protein genes. *Journal of neuropathology and experimental neurology,* 61**,** 1056-68.

IWATA, A., STYS, P. K., WOLF, J. A., CHEN, X. H., TAYLOR, A. G., MEANEY, D. F. & SMITH, D. H. 2004. Traumatic axonal injury induces proteolytic cleavage of the voltage-gated sodium channels modulated by tetrodotoxin and protease inhibitors. *The Journal of neuroscience,* 24**,** 4605-13.

IWATA, N., TSUBUKI, S., TAKAKI, Y., SHIROTANI, K., LU, B., GERARD, N. P., GERARD, C., HAMA, E., LEE, H. J. & SAIDO, T. C. 2001. Metabolic regulation of brain Abeta by neprilysin. *Science,* 292**,** 1550-2.

IWATA, N., TSUBUKI, S., TAKAKI, Y., WATANABE, K., SEKIGUCHI, M., HOSOKI, E., KAWASHIMA-MORISHIMA, M., LEE, H. J., HAMA, E., SEKINE-AIZAWA, Y. & SAIDO, T. C. 2000. Identification of the

major Abeta1-42-degrading catabolic pathway in brain parenchyma: suppression leads to biochemical and pathological deposition. *Nature medicine,* 6**,** 143-50.

JANKOWSKY, J. L., FADALE, D. J., ANDERSON, J., XU, G. M., GONZALES, V., JENKINS, N. A., COPELAND, N. G., LEE, M. K., YOUNKIN, L. H., WAGNER, S. L., YOUNKIN, S. G. & BORCHELT, D. R. 2004. Mutant presenilins specifically elevate the levels of the 42 residue beta-amyloid peptide in vivo: evidence for augmentation of a 42-specific gamma secretase. *Human molecular genetics,* 13**,** 159-70.

JANKOWSKY, J. L., SLUNT, H. H., RATOVITSKI, T., JENKINS, N. A., COPELAND, N. G. & BORCHELT, D. R. 2001. Co-expression of multiple transgenes in mouse CNS: a comparison of strategies. *Biomolecular engineering,* 17**,** 157-65.

JELLINGER, K. A., PAULUS, W., WROCKLAGE, C. & LITVAN, I. 2001a. Effects of closed traumatic brain injury and genetic factors on the development of Alzheimer's disease. *European journal of neurology : the official journal of the European Federation of Neurological Societies,* 8**,** 707-10.

JELLINGER, K. A., PAULUS, W., WROCKLAGE, C. & LITVAN, I. 2001b. Traumatic brain injury as a risk factor for Alzheimer disease. Comparison of two retrospective autopsy cohorts with evaluation of ApoE genotype. *BMC neurology,* 1**,** 3.

JOHNSON, V. E., STEWART, J. E., BEGBIE, F. D., TROJANOWSKI, J. Q., SMITH, D. H. & STEWART, W. 2013a. Inflammation and white matter degeneration persist for years after a single traumatic brain injury. *Brain,* 136**,** 28-42.

JOHNSON, V. E., STEWART, W., GRAHAM, D. I., STEWART, J. E., PRAESTGAARD, A. H. & SMITH, D. H. 2009. A neprilysin polymorphism and amyloid-beta plaques after traumatic brain injury. *Journal of neurotrauma,* 26**,** 1197-202.

JOHNSON, V. E., STEWART, W. & SMITH, D. H. 2010. Traumatic brain injury and amyloid-beta pathology: a link to Alzheimer's disease? *Nature reviews. Neuroscience,* 11**,** 361-70.

JOHNSON, V. E., STEWART, W. & SMITH, D. H. 2012. Widespread tau and amyloid-Beta pathology many years after a single traumatic brain injury in humans. *Brain pathology,* 22**,** 142-9.

JOHNSON, V. E., STEWART, W. & SMITH, D. H. 2013b. Axonal pathology in traumatic brain injury. *Experimental neurology,* 246**,** 35-43.

JOHNSTONE, E. M., CHANEY, M. O., NORRIS, F. H., PASCUAL, R. & LITTLE, S. P. 1991. Conservation of the sequence of the Alzheimer's disease amyloid peptide in dog, polar bear and five other mammals by cross-species polymerase chain reaction analysis. *Brain research. Molecular brain research,* 10**,** 299-305.

KAMAL, A., ALMENAR-QUERALT, A., LEBLANC, J. F., ROBERTS, E. A. & GOLDSTEIN, L. S. 2001. Kinesin-mediated axonal transport of a membrane compartment containing beta-secretase and presenilin-1 requires APP. *Nature,* 414**,** 643-8.

KAMAL, A., STOKIN, G. B., YANG, Z., XIA, C. H. & GOLDSTEIN, L. S. 2000. Axonal transport of amyloid precursor protein is mediated by direct binding to the kinesin light chain subunit of kinesin-I. *Neuron,* 28**,** 449-59.

KATSOURI, L., ASHRAF, A., BIRCH, A. M., LEE, K. K., MIRZAEI, N. & SASTRE, M. 2014. Systemic administration of fibroblast growth factor-2 (FGF2) reduces BACE1 expression and amyloid pathology in APP23 mice. *Neurobiology of aging*.

KATZMAN, R., GALASKO, D. R., SAITOH, T., CHEN, X., PAY, M. M., BOOTH, A. & THOMAS, R. G. 1996. Apolipoprotein-epsilon4 and head trauma: Synergistic or additive risks? *Neurology,* 46**,** 889-91.

KHAN, F., BAGULEY, I. J. & CAMERON, I. D. 2003. 4: Rehabilitation after traumatic brain injury. *The Medical journal of Australia,* 178**,** 290-5.

KIENLEN-CAMPARD, P., MIOLET, S., TASIAUX, B. & OCTAVE, J. N. 2002. Intracellular amyloid-beta 1-42, but not extracellular soluble amyloid-beta peptides, induces neuronal apoptosis. *The Journal of biological chemistry,* 277**,** 15666-70.

KILINC, D., GALLO, G. & BARBEE, K. A. 2009. Mechanical membrane injury induces axonal beading through localized activation of calpain. *Experimental neurology,* 219**,** 553-61.

KING, C. E., CANTY, A. J. & VICKERS, J. C. 2001. Alterations in neurofilaments associated with reactive brain changes and axonal sprouting following acute physical injury to the rat neocortex. *Neuropathology and applied neurobiology,* 27**,** 115-26.

KIRKCALDIE, M. T., DICKSON, T. C., KING, C. E., GRASBY, D., RIEDERER, B. M. & VICKERS, J. C. 2002. Neurofilament triplet proteins are restricted to a subset of neurons in the rat neocortex. *Journal of chemical neuroanatomy,* 24**,** 163-71.

KIRKITADZE, M. D., CONDRON, M. M. & TEPLOW, D. B. 2001. Identification and characterization of key kinetic intermediates in amyloid beta-protein fibrillogenesis. *Journal of molecular biology,* 312**,** 1103-19.

KIRSCHNER, D. A., INOUYE, H., DUFFY, L. K., SINCLAIR, A., LIND, M. & SELKOE, D. J. 1987. Synthetic peptide homologous to beta protein from Alzheimer disease forms amyloid-like fibrils in vitro. *Proceedings of the National Academy of Sciences of the United States of America,* 84**,** 6953-7.

KONDO, K., NIINO, M. & SHIDO, K. 1994. A case-control study of Alzheimer's disease in Japan--significance of life-styles. *Dementia,* 5**,** 314-26.

KOO, E. H., SISODIA, S. S., ARCHER, D. R., MARTIN, L. J., WEIDEMANN, A., BEYREUTHER, K., FISCHER, P., MASTERS, C. L. & PRICE, D. L. 1990. Precursor of amyloid protein in Alzheimer disease undergoes fast anterograde axonal transport. *Proceedings of the National Academy of Sciences of the United States of America,* 87**,** 1561-5.

KOO, E. H. & SQUAZZO, S. L. 1994. Evidence that production and release of amyloid beta-protein involves the endocytic pathway. *The Journal of biological chemistry,* 269**,** 17386-9.

KOO, E. H., SQUAZZO, S. L., SELKOE, D. J. & KOO, C. H. 1996. Trafficking of cell-surface amyloid beta-protein precursor. I. Secretion, endocytosis and recycling as detected by labeled monoclonal antibody. *Journal of cell science,* 109 (Pt 5)**,** 991-8.

KREPLAK, L., BAR, H., LETERRIER, J. F., HERRMANN, H. & AEBI, U. 2005. Exploring the mechanical behavior of single intermediate filaments. *Journal of molecular biology,* 354**,** 569-77.

KRESS, B. T., ILIFF, J. J., XIA, M., WANG, M., WEI, H. S., ZEPPENFELD, D., XIE, L., KANG, H., XU, Q., LIEW, J. A., PLOG, B. A., DING, F., DEANE, R. & NEDERGAARD, M. 2014. Impairment of paravascular clearance pathways in the aging brain. *Annals of neurology,* 76**,** 845-61.

KUCHIBHOTLA, K. V., GOLDMAN, S. T., LATTARULO, C. R., WU, H. Y., HYMAN, B. T. & BACSKAI, B. J. 2008. Abeta plaques lead to aberrant regulation of calcium homeostasis in vivo resulting in structural and functional disruption of neuronal networks. *Neuron,* 59**,** 214-25.

KUMAR, A. & LOANE, D. J. 2012. Neuroinflammation after traumatic brain injury: opportunities for therapeutic intervention. *Brain, behavior, and immunity,* 26**,** 1191-201.

LAUNER, L. J., ANDERSEN, K., DEWEY, M. E., LETENNEUR, L., OTT, A., AMADUCCI, L. A., BRAYNE, C., COPELAND, J. R., DARTIGUES, J. F., KRAGH-SORENSEN, P., LOBO, A., MARTINEZ-LAGE, J. M., STIJNEN, T. & HOFMAN, A. 1999. Rates and risk factors for dementia and Alzheimer's disease: results from EURODEM pooled analyses. EURODEM Incidence Research Group and Work Groups. European Studies of Dementia. *Neurology,* 52**,** 78-84.

LEE, J. E. & HAN, P. L. 2013. An update of animal models of Alzheimer disease with a reevaluation of plaque depositions. *Experimental neurobiology,* 22**,** 84-95.

LEVITES, Y., DAS, P., PRICE, R. W., ROCHETTE, M. J., KOSTURA, L. A., MCGOWAN, E. M., MURPHY, M. P. & GOLDE, T. E. 2006. Anti-Abeta42- and anti-Abeta40-specific mAbs attenuate amyloid deposition in an Alzheimer disease mouse model. *The Journal of clinical investigation,* 116**,** 193-201.

LEWEN, A., LI, G. L., NILSSON, P., OLSSON, Y. & HILLERED, L. 1995. Traumatic brain injury in rat produces changes of beta-amyloid precursor protein immunoreactivity. *Neuroreport,* 6**,** 357-60.

LI, G., SHEN, Y. C., LI, Y. T., CHEN, C. H., ZHAU, Y. W. & SILVERMAN, J. M. 1992. A case-control study of Alzheimer's disease in China. *Neurology,* 42**,** 1481-8.

LIGHTHALL, J. W. 1988. Controlled cortical impact: a new experimental brain injury model. *Journal of neurotrauma,* 5**,** 1-15.

LILIUS, L., FORSELL, C., AXELMAN, K., WINBLAD, B., GRAFF, C. & TJERNBERG, L. 2003. No association between polymorphisms in the neprilysin promoter region and Swedish Alzheimer's disease patients. *Neuroscience letters,* 337**,** 111-3.

LINDGREN, M. & HAMMARSTROM, P. 2010. Amyloid oligomers: spectroscopic characterization of amyloidogenic protein states. *The FEBS journal,* 277**,** 1380-8.

LIU, Y., STAAL, J. A., CANTY, A. J., KIRKCALDIE, M. T., KING, A. E., BIBARI, O., MITEW, S. T., DICKSON, T. C. & VICKERS, J. C. 2013. Cytoskeletal changes during development and aging in the cortex of neurofilament light protein knockout mice. *The Journal of comparative neurology,* 521**,** 1817-27.

LIU, Z., CONDELLO, C., SCHAIN, A., HARB, R. & GRUTZENDLER, J. 2010. CX3CR1 in microglia regulates brain amyloid deposition through selective protofibrillar amyloid-beta phagocytosis. *The Journal of neuroscience,* 30**,** 17091-101.

LOANE, D. J. & BYRNES, K. R. 2010. Role of microglia in neurotrauma. *Neurotherapeutics,* 7**,** 366-77.

LOUVEAU, A., SMIRNOV, I., KEYES, T. J., ECCLES, J. D., ROUHANI, S. J., PESKE, J. D., DERECKI, N. C., CASTLE, D., MANDELL, J. W., LEE, K. S., HARRIS, T. H. & KIPNIS, J. 2015. Structural and functional features of central nervous system lymphatic vessels. *Nature*.

MA, M., FERGUSON, T. A., SCHOCH, K. M., LI, J., QIAN, Y., SHOFER, F. S., SAATMAN, K. E. & NEUMAR, R. W. 2013. Calpains mediate axonal cytoskeleton disintegration during Wallerian degeneration. *Neurobiology of disease,* 56**,** 34-46.

MAAS, A. I., STOCCHETTI, N. & BULLOCK, R. 2008. Moderate and severe traumatic brain injury in adults. *Lancet neurology,* 7**,** 728-41.

MALM, T. M., JAY, T. R. & LANDRETH, G. E. 2015. The evolving biology of microglia in Alzheimer's disease. *Neurotherapeutics,* 12**,** 81-93.

MALM, T. M., KOISTINAHO, M., PAREPALO, M., VATANEN, T., OOKA, A., KARLSSON, S. & KOISTINAHO, J. 2005. Bone-marrow-derived cells contribute to the recruitment of microglial cells in response to beta-amyloid deposition in APP/PS1 double transgenic Alzheimer mice. *Neurobiology of disease,* 18**,** 134-42.

MARKLUND, N. & HILLERED, L. 2011. Animal modelling of traumatic brain injury in preclinical drug development: where do we go from here? *British journal of pharmacology,* 164**,** 1207-29.

MARMAROU, C. R., LIANG, X., ABIDI, N. H., PARVEEN, S., TAYA, K., HENDERSON, S. C., YOUNG, H. F., FILIPPIDIS, A. S. & BAUMGARTEN, C. M. 2014. Selective vasopressin-1a receptor antagonist prevents brain edema, reduces astrocytic cell swelling and GFAP, V1aR and AQP4 expression after focal traumatic brain injury. *Brain research,* 1581**,** 89-102.

MARMAROU, C. R., WALKER, S. A., DAVIS, C. L. & POVLISHOCK, J. T. 2005. Quantitative analysis of the relationship between intra- axonal neurofilament compaction and impaired axonal transport following diffuse traumatic brain injury. *Journal of neurotrauma,* 22**,** 1066-80.

MARR, R. A., ROCKENSTEIN, E., MUKHERJEE, A., KINDY, M. S., HERSH, L. B., GAGE, F. H., VERMA, I. M. & MASLIAH, E. 2003. Neprilysin gene transfer reduces human amyloid pathology in transgenic mice. *The Journal of neuroscience,* 23**,** 1992-6.

MARTLAND, H. S. 1928. Punch drunk. *JAMA : the journal of the American Medical Association,* 91**,** 1103-1107.

MASLIAH, E., MALLORY, M., HANSEN, L., ALFORD, M., DETERESA, R. & TERRY, R. 1993. An antibody against phosphorylated neurofilaments identifies a subset of damaged association axons in Alzheimer's disease. *The American journal of pathology,* 142**,** 871-82.

MASUMURA, M., HATA, R., URAMOTO, H., MURAYAMA, N., OHNO, T. & SAWADA, T. 2000. Altered expression of amyloid precursors proteins after traumatic brain injury in rats: in situ hybridization and immunohistochemical study. *Journal of neurotrauma,* 17**,** 123-34.

MAURI, M., SINFORIANI, E., BONO, G., CITTADELLA, R., QUATTRONE, A., BOLLER, F. & NAPPI, G. 2006. Interaction between Apolipoprotein epsilon 4 and traumatic brain injury in patients with Alzheimer's disease and Mild Cognitive Impairment. *Functional neurology,* 21**,** 223-8.

MAYEUX, R., OTTMAN, R., MAESTRE, G., NGAI, C., TANG, M. X., GINSBERG, H., CHUN, M., TYCKO, B. & SHELANSKI, M. 1995. Synergistic effects of traumatic head injury and apolipoprotein-epsilon 4 in patients with Alzheimer's disease. *Neurology,* 45**,** 555-7.

MAYEUX, R., OTTMAN, R., TANG, M. X., NOBOA-BAUZA, L., MARDER, K., GURLAND, B. & STERN, Y. 1993. Genetic susceptibility and head injury as risk factors for Alzheimer's disease among community-dwelling elderly persons and their first-degree relatives. *Annals of neurology,* 33**,** 494-501.

MCALLISTER, T. W. 2011. Neurobiological consequences of traumatic brain injury. *Dialogues in clinical neuroscience,* 13**,** 287-300.

MCGINN, M. J., KELLEY, B. J., AKINYI, L., OLI, M. W., LIU, M. C., HAYES, R. L., WANG, K. K. & POVLISHOCK, J. T. 2009. Biochemical, structural, and biomarker evidence for calpain-mediated cytoskeletal change after diffuse brain injury uncomplicated by contusion. *Journal of neuropathology and experimental neurology,* 68**,** 241-9.

MCINTYRE, A., MEHTA, S., AUBUT, J., DIJKERS, M. & TEASELL, R. W. 2013. Mortality among older adults after a traumatic brain injury: a meta-analysis. *Brain injury,* 27**,** 31-40.

MCKEE, A. C., CANTU, R. C., NOWINSKI, C. J., HEDLEY-WHYTE, E. T., GAVETT, B. E., BUDSON, A. E., SANTINI, V. E., LEE, H. S., KUBILUS, C. A. & STERN, R. A. 2009. Chronic traumatic encephalopathy in athletes: progressive tauopathy after repetitive head injury. *Journal of neuropathology and experimental neurology,* 68**,** 709-35.

MCKEE, A. C., STERN, R. A., NOWINSKI, C. J., STEIN, T. D., ALVAREZ, V. E., DANESHVAR, D. H., LEE, H. S., WOJTOWICZ, S. M., HALL, G., BAUGH, C. M., RILEY, D. O., KUBILUS, C. A., CORMIER, K. A., JACOBS, M. A., MARTIN, B. R., ABRAHAM, C. R., IKEZU, T.,

REICHARD, R. R., WOLOZIN, B. L., BUDSON, A. E., GOLDSTEIN, L. E., KOWALL, N. W. & CANTU, R. C. 2013. The spectrum of disease in chronic traumatic encephalopathy. *Brain,* 136**,** 43-64.

MCKENZIE, K. J., MCLELLAN, D. R., GENTLEMAN, S. M., MAXWELL, W. L., GENNARELLI, T. A. & GRAHAM, D. I. 1996. Is beta-APP a marker of axonal damage in short-surviving head injury? *Acta neuropathologica,* 92**,** 608-13.

MEHTA, K. M., OTT, A., KALMIJN, S., SLOOTER, A. J., VAN DUIJN, C. M., HOFMAN, A. & BRETELER, M. M. 1999. Head trauma and risk of dementia and Alzheimer's disease: The Rotterdam Study. *Neurology,* 53**,** 1959-62.

MEYER-LUEHMANN, M., SPIRES-JONES, T. L., PRADA, C., GARCIA-ALLOZA, M., DE CALIGNON, A., ROZKALNE, A., KOENIGSKNECHT-TALBOO, J., HOLTZMAN, D. M., BACSKAI, B. J. & HYMAN, B. T. 2008. Rapid appearance and local toxicity of amyloid-beta plaques in a mouse model of Alzheimer's disease. *Nature,* 451**,** 720-4.

MIELKE, M. M., SAVICA, R., WISTE, H. J., WEIGAND, S. D., VEMURI, P., KNOPMAN, D. S., LOWE, V. J., ROBERTS, R. O., MACHULDA, M. M., GEDA, Y. E., PETERSEN, R. C. & JACK, C. R., JR. 2014. Head trauma and in vivo measures of amyloid and neurodegeneration in a population-based study. *Neurology,* 82**,** 70-6.

MINERS, J. S., BAIG, S., PALMER, J., PALMER, L. E., KEHOE, P. G. & LOVE, S. 2008. Abeta-degrading enzymes in Alzheimer's disease. *Brain pathology,* 18**,** 240-52.

MITEW, S., KIRKCALDIE, M. T., DICKSON, T. C. & VICKERS, J. C. 2013a. Altered synapses and gliotransmission in Alzheimer's disease and AD model mice. *Neurobiology of aging,* 34**,** 2341-51.

MITEW, S., KIRKCALDIE, M. T., DICKSON, T. C. & VICKERS, J. C. 2013b. Neurites containing the neurofilament-triplet proteins are selectively vulnerable to cytoskeletal pathology in Alzheimer's disease and transgenic mouse models. *Frontiers in neuroanatomy,* 7**,** 30.

MITEW, S., KIRKCALDIE, M. T., HALLIDAY, G. M., SHEPHERD, C. E., VICKERS, J. C. & DICKSON, T. C. 2010. Focal demyelination in

Alzheimer's disease and transgenic mouse models. *Acta neuropathologica,* 119**,** 567-77.

MORALES, D. M., MARKLUND, N., LEBOLD, D., THOMPSON, H. J., PITKANEN, A., MAXWELL, W. L., LONGHI, L., LAURER, H., MAEGELE, M., NEUGEBAUER, E., GRAHAM, D. I., STOCCHETTI, N. & MCINTOSH, T. K. 2005. Experimental models of traumatic brain injury: do we really need to build a better mousetrap? *Neuroscience,* 136**,** 971-89.

MORTIMER, J. A., VAN DUIJN, C. M., CHANDRA, V., FRATIGLIONI, L., GRAVES, A. B., HEYMAN, A., JORM, A. F., KOKMEN, E., KONDO, K., ROCCA, W. A. & ET AL. 1991. Head trauma as a risk factor for Alzheimer's disease: a collaborative re-analysis of case-control studies. EURODEM Risk Factors Research Group. *International journal of epidemiology,* 20 Suppl 2**,** S28-35.

MURAI, H., PIERCE, J. E., RAGHUPATHI, R., SMITH, D. H., SAATMAN, K. E., TROJANOWSKI, J. Q., LEE, V. M., LORING, J. F., ECKMAN, C., YOUNKIN, S. & MCINTOSH, T. K. 1998. Twofold overexpression of human beta-amyloid precursor proteins in transgenic mice does not affect the neuromotor, cognitive, or neurodegenerative sequelae following experimental brain injury. *The journal of comparative neurology,* 392**,** 428-38.

MURAKAMI, N., YAMAKI, T., IWAMOTO, Y., SAKAKIBARA, T., KOBORI, N., FUSHIKI, S. & UEDA, S. 1998. Experimental brain injury induces expression of amyloid precursor protein, which may be related to neuronal loss in the hippocampus. *Journal of neurotrauma,* 15**,** 993-1003.

MYBURGH, J. A., COOPER, D. J., FINFER, S. R., VENKATESH, B., JONES, D., HIGGINS, A., BISHOP, N., HIGLETT, T., AUSTRALASIAN TRAUMATIC BRAIN INJURY STUDY INVESTIGATORS FOR THE, A. & NEW ZEALAND INTENSIVE CARE SOCIETY CLINICAL TRIALS, G. 2008. Epidemiology and 12-month outcomes from traumatic brain injury in australia and new zealand. *The Journal of trauma,* 64**,** 854-62.

NAGELE, R. G., WEGIEL, J., VENKATARAMAN, V., IMAKI, H. & WANG, K. C. 2004. Contribution of glial cells to the development of amyloid plaques in Alzheimer's disease. *Neurobiology of aging,* 25**,** 663-74.

NAKAGAWA, Y., NAKAMURA, M., MCINTOSH, T. K., RODRIGUEZ, A., BERLIN, J. A., SMITH, D. H., SAATMAN, K. E., RAGHUPATHI, R., CLEMENS, J., SAIDO, T. C., SCHMIDT, M. L., LEE, V. M. & TROJANOWSKI, J. Q. 1999. Traumatic brain injury in young, amyloid-beta peptide overexpressing transgenic mice induces marked ipsilateral hippocampal atrophy and diminished Abeta deposition during aging. *The journal of comparative neurology,* 411**,** 390-8.

NAKAGAWA, Y., REED, L., NAKAMURA, M., MCINTOSH, T. K., SMITH, D. H., SAATMAN, K. E., RAGHUPATHI, R., CLEMENS, J., SAIDO, T. C., LEE, V. M. & TROJANOWSKI, J. Q. 2000. Brain trauma in aged transgenic mice induces regression of established abeta deposits. *Experimental neurology,* 163**,** 244-52.

NEDERGAARD, M. 2013. Neuroscience. Garbage truck of the brain. *Science,* 340**,** 1529-30.

NEMETZ, P. N., LEIBSON, C., NAESSENS, J. M., BEARD, M., KOKMEN, E., ANNEGERS, J. F. & KURLAND, L. T. 1999. Traumatic brain injury and time to onset of Alzheimer's disease: a population-based study. *American journal of epidemiology,* 149**,** 32-40.

NICOLL, J. A., ROBERTS, G. W. & GRAHAM, D. I. 1995. Apolipoprotein E epsilon 4 allele is associated with deposition of amyloid beta-protein following head injury. *Nature medicine,* 1**,** 135-7.

O'BRIEN, R. J. & WONG, P. C. 2011. Amyloid precursor protein processing and Alzheimer's disease. *Annual review of neuroscience,* 34**,** 185-204.

O'MEARA, E. S., KUKULL, W. A., SHEPPARD, L., BOWEN, J. D., MCCORMICK, W. C., TERI, L., PFANSCHMIDT, M., THOMPSON, J. D., SCHELLENBERG, G. D. & LARSON, E. B. 1997. Head injury and risk of Alzheimer's disease by apolipoprotein E genotype. *American journal of epidemiology,* 146**,** 373-84.

OTSUKA, N., TOMONAGA, M. & IKEDA, K. 1991. Rapid appearance of beta-amyloid precursor protein immunoreactivity in damaged axons and

reactive glial cells in rat brain following needle stab injury. *Brain research,* 568**,** 335-8.

OTVOS, L., JR., SZENDREI, G. I., LEE, V. M. & MANTSCH, H. H. 1993. Human and rodent Alzheimer beta-amyloid peptides acquire distinct conformations in membrane-mimicking solvents. *European journal of biochemistry / FEBS,* 211**,** 249-57.

PARACHIKOVA, A., VASILEVKO, V., CRIBBS, D. H., LAFERLA, F. M. & GREEN, K. N. 2010. Reductions in amyloid-beta-derived neuroinflammation, with minocycline, restore cognition but do not significantly affect tau hyperphosphorylation. *Journal of Alzheimer's disease : JAD,* 21**,** 527-42.

PARESCE, D. M., GHOSH, R. N. & MAXFIELD, F. R. 1996. Microglial cells internalize aggregates of the Alzheimer's disease amyloid beta-protein via a scavenger receptor. *Neuron,* 17**,** 553-65.

PEREZ, S. E., RAGHANTI, M. A., HOF, P. R., KRAMER, L., IKONOMOVIC, M. D., LACOR, P. N., ERWIN, J. M., SHERWOOD, C. C. & MUFSON, E. J. 2013. Alzheimer's disease pathology in the neocortex and hippocampus of the western lowland gorilla (Gorilla gorilla gorilla). *The Journal of comparative neurology,* 521**,** 4318-38.

PERICAK-VANCE, M. A., BEBOUT, J. L., GASKELL, P. C., JR., YAMAOKA, L. H., HUNG, W. Y., ALBERTS, M. J., WALKER, A. P., BARTLETT, R. J., HAYNES, C. A., WELSH, K. A. & ET AL. 1991. Linkage studies in familial Alzheimer disease: evidence for chromosome 19 linkage. *American journal of human genetics,* 48**,** 1034-50.

PERROT, R. & JULIEN, J. P. 2009. Real-time imaging reveals defects of fast axonal transport induced by disorganization of intermediate filaments. *FASEB journal,* 23**,** 3213-25.

PETTUS, E. H., CHRISTMAN, C. W., GIEBEL, M. L. & POVLISHOCK, J. T. 1994. Traumatically induced altered membrane permeability: its relationship to traumatically induced reactive axonal change. *Journal of neurotrauma,* 11**,** 507-22.

PIERCE, J. E., TROJANOWSKI, J. Q., GRAHAM, D. I., SMITH, D. H. & MCINTOSH, T. K. 1996. Immunohistochemical characterization of alterations in the distribution of amyloid precursor proteins and beta-

amyloid peptide after experimental brain injury in the rat. *The Journal of neuroscience,* 16**,** 1083-90.

PIKE, C. J., CUMMINGS, B. J. & COTMAN, C. W. 1995. Early association of reactive astrocytes with senile plaques in Alzheimer's disease. *Experimental neurology,* 132**,** 172-9.

PLASSMAN, B. L., HAVLIK, R. J., STEFFENS, D. C., HELMS, M. J., NEWMAN, T. N., DROSDICK, D., PHILLIPS, C., GAU, B. A., WELSH-BOHMER, K. A., BURKE, J. R., GURALNIK, J. M. & BREITNER, J. C. 2000. Documented head injury in early adulthood and risk of Alzheimer's disease and other dementias. *Neurology,* 55**,** 1158-66.

PODLISNY, M. B., TOLAN, D. R. & SELKOE, D. J. 1991. Homology of the amyloid beta protein precursor in monkey and human supports a primate model for beta amyloidosis in Alzheimer's disease. *The American journal of pathology,* 138**,** 1423-35.

POVLISHOCK, J. T., MARMAROU, A., MCINTOSH, T., TROJANOWSKI, J. Q. & MOROI, J. 1997. Impact acceleration injury in the rat: evidence for focal axolemmal change and related neurofilament sidearm alteration. *Journal of neuropathology and experimental neurology,* 56**,** 347-59.

POVLISHOCK, J. T. & PETTUS, E. H. 1996. Traumatically induced axonal damage: evidence for enduring changes in axolemmal permeability with associated cytoskeletal change. *Acta neurochirurgica. Supplement,* 66**,** 81-6.

PRENDERGAST, B. J., ONISHI, K. G. & ZUCKER, I. 2014. Female mice liberated for inclusion in neuroscience and biomedical research. *Neuroscience and biobehavioral reviews,* 40**,** 1-5.

PRILLER, J., FLUGEL, A., WEHNER, T., BOENTERT, M., HAAS, C. A., PRINZ, M., FERNANDEZ-KLETT, F., PRASS, K., BECHMANN, I., DE BOER, B. A., FROTSCHER, M., KREUTZBERG, G. W., PERSONS, D. A. & DIRNAGL, U. 2001. Targeting gene-modified hematopoietic cells to the central nervous system: use of green fluorescent protein uncovers microglial engraftment. *Nature medicine,* 7**,** 1356-61.

RAJENDRAN, L. & ANNAERT, W. 2012. Membrane trafficking pathways in Alzheimer's disease. *Traffic,* 13**,** 759-70.

RASMUSSON, D. X., BRANDT, J., MARTIN, D. B. & FOLSTEIN, M. F. 1995. Head injury as a risk factor in Alzheimer's disease. *Brain injury : [BI],* 9**,** 213-9.

REAUME, A. G., HOWLAND, D. S., TRUSKO, S. P., SAVAGE, M. J., LANG, D. M., GREENBERG, B. D., SIMAN, R. & SCOTT, R. W. 1996. Enhanced amyloidogenic processing of the beta-amyloid precursor protein in gene-targeted mice bearing the Swedish familial Alzheimer's disease mutations and a "humanized" Abeta sequence. *The Journal of biological chemistry,* 271**,** 23380-8.

REN, Z., ILIFF, J. J., YANG, L., YANG, J., CHEN, X., CHEN, M. J., GIESE, R. N., WANG, B., SHI, X. & NEDERGAARD, M. 2013. 'Hit & Run' model of closed-skull traumatic brain injury (TBI) reveals complex patterns of post-traumatic AQP4 dysregulation. *Journal of cerebral blood flow and metabolism,* 33**,** 834-45.

ROBERTS, G. W., GENTLEMAN, S. M., LYNCH, A. & GRAHAM, D. I. 1991. Beta A4 amyloid protein deposition in brain after head trauma. *Lancet,* 338**,** 1422-3.

ROBERTS, G. W., GENTLEMAN, S. M., LYNCH, A., MURRAY, L., LANDON, M. & GRAHAM, D. I. 1994. Beta amyloid protein deposition in the brain after severe head injury: implications for the pathogenesis of Alzheimer's disease. *Journal of neurology, neurosurgery, and psychiatry,* 57**,** 419-25.

ROOZENBEEK, B., MAAS, A. I. & MENON, D. K. 2013. Changing patterns in the epidemiology of traumatic brain injury. *Nature reviews. Neurology,* 9**,** 231-6.

SAKAI, A., UJIKE, H., NAKATA, K., TAKEHISA, Y., IMAMURA, T., UCHIDA, N., KANZAKI, A., YAMAMOTO, M., FUJISAWA, Y., OKUMURA, K. & KURODA, S. 2004. Association of the Neprilysin gene with susceptibility to late-onset Alzheimer's disease. *Dementia and geriatric cognitive disorders,* 17**,** 164-9.

SALIB, E. & HILLIER, V. 1997. Head injury and the risk of Alzheimer's disease: a case control study. *International journal of geriatric psychiatry,* 12**,** 363-8.

SAMAROO, H. D., OPSAHL, A. C., SCHREIBER, J., O'NEILL, S. M., MARCONI, M., QIAN, J., CARVAJAL-GONZALEZ, S., TATE, B., MILICI, A. J., BALES, K. R. & STEPHENSON, D. T. 2012. High throughput object-based image analysis of beta-amyloid plaques in human and transgenic mouse brain. *Journal of neuroscience methods,* 204**,** 179-88.

SCHNEIDER, C. A., RASBAND, W. S. & ELICEIRI, K. W. 2012. NIH Image to ImageJ: 25 years of image analysis. *Nature methods,* 9**,** 671-5.

SCHOFIELD, P. W., TANG, M., MARDER, K., BELL, K., DOONEIEF, G., CHUN, M., SANO, M., STERN, Y. & MAYEUX, R. 1997. Alzheimer's disease after remote head injury: an incidence study. *Journal of neurology, neurosurgery, and psychiatry,* 62**,** 119-24.

SELKOE, D. J. 1989. Biochemistry of altered brain proteins in Alzheimer's disease. *Annual review of neuroscience,* 12**,** 463-90.

SELKOE, D. J., BELL, D. S., PODLISNY, M. B., PRICE, D. L. & CORK, L. C. 1987. Conservation of brain amyloid proteins in aged mammals and humans with Alzheimer's disease. *Science,* 235**,** 873-7.

SHALAT, S. L., SELTZER, B., PIDCOCK, C. & BAKER, E. L., JR. 1987. Risk factors for Alzheimer's disease: a case-control study. *Neurology,* 37**,** 1630-3.

SHENTON, M. E., HAMODA, H. M., SCHNEIDERMAN, J. S., BOUIX, S., PASTERNAK, O., RATHI, Y., VU, M. A., PUROHIT, M. P., HELMER, K., KOERTE, I., LIN, A. P., WESTIN, C. F., KIKINIS, R., KUBICKI, M., STERN, R. A. & ZAFONTE, R. 2012. A review of magnetic resonance imaging and diffusion tensor imaging findings in mild traumatic brain injury. *Brain imaging and behavior,* 6**,** 137-92.

SHERRIFF, F. E., BRIDGES, L. R. & SIVALOGANATHAN, S. 1994. Early detection of axonal injury after human head trauma using immunocytochemistry for beta-amyloid precursor protein. *Acta neuropathologica,* 87**,** 55-62.

SHERRINGTON, R., ROGAEV, E. I., LIANG, Y., ROGAEVA, E. A., LEVESQUE, G., IKEDA, M., CHI, H., LIN, C., LI, G., HOLMAN, K., TSUDA, T., MAR, L., FONCIN, J. F., BRUNI, A. C., MONTESI, M. P., SORBI, S., RAINERO, I., PINESSI, L., NEE, L., CHUMAKOV, I.,

POLLEN, D., BROOKES, A., SANSEAU, P., POLINSKY, R. J., WASCO, W., DA SILVA, H. A., HAINES, J. L., PERKICAK-VANCE, M. A., TANZI, R. E., ROSES, A. D., FRASER, P. E., ROMMENS, J. M. & ST GEORGE-HYSLOP, P. H. 1995. Cloning of a gene bearing missense mutations in early-onset familial Alzheimer's disease. *Nature,* 375**,** 754-60.

SHI, J., ZHANG, S., TANG, M., MA, C., ZHAO, J., LI, T., LIU, X., SUN, Y., GUO, Y., HAN, H., MA, Y. & ZHAO, Z. 2005. Mutation screening and association study of the neprilysin gene in sporadic Alzheimer's disease in Chinese persons. *The journals of gerontology. Series A, Biological sciences and medical sciences,* 60**,** 301-6.

SIMARD, A. R., SOULET, D., GOWING, G., JULIEN, J. P. & RIVEST, S. 2006. Bone marrow-derived microglia play a critical role in restricting senile plaque formation in Alzheimer's disease. *Neuron,* 49**,** 489-502.

SMITH, D. H., CHEN, X. H., IWATA, A. & GRAHAM, D. I. 2003. Amyloid beta accumulation in axons after traumatic brain injury in humans. *Journal of neurosurgery,* 98**,** 1072-7.

SMITH, D. H., CHEN, X. H., NONAKA, M., TROJANOWSKI, J. Q., LEE, V. M., SAATMAN, K. E., LEONI, M. J., XU, B. N., WOLF, J. A. & MEANEY, D. F. 1999. Accumulation of amyloid beta and tau and the formation of neurofilament inclusions following diffuse brain injury in the pig. *Journal of neuropathology and experimental neurology,* 58**,** 982-92.

SMITH, D. H. & MEANEY, D. F. 2000. Axonal damage in traumatic brain injury. *Neuroscientist,* 6**,** 483-495.

SMITH, D. H., NAKAMURA, M., MCINTOSH, T. K., WANG, J., RODRIGUEZ, A., CHEN, X. H., RAGHUPATHI, R., SAATMAN, K. E., CLEMENS, J., SCHMIDT, M. L., LEE, V. M. & TROJANOWSKI, J. Q. 1998. Brain trauma induces massive hippocampal neuron death linked to a surge in beta-amyloid levels in mice overexpressing mutant amyloid precursor protein. *The American journal of pathology,* 153**,** 1005-10.

SMITH, D. H., SOARES, H. D., PIERCE, J. S., PERLMAN, K. G., SAATMAN, K. E., MEANEY, D. F., DIXON, C. E. & MCINTOSH, T.

K. 1995. A model of parasagittal controlled cortical impact in the mouse: cognitive and histopathologic effects. *Journal of neurotrauma,* 12**,** 169-78.

SODEYAMA, N., MIZUSAWA, H., YAMADA, M., ITOH, Y., OTOMO, E. & MATSUSHITA, M. 2001. Lack of association of neprilysin polymorphism with Alzheimer's disease and Alzheimer's disease-type neuropathological changes. *Journal of neurology, neurosurgery, and psychiatry,* 71**,** 817-8.

SOFRONIEW, M. V. 2009. Molecular dissection of reactive astrogliosis and glial scar formation. *Trends in neurosciences,* 32**,** 638-47.

SOMMER, C., STRAEHLE, C., KOTHE, U. & HAMPRECHT, F. A. 2011. Ilastik: Interactive learning and segmentation toolkit. Biomedical Imaging: From Nano to Macro. *Biomedical Imaging: From Nano to Macro, 2011 IEEE International Symposium***,** 230-233.

SOULET, D. & RIVEST, S. 2008. Bone-marrow-derived microglia: myth or reality? *Current opinion in pharmacology,* 8**,** 508-18.

SPAIN, A., DAUMAS, S., LIFSHITZ, J., RHODES, J., ANDREWS, P. J., HORSBURGH, K. & FOWLER, J. H. 2010. Mild fluid percussion injury in mice produces evolving selective axonal pathology and cognitive deficits relevant to human brain injury. *Journal of neurotrauma,* 27**,** 1429-38.

STEIN, T. D., MONTENIGRO, P. H., ALVAREZ, V. E., XIA, W., CRARY, J. F., TRIPODIS, Y., DANESHVAR, D. H., MEZ, J., SOLOMON, T., MENG, G., KUBILUS, C. A., CORMIER, K. A., MENG, S., BABCOCK, K., KIERNAN, P., MURPHY, L., NOWINSKI, C. J., MARTIN, B., DIXON, D., STERN, R. A., CANTU, R. C., KOWALL, N. W. & MCKEE, A. C. 2015. Beta-amyloid deposition in chronic traumatic encephalopathy. *Acta neuropathologica,* 130**,** 21-34.

STERNBERGER, L. A. & STERNBERGER, N. H. 1983. Monoclonal antibodies distinguish phosphorylated and nonphosphorylated forms of neurofilaments in situ. *Proceedings of the National Academy of Sciences of the United States of America,* 80**,** 6126-30.

STOKIN, G. B., LILLO, C., FALZONE, T. L., BRUSCH, R. G., ROCKENSTEIN, E., MOUNT, S. L., RAMAN, R., DAVIES, P.,

MASLIAH, E., WILLIAMS, D. S. & GOLDSTEIN, L. S. 2005. Axonopathy and transport deficits early in the pathogenesis of Alzheimer's disease. *Science,* 307**,** 1282-8.

STONE, J. R., SINGLETON, R. H. & POVLISHOCK, J. T. 2001. Intra-axonal neurofilament compaction does not evoke local axonal swelling in all traumatically injured axons. *Experimental neurology,* 172**,** 320-31.

STREIT, W. J. 2004a. Microglia and Alzheimer's disease pathogenesis. *J Neurosci Res,* 77**,** 1-8.

STREIT, W. J. 2004b. Microglia and Alzheimer's disease pathogenesis. *Journal of neuroscience research,* 77**,** 1-8.

STRICH, S. J. 1956. Diffuse degeneration of the cerebral white matter in severe dementia following head injury. *Journal of neurology, neurosurgery, and psychiatry,* 19**,** 163-85.

STRICH, S. J. & OXON, D. M. 1961. Shearing of nerve fibres as a cause of brain damage due to head injury: A pathological study of twenty cases. *The Lancet,* 278**,** 443-448.

STRITTMATTER, W. J., SAUNDERS, A. M., SCHMECHEL, D., PERICAK-VANCE, M., ENGHILD, J., SALVESEN, G. S. & ROSES, A. D. 1993. Apolipoprotein E: high-avidity binding to beta-amyloid and increased frequency of type 4 allele in late-onset familial Alzheimer disease. *Proceedings of the National Academy of Sciences of the United States of America,* 90**,** 1977-81.

SULLIVAN, P., PETITTI, D. & BARBACCIA, J. 1987. Head trauma and age of onset of dementia of the Alzheimer type. *JAMA : the journal of the American Medical Association,* 257**,** 2289-90.

TAKAHASHI, R. H., MILNER, T. A., LI, F., NAM, E. E., EDGAR, M. A., YAMAGUCHI, H., BEAL, M. F., XU, H., GREENGARD, P. & GOURAS, G. K. 2002. Intraneuronal Alzheimer abeta42 accumulates in multivesicular bodies and is associated with synaptic pathology. *The American journal of pathology,* 161**,** 1869-79.

TANG-SCHOMER, M. D., JOHNSON, V. E., BAAS, P. W., STEWART, W. & SMITH, D. H. 2012. Partial interruption of axonal transport due to microtubule breakage accounts for the formation of periodic varicosities after traumatic axonal injury. *Experimental neurology,* 233**,** 364-72.

TANG-SCHOMER, M. D., PATEL, A. R., BAAS, P. W. & SMITH, D. H. 2010. Mechanical breaking of microtubules in axons during dynamic stretch injury underlies delayed elasticity, microtubule disassembly, and axon degeneration. *FASEB journal* 24**,** 1401-10.

THOMPSON, H. J., LIFSHITZ, J., MARKLUND, N., GRADY, M. S., GRAHAM, D. I., HOVDA, D. A. & MCINTOSH, T. K. 2005. Lateral fluid percussion brain injury: a 15-year review and evaluation. *Journal of neurotrauma,* 22**,** 42-75.

THORNTON, E., VINK, R., BLUMBERGS, P. C. & VAN DEN HEUVEL, C. 2006. Soluble amyloid precursor protein alpha reduces neuronal injury and improves functional outcome following diffuse traumatic brain injury in rats. *Brain research,* 1094**,** 38-46.

TRAN, H. T., LAFERLA, F. M., HOLTZMAN, D. M. & BRODY, D. L. 2011a. Controlled cortical impact traumatic brain injury in 3xTg-AD mice causes acute intra-axonal amyloid-beta accumulation and independently accelerates the development of tau abnormalities. *The Journal of neuroscience,* 31**,** 9513-25.

TRAN, H. T., SANCHEZ, L., ESPARZA, T. J. & BRODY, D. L. 2011b. Distinct temporal and anatomical distributions of amyloid-beta and tau abnormalities following controlled cortical impact in transgenic mice. *PloS one,* 6**,** e25475.

TSOLAKI, M., FOUNTOULAKIS, K., CHANTZI, E. & KAZIS, A. 1997. Risk factors for clinically diagnosed Alzheimer's disease: a case-control study of a Greek population. *International psychogeriatrics / IPA,* 9**,** 327-41.

TURNER, A. J., ISAAC, R. E. & COATES, D. 2001. The neprilysin (NEP) family of zinc metalloendopeptidases: genomics and function. *Bioessays,* 23**,** 261-9.

URYU, K., CHEN, X. H., MARTINEZ, D., BROWNE, K. D., JOHNSON, V. E., GRAHAM, D. I., LEE, V. M., TROJANOWSKI, J. Q. & SMITH, D. H. 2007. Multiple proteins implicated in neurodegenerative diseases accumulate in axons after brain trauma in humans. *Experimental neurology,* 208**,** 185-92.

URYU, K., LAURER, H., MCINTOSH, T., PRATICO, D., MARTINEZ, D., LEIGHT, S., LEE, V. M. & TROJANOWSKI, J. Q. 2002. Repetitive

mild brain trauma accelerates Abeta deposition, lipid peroxidation, and cognitive impairment in a transgenic mouse model of Alzheimer amyloidosis. *The Journal of neuroscience,* 22**,** 446-54.

VAN DEN HEUVEL, C., BLUMBERGS, P. C., FINNIE, J. W., MANAVIS, J., JONES, N. R., REILLY, P. L. & PEREIRA, R. A. 1999. Upregulation of amyloid precursor protein messenger RNA in response to traumatic brain injury: an ovine head impact model. *Experimental neurology,* 159**,** 441-50.

VAN DUIJN, C. M., TANJA, T. A., HAAXMA, R., SCHULTE, W., SAAN, R. J., LAMERIS, A. J., ANTONIDES-HENDRIKS, G. & HOFMAN, A. 1992. Head trauma and the risk of Alzheimer's disease. *American journal of epidemiology,* 135**,** 775-82.

VERKHRATSKY, A., OLABARRIA, M., NORISTANI, H. N., YEH, C. Y. & RODRIGUEZ, J. J. 2010. Astrocytes in Alzheimer's disease. *Neurotherapeutics,* 7**,** 399-412.

VICKERS, J. C., CHIN, D., EDWARDS, A. M., SAMPSON, V., HARPER, C. & MORRISON, J. 1996. Dystrophic neurite formation associated with age-related beta amyloid deposition in the neocortex: clues to the genesis of neurofibrillary pathology. *Experimental neurology,* 141**,** 1-11.

VICKERS, J. C. & COSTA, M. 1992. The neurofilament triplet is present in distinct subpopulations of neurons in the central nervous system of the guinea-pig. *Neuroscience,* 49**,** 73-100.

VICKERS, J. C., RIEDERER, B. M., MARUGG, R. A., BUEE-SCHERRER, V., BUEE, L., DELACOURTE, A. & MORRISON, J. H. 1994. Alterations in neurofilament protein immunoreactivity in human hippocampal neurons related to normal aging and Alzheimer's disease. *Neuroscience,* 62**,** 1-13.

WANG, A., DAS, P., SWITZER, R. C., 3RD, GOLDE, T. E. & JANKOWSKY, J. L. 2011. Robust amyloid clearance in a mouse model of Alzheimer's disease provides novel insights into the mechanism of amyloid-beta immunotherapy. *The Journal of neuroscience,* 31**,** 4124-36.

WANG, H. K., LIN, S. H., SUNG, P. S., WU, M. H., HUNG, K. W., WANG, L. C., HUANG, C. Y., LU, K., CHEN, H. J. & TSAI, K. J. 2012. Population based study on patients with traumatic brain injury suggests increased

risk of dementia. *Journal of neurology, neurosurgery, and psychiatry,* 83**,** 1080-5.

WASHINGTON, P. M., MORFFY, N., PARSADANIAN, M., ZAPPLE, D. N. & BURNS, M. P. 2014. Experimental traumatic brain injury induces rapid aggregation and oligomerization of amyloid-beta in an Alzheimer's disease mouse model. *Journal of neurotrauma,* 31**,** 125-34.

WEGIEL, J., WANG, K. C., TARNAWSKI, M. & LACH, B. 2000. Microglia cells are the driving force in fibrillar plaque formation, whereas astrocytes are a leading factor in plague degradation. *Acta neuropathologica,* 100**,** 356-64.

WOLF, J. A., STYS, P. K., LUSARDI, T., MEANEY, D. & SMITH, D. H. 2001. Traumatic axonal injury induces calcium influx modulated by tetrodotoxin-sensitive sodium channels. *The Journal of neuroscience,* 21**,** 1923-30.

WOOD, L. S., PICKERING, E. H., MCHALE, D. & DECHAIRO, B. M. 2007. Association between neprilysin polymorphisms and sporadic Alzheimer's disease. *Neuroscience letters,* 427**,** 103-6.

WOODHOUSE, A., VICKERS, J. C., ADLARD, P. A. & DICKSON, T. C. 2009. Dystrophic neurites in TgCRND8 and Tg2576 mice mimic human pathological brain aging. *Neurobiology of aging,* 30**,** 864-74.

WYSS-CORAY, T., LOIKE, J. D., BRIONNE, T. C., LU, E., ANANKOV, R., YAN, F., SILVERSTEIN, S. C. & HUSEMANN, J. 2003a. Adult mouse astrocytes degrade amyloid-beta in vitro and in situ. *Nature medicine,* 9**,** 453-7.

WYSS-CORAY, T., LOIKE, J. D., BRIONNE, T. C., LU, E., ANANKOV, R., YAN, F., SILVERSTEIN, S. C. & HUSEMANN, J. 2003b. Adult mouse astrocytes degrade amyloid-beta in vitro and in situ. *Nat Med,* 9**,** 453-7.

XIONG, Y., MAHMOOD, A. & CHOPP, M. 2013. Animal models of traumatic brain injury. *Nature reviews. Neuroscience,* 14**,** 128-42.

YAMADA, T., SASAKI, H., FURUYA, H., MIYATA, T., GOTO, I. & SAKAKI, Y. 1987. Complementary DNA for the mouse homolog of the human amyloid beta protein precursor. *Biochemical and biophysical research communications,* 149**,** 665-71.

YAMAZAKI, T., KOO, E. H. & SELKOE, D. J. 1996. Trafficking of cell-surface amyloid beta-protein precursor. II. Endocytosis, recycling and lysosomal targeting detected by immunolocalization. *Journal of cell science,* 109 (Pt 5)**,** 999-1008.

YASOJIMA, K., AKIYAMA, H., MCGEER, E. G. & MCGEER, P. L. 2001. Reduced neprilysin in high plaque areas of Alzheimer brain: a possible relationship to deficient degradation of beta-amyloid peptide. *Neuroscience letters,* 297**,** 97-100.

YOUMANS, K. L., TAI, L. M., KANEKIYO, T., STINE, W. B., JR., MICHON, S. C., NWABUISI-HEATH, E., MANELLI, A. M., FU, Y., RIORDAN, S., EIMER, W. A., BINDER, L., BU, G., YU, C., HARTLEY, D. M. & LADU, M. J. 2012a. Intraneuronal Abeta detection in 5xFAD mice by a new Abeta-specific antibody. *Molecular neurodegeneration,* 7**,** 8.

YOUMANS, K. L., TAI, L. M., NWABUISI-HEATH, E., JUNGBAUER, L., KANEKIYO, T., GAN, M., KIM, J., EIMER, W. A., ESTUS, S., REBECK, G. W., WEEBER, E. J., BU, G., YU, C. & LADU, M. J. 2012b. APOE4-specific changes in Abeta accumulation in a new transgenic mouse model of Alzheimer disease. *The Journal of biological chemistry,* 287**,** 41774-86.

YUAN, A., RAO, M. V., VEERANNA & NIXON, R. A. 2012. Neurofilaments at a glance. *J Cell Sci,* 125**,** 3257-63.

ZAHS, K. R. & ASHE, K. H. 2010. 'Too much good news' - are Alzheimer mouse models trying to tell us how to prevent, not cure, Alzheimer's disease? *Trends in neurosciences,* 33**,** 381-9.

ZHANG, D., HU, X., QIAN, L., O'CALLAGHAN, J. P. & HONG, J. S. 2010. Astrogliosis in CNS pathologies: is there a role for microglia? *Molecular neurobiology,* 41**,** 232-41.

ZHAO, W., DUMANIS, S. B., TAMBOLI, I. Y., RODRIGUEZ, G. A., JO LADU, M., MOUSSA, C. E. & WILLIAM REBECK, G. 2014a. Human APOE genotype affects intraneuronal Abeta1-42 accumulation in a lentiviral gene transfer model. *Human molecular genetics,* 23**,** 1365-75.

ZHAO, W., ZHANG, J., DAVIS, E. G. & REBECK, G. W. 2014b. Aging reduces glial uptake and promotes extracellular accumulation of Abeta from a lentiviral vector. *Frontiers in aging neuroscience,* 6**,** 210.

ZHU, Q., COUILLARD-DESPRES, S. & JULIEN, J. P. 1997. Delayed maturation of regenerating myelinated axons in mice lacking neurofilaments. *Experimental neurology,* 148**,** 299-316.

Appendix A – Commonly used solutions

0.27M sodium phosphate monobasic

32.2g sodium phosphate monobasic (Sigma-Aldrich, S8282-500G)

1000mL milli-Q® water

0.16M sodium phosphate dibasic dihydrate

28.4g sodium phosphate dibasic dehydrate (Sigma-Aldrich, S0876-1KG)

1000mL milli-Q® water

1.54M sodium chloride

90g sodium chloride (Sigma-Aldrich, S3014-5KG)

1000mL milli-Q® water

0.01M Phosphate buffered saline (PBS)

10mL of 0.27M sodium phosphate monobasic

40mL of 0.16M sodium phosphate dibasic dihydrate

100mL of 1.54M sodium chloride

850mL milli-Q® water

0.2% PBS Azide

1g sodium azide (Sigma-Aldrich, S2002-500G)

500mL 0.1M PBS

0.01% Sodium Azide

10mL 0.2% sodium azide

190mL 0.01M PBS

Antibody Diluent – 0.3% Triton-x-100 in 0.1MPBS

600ul Triton-X-100 (Sigma-Aldrich, X-100-500ML)

200mL 0.1M PBS

PBSX 0.25% Triton-X-100 in 0.1M PBS

250ul Triton-X-100

100mL 0.1M PBS

10x TBS

60.5g Trizma Base (Sigma-Aldrich, T1S03-1KG)

87.6g NaCl

pH to 7.5

Make up to 1L with deionized water.

1xTBS

100mL 10× TBS

900mL 1×TBS

TBST

100mL TBS 10×

900mL dH_2O

1mL Tween-20 (P2287-500ML)

Artificial cerebral spinal fluid (aCSF)

7.305g Sodium chloride

0.372g Potassium chloride

1.802g Glucose

2.383g HEPES

0.294g Calcium chloride

0.493g Magnesium sulfate

pH to 7.4, make up to 1L with milli-Q® water and filter sterilize.

4% paraformaldehyde (PFA)

20g paraformaldehyde (granular) (Electron Microscopy Sciences, 19210)

500mL of 0.01M PBS

0.5M EDTA

292.24g EDTA (Sigma-Aldrich, EDS-500G)

pH to 8.0, make up to 500mL.

50×TAE

100mL 0.5M EDTA ph8.0

242g Trizma base in 750mL milli-Q® water

57.1ml glacial acetic acid

Make up to 1L with milli-Q® water.

1×TAE

20mL 50×TAE

980mL milli-Q® water

Appendix B - Segmentation of a stiched montage image

Figure B1 Segmentation of a stitched montage image. (A) Stitched montage image with grid-like pattern prior to segmenting. (B) Image in (A) following segmentation. The grid-like pattern did not effect the segmentation of plaques in different regions across the grid-like patterned image.

A

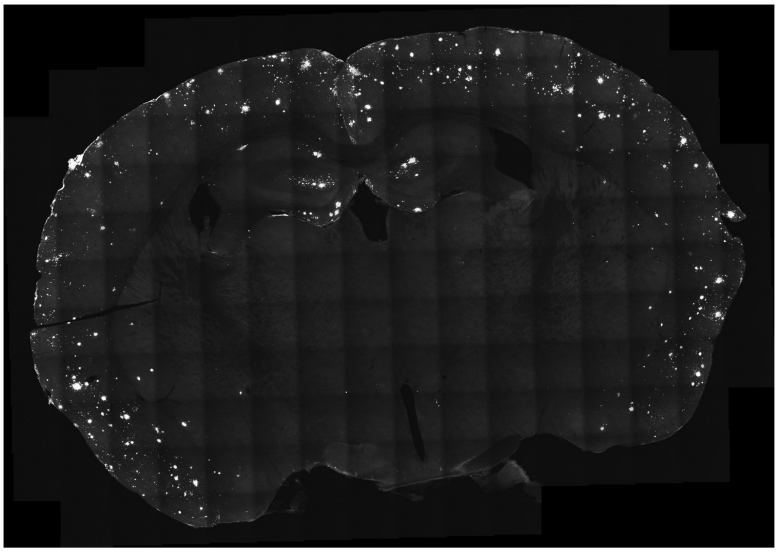

B